Effects of mucilage and extracellular polymeric substances on soil gas diffusion

Adrian Haupenthal

Energie & Umwelt / Energy & Environment
Band / Volume 668
ISBN 978-3-95806-834-6

Mitglied der Helmholtz-Gemeinschaft

JÜLICH
Forschungszentrum

Schriften des Forschungszentrums Jülich
Reihe Energie & Umwelt / Energy & Environment Band / Volume 668

Forschungszentrum Jülich GmbH
Institut für Bio- und Geowissenschaften (IBG)
Agrosphäre (IBG-3)

Effects of mucilage and extracellular polymeric substances on soil gas diffusion

Adrian Haupenthal

Schriften des Forschungszentrums Jülich
Reihe Energie & Umwelt / Energy & Environment Band / Volume 668

ISSN 1866-1793 ISBN 978-3-95806-834-6

Bibliografische Information der Deutschen Nationalbibliothek.
Die Deutsche Nationalbibliothek verzeichnet diese Publikation in der
Deutschen Nationalbibliografie; detaillierte Bibliografische Daten
sind im Internet über http://dnb.d-nb.de abrufbar.

Herausgeber und Vertrieb:	Forschungszentrum Jülich GmbH Zentralbibliothek, Verlag 52425 Jülich Tel.: +49 2461 61-5368 Fax: +49 2461 61-6103 zb-publikation@fz-juelich.de www.fz-juelich.de/zb
Umschlaggestaltung:	Grafische Medien, Forschungszentrum Jülich GmbH
Druck:	Grafische Medien, Forschungszentrum Jülich GmbH
Copyright:	Forschungszentrum Jülich 2025

Schriften des Forschungszentrums Jülich
Reihe Energie & Umwelt / Energy & Environment, Band / Volume 668

D 5 (Diss. Bonn, Univ., 2025)

ISSN 1866-1793
ISBN 978-3-95806-834-6

Vollständig frei verfügbar über das Publikationsportal des Forschungszentrums Jülich (JuSER)
unter www.fz-juelich.de/zb/openaccess.

Acknowledgments

I would like to express my sincere gratitude to my initial supervisor, Eva Kröner, for introducing me to the topic of this thesis and for providing many inspiring ideas during the early stages of my research, and to my current supervisor, Nicolas Brüggemann, for his mentorship and encouragement in guiding my research to its conclusion. This thesis is a result of the collaborative efforts and insights of both, for which I am truly grateful.

I would like to thank Hermann Jungkunst, whose expertise and feedback have been instrumental in advancing this research. I am also grateful to him for accepting the role of external reviewer for this thesis.

This work was made possible through the support and collaboration of many people, to whom I am deeply grateful.

I would like to express my heartfelt gratitude to all my colleagues and friends from the Geophysics group at the University of Landau and the Plant-Soil-Atmosphere Exchange Processes group at Forschungszentrum Jülich. You have all been such wonderful colleagues and friends, and I truly appreciate the support, fun moments, and collaboration we shared throughout this journey.

I would like to thank all my colleagues who contributed to the research presented in this thesis. Collaborating with you has been an enriching experience, and your insights, expertise, and dedication have significantly enhanced the quality of this work. Thank you for your partnership and for sharing your knowledge and ideas throughout this process.

I would like to thank all my office mates over the years for fostering such a welcoming and friendly atmosphere.

I would also like to express my gratitude to Andrea Carminati and all members of the POSE group at ETH Zurich for welcoming me during my research stay. The opportunity to collaborate with such a talented group of researchers was incredibly enriching, and I greatly appreciate the support, resources, and knowledge shared during my time there. A special thank you goes to Patrick Duddek and Pascal Benard

for assisting with CT imaging. Beyond the scientific work, I am especially thankful for the non-scientific activities that made my stay so enjoyable, including the opportunity to join the group retreat.

I would like to thank my dear friends Jonas and Patrick. From our early days studying together at university to doing our PhDs in the same research field, it has been an incredible journey. The regular meet-ups, discussions, and countless moments of support and laughter have been a constant source of motivation and joy. I feel truly fortunate to have shared this journey with you both.

I extend my heartfelt thanks to my family for their unconditional support throughout the entirety of this endeavor. I owe a very special thank you to my girlfriend, Lisa, whose love, patience, and constant encouragement have been my anchor during this journey. Her belief in me and her unwavering support, especially during challenging times, have been a source of immense strength and inspiration.

Lastly, I would like to extend my gratitude to anyone whose support or contributions I may have unintentionally overlooked. Each interaction, no matter how small, has played a role in shaping this journey, and I am truly grateful for the kindness, encouragement, and assistance I have received along the way.

This work has been supported by the Deutsche Forschungsgemeinschaft (DFG, German Research Foundation) under Germany's Excellence Strategy – EXC 2070 – 390732324.

Abstract

Gas exchange in the soil is determined by the size and connectivity of air-filled pores. Thereby, water saturation, soil compaction, and organic matter fraction are the main barriers for gas movement in soil. For optimal growth, life in soil requires a balance between water and oxygen content. However, fluctuations in moisture conditions challenge this balance. By exuding mucilage and extracellular polymeric substances (EPS), plants and bacteria can alter the physical properties of the soil in their vicinity. It is considered that by releasing these hydrogel-like substances, plants and bacteria increase their resilience against drought stress. However, we still lack knowledge on how these substances affect the soil gas diffusion. An improved understanding of the complex interactions between plants, bacteria, and soil, which have great implications for root water and nutrient uptake, and biogeochemical turnover and respiration processes in the soil, could provide valuable insights for optimizing crop performance and improving water and nutrient use efficiency.

The focus of this thesis was to investigate the effect of mucilage and EPS on soil gas diffusion, aiming to improve understanding of gas diffusion processes in in soil by explaining the geometric alterations of the pore space induced by mucilage and EPS. Laboratory measurements were conducted to determine soil gas diffusion coefficient (D_p) supported by advanced imaging techniques such as X-ray Computed Tomography (X-ray CT) and Environmental Scanning Electron Microscopy (ESEM) to quantify and visualize mucilage-induced alterations of the pore space and simulations to characterize the geometric distribution of mucilage within soil during the drying process.

Initially, a conceptual model was developed to describe alterations in the pore space geometry induced by mucilage under dry soil conditions. Laboratory measurements indicated that mucilage decreases the gas diffusion coefficient under dry conditions without affecting bulk density or porosity. Depending on its content in the soil, mucilage forms various structures within the pore space. The evolution of these structures was explained via pore scale modeling based on identifying the elastic strength of rhizodeposition during soil drying. Next, the influence of mucilage on soil gas diffusion at different water contents during a drying-rewetting cycle was investigated. In soils without mucilage, a hysteresis in the gas diffusion coefficient was observed. The extent of the hysteresis depended on particle size. Furthermore, X-ray CT imaging indicated a hysteresis in gas-phase connectivity for samples without mucilage. The effect diminished with increasing mucilage content. In addition, ESEM

imaging of sandy soil samples mixed with mucilage confirmed the formation of liquid structures in the pore space. However, these structures showed slightly different shapes in comparison to those in glass bead samples, likely due to the higher surface roughness of soil particles. Finally, diffusion measurements conducted on soil samples containing EPS demonstrated a similar effect of EPS and mucilage on gas diffusivity.

In conclusion, the findings of this thesis suggest that plants and bacteria balance oxygen availability and water content by releasing polymeric substances, even under fluctuating moisture conditions. Through these exudates, they employ similar strategies to engineer their surroundings, modifying the physical properties of their local environment in ways that enhance their survival and resilience.

Zusammenfassung

Der Gasaustausch im Boden wird durch die Größe und Vernetzung der luftgefüllten Poren bestimmt. Dabei stellen Wassersättigung, Bodenverdichtung und der Anteil an organischer Substanz die Hauptbarrieren für die Gasbewegung im Boden dar. Für optimales Wachstum erfordert das Leben im Boden ein Gleichgewicht zwischen Wasser- und Sauerstoffgehalt. Schwankungen der Feuchtigkeitsbedingungen stellen jedoch eine Herausforderung für dieses Gleichgewicht dar. Pflanzen und Bakterien können durch die Ausscheidung von Mucilage und extrazellulären polymeren Substanzen (EPS) die physikalischen Eigenschaften des Bodens in ihrer Umgebung beeinflussen. Es wird angenommen, dass diese hydrogelartigen Substanzen die Widerstandsfähigkeit von Pflanzen und Bakterien gegenüber Trockenstress erhöhen. Dennoch mangelt es an Kenntnissen darüber, wie diese Substanzen die Gasdiffusion im Boden beeinflussen. Ein besseres Verständnis der komplexen Wechselwirkungen zwischen Pflanzen, Bakterien und Boden, die weitreichende Implikationen für die Wasser- und Nährstoffaufnahme der Wurzeln sowie für biogeochemische Umsetzungen und Atmungsprozesse im Boden haben, könnte wertvolle Erkenntnisse für die Optimierung des Ernteertrags und die Verbesserung der Wasser- und Nährstoffnutzungseffizienz liefern.

Der Fokus dieser Dissertation lag auf der Untersuchung des Einflusses von Mucilage und EPS auf die Gasdiffusion im Boden. Ziel war es, das Verständnis der Gasdiffusionsprozesse im Boden zu vertiefen, indem die durch Mucilage und EPS induzierten geometrischen Veränderungen des Porenraums erklärt wurden. Zu diesem Zweck wurden Laboruntersuchungen durchgeführt, um den Boden-Gasdiffusionskoeffizienten (D_p) zu bestimmen. Diese Untersuchungen wurden durch fortschrittliche Bildgebungstechniken wie Röntgen-Computertomographie (X-ray CT) und Rasterelektronenmikroskopie (Environmental Scanning Electron Microscopy, kurz ESEM) ergänzt. Dabei wurden durch Mucilage hervorgerufene Veränderungen des Porenraums quantifiziert und visualisiert. Zudem wurden Simulationen durchgeführt, um die geometrische Verteilung von Mucilage im Boden während des Trocknungsprozesses zu charakterisieren.

Zunächst wurde ein konzeptionelles Modell entwickelt, um die Veränderungen der Porenraumgeometrie durch Mucilage unter trockenen Bodenbedingungen zu beschreiben. Labormessungen zeigten, dass Mucilage den Gasdiffusionskoeffizienten unter trockenen Bedingungen verringert, ohne die Schüttdichte oder Porosität zu beeinflussen. Je nach Mucilagegehalt im Boden bildet Mucilage unterschiedliche Strukturen im Porenraum aus. Die Entwicklung dieser Strukturen wurde durch Modellierungen

im Porenmaßstab erklärt, die auf der elastischen Festigkeit von Rhizodepositionen während der Trocknung des Bodens basieren.

Im nächsten Schritt wurde der Einfluss von Mucilage auf die Gasdiffusion im Boden bei unterschiedlichen Wassergehalten während eines Trocknungs-Wiederbefeuchtungszyklus untersucht. In Böden ohne Mucilage wurde eine Hysterese im Gasdiffusionskoeffizienten beobachtet, deren Ausmaß von der Partikelgröße abhing. Darüber hinaus zeigte die Röntgen-CT-Bildgebung eine Hysterese in der Gasphasenkonnektivität bei Proben ohne Mucilage. Dieser Effekt nahm mit zunehmendem Mucilagegehalt ab. Zusätzlich bestätigte die ESEM-Bildgebung von sandigen Bodenproben, die mit Mucilage gemischt waren, die Bildung von Flüssigkeitsstrukturen im Porenraum. Diese Strukturen wiesen jedoch im Vergleich zu Glasperlenproben leicht unterschiedliche Formen auf, was vermutlich auf die höhere Oberflächenrauheit der Bodenpartikel zurückzuführen ist. Schließlich zeigten Diffusionsmessungen an Bodenproben mit EPS einen ähnlichen Effekt von EPS und Mucilage auf die Gasdiffusivität.

Abschließend legen die Ergebnisse dieser Dissertation nahe, dass Pflanzen und Bakterien die Verfügbarkeit von Sauerstoff und Wassergehalt durch die Freisetzung polymerer Substanzen auch unter schwankenden Feuchtigkeitsbedingungen ausgleichen können. Durch diese Exsudate wenden sie ähnliche Strategien an, um ihre Umgebung zu gestalten und die physikalischen Eigenschaften des Bodens so zu verändern, dass ihr Überleben und ihre Widerstandsfähigkeit verbessert werden.

List of Publications

Parts of this thesis have been published in peer-reviewed journals:

1. Haupenthal, Adrian, Mathilde Brax, Jonas Bentz, Hermann F. Jungkunst, Klaus Schützenmeister, and Eva Kroener. 2021. "Plants control soil gas exchanges possibly via mucilage." Journal of Plant Nutrition and Soil Science 184 (3):320–328. DOI: 10.1002/jpln.202000496
   Chapter 2 is based on the published version.

2. Haupenthal, Adrian, Patrick Duddek, Pascal Benard, Mathilde Knott, Andrea Carminati, Hermann F. Jungkunst, Eva Kroener, and Nicolas Brüggemann. 2024. "A root mucilage analogue from chia seeds reduces soil gas diffusivity." European Journal of Soil Science 75 (5): e13576.
   DOI: 10.1111/ejss.13576
   Chapter 3 is based on the published version.

Contents

List of Figures

List of Tables

1. Introduction

1.1. Rationale

The world population is increasing, and with it, the demand for food. At the same time, climatic change leads to an increase in global temperature. Both will affect the availability of fresh water. In the future, water scarcity will be a major threat to food production (Gerten et al. 2011; Dinar, Tieu, and Huynh 2019). To address these challenges, an agricultural production that optimizes the use of limited resources is needed (Lynch and Brown 2012).

Considering soils as a main priority for food security, climate resilience, and biodiversity, physical and mechanical soil properties will play a key role (Scherer et al. 2020; FAO 2023; Tolk 2003). Therefore, a sound understanding of physical processes in soil can contribute to an agricultural system with increased crop performance and higher nutrient and water use efficiency. Plants are obligate aerobic organisms. Optimal plant growth requires the availability of water and nutrients and an adequate supply of O_2 in the soil. Maintaining a balance between water and O_2 contents that are favorable for optimal plant growth demands management strategies that are based on a profound understanding of soil aeration and soil respiration processes (Lazarovitch et al. 2018). After water and nutrient availability, these processes are the most important factors affecting soil fertility and plant growth (Ben-Noah and Friedman 2018).

The primary natural mechanism for gas movement in soil is the diffusion of air from the soil surface down through the soil profile and toward the plant roots, and conversely, the diffusion of CO_2 and other gases from the soil to the atmosphere (Jensen and Kirkham 1963). Within the soil, gas diffusion depends on the distribution and connectivity of air-filled pores. Thereby, water saturation and compaction are the main barriers for soil gas diffusion. The diffusivity of gas in water is 10^4 times lower than in air. The presence of water filling the pore space can create anaerobic conditions within several hours to several days, as the soil becomes rapidly oxygen-deprived due to the rapid consumption of the remaining oxygen before diffusion limitations set in

(Stępniewski et al. 2005). Drying and rewetting cycles lead to recurring fluctuations in soil moisture conditions. In order to counteract negative effects on growth conditions, plants modify the soil in their vicinity by releasing polymeric substances. Mucilage, a polymeric blend composed mainly of glucose and organic acids, and secreted at the root tip during growth, is one of these substances (Read and Gregory 1997; Naveed et al. 2017). As the roots grow into the soil, they create the rhizosphere, a thin layer of soil around the root actively modified by growth rate and exudation, and a hotspot for microbial activity (Gregory 2006; Hinsinger et al. 2009; Kuzyakov and Blagodatskaya 2015). In addition to plant roots, microorganisms are also capable of shaping their local environment in the soil. By producing extracellular polymeric substances (EPS), they form a biofilm to better withstand environmental stresses (Flemming and Wingender 2010). Both mucilage and EPS are known for improving the availability of water by forming a three-dimensional network in the soil (Carminati et al. 2010; Roberson and Firestone 1992). Yet, this network represents a further barrier to the diffusion of soil gases, which must be overcome before O_2 becomes available for plant roots. A complete (anoxia) or even partial (hypoxia) deficiency of O_2 can cause severe damage to the plant (Stępniewski et al. 2005). A lack of O_2 can lead to oxygen stress conditions in the roots, resulting in major reductions in crop yield (Drew 1997). The severity of damage caused by O_2 shortage varies among species and the stage of plant development, as well as the different biotic and abiotic conditions they are exposed to (Stępniewski et al. 2005).
Plants require oxygen to carry out their life-sustaining processes, including root growth and maintenance, as well as ion absorption and transport to the xylem (Amthor 2000; Lambers, Steingröver, and Smakman 1978). The energy they need for this is obtained by the plant through root respiration. Therefore, a proper understanding of soil aeration and root respiration, especially the influence of mucilage and EPS on soil gas diffusivity, can help to optimize the use of limited resources, irrigation techniques, and consequently crop performance.

1.2. State of the art

1.2.1. Soil aeration

The soil gas phase, similar to the atmosphere, consists mainly of nitrogen and oxygen, but also contains higher concentrations of carbon dioxide and variable amounts of

argon and water vapor depending on environmental conditions. However, autotrophic (roots) and heterotrophic (microbes, soil fauna) respiration processes lead to greater fluctuations in the soil gas composition, with the proportion of CO_2 being higher and O_2 lower than in the atmosphere (Russell and Appleyard 1915). Soil aeration is an important factor for plant root growth and consequently crop growth (Vermoesen, Ramon, and Van Cleemput 1991). Despite the fact that plants are one of the main atmospheric oxygen producers (Hocke 2023), their roots can still lack O_2 because the O_2 supply from the aerial parts of the plant to the roots is often insufficient (Scanlon, Nicot, and Massmann 2001) and the demand for O_2 in soil varies with climatic conditions and vegetation (Ben-Noah and Friedman 2018). Soil aeration processes occur mainly by diffusion (Jensen and Kirkham 1963). Thereby, the diffusion of oxygen is considered the major process of soil gas exchange (Armstrong 1980). The driving force for gas diffusion is the concentration gradient within the soil, e.g. caused by root O_2 consumption. Due to the low solubility of O_2 in water ($1.22 \times 10^{-3}\,\mathrm{mol\,L^{-1}}$, at 25 °C and 1 atm (Xing et al. 2014)), soil air content determines the storage of O_2. Hence, the gas diffusivity in soil depends highly on the geometry of the soil pore system, including air-filled porosity, pore tortuosity, and connectivity (Hamamoto et al. 2009). Thus, soil texture and compaction have a major impact on soil gas diffusion as they affect the size, connectivity, and tortuosity of the pores. Furthermore, water-filled pore space reduces soil air content and is seen as the main limiting factor for gas diffusion. Besides soil traits, land cover and management affect soil aeration. Although the destructive effects of tillage on soil structure are well known, it is still the most common practice for improving soil aeration (Ben-Noah and Friedman 2018).

1.2.2. Consequences of oxygen deficiency in the soil

Plants can suffer from a partial (hypoxia) and even complete (anoxia) oxygen deficiency. In both cases, there is an insufficient supply of O_2 from the soil to the roots. Water-filled pore space, paired with poor O_2 transportation mechanisms, are the main drivers (Ben-Noah and Friedman 2018; Stępniewski et al. 2005). The limitation of the available O_2 has a negative effect on plant growth and development. The common field crops maize, wheat, and barley are all sensitive to an oxygen deficiency stress, which can lead to an impaired growth and yield formation up to the death of the plants (Zahra et al. 2021).

Oxygen deficiency can have direct (physiological) and indirect (soil processes) effects on plants (Gliński and Stępniewski 1985). The main physiological effect is the limited

cellular respiration. Oxidative phosphorylation leads to the release of energy in the form of adenosine triphosphate (ATP). Under oxygen deficiency, plant cells are forced to switch from this aerobic respiration to anaerobic respiration. Thereby, the ATP generation is reduced (Stępniewski et al. 2005; Zahra et al. 2021). Furthermore, anaerobic respiration produces toxic by-products, like lactate and ethanol, that can accumulate in and around the root (Drew 1997; Rivoal and Hanson 1994). Negative effects associated with processes in the soil are mainly caused by flooding when water displaces the air in the pore space. The resulting anaerobic conditions impair redox processes and the pH value, which in turn affects the availability of nutrients for the plants (Stępniewski et al. 2005). As the diffusion of oxygen in water is 10,000 times lower than in air, and the solubility of oxygen in water is low, the O_2 supply via the water absorption of the roots is negligible.

1.2.3. Root respiration

Plants require oxygen to carry out their vital processes. O_2 provided by the above ground part of the plant is often insufficient for below ground processes, like root growth and maintenance. For this reason, plants respire O_2 directly through their roots from the soil, enabling them to meet the respiratory demands of these processes. Besides this, also microbial communities in the soil are in demand of O_2. In the rhizosphere, roots and microorganisms compete for the same O_2. Due to the lack of measurement techniques capable of isolating these processes, current definitions of root respiration include, in addition to root respiration itself, the respiration of mycorrhizal, microbial, and other decomposing organisms that feed on root exudates and dead root tissue (Wiant 1967). The respiration of roots varies among plant types and depends on soil and environmental conditions. Differences in root traits, soil physical properties and structure as well as temperature and precipitation can affect O_2 consumption rates. During the different seasons, the proportion of root respiration accounts for $< 10\%$ to $> 90\%$ of total soil respiration processes (Hanson et al. 2000). The consumption of O_2 by plant roots leads to concentration gradients that force the gas to diffuse from the soil surface to the root. But before the oxygen reaches the root, it has to pass through the rhizosphere. Root exudates, such as mucilage, alter the physical properties of the rhizosphere compared to the surrounding bulk soil. It is reported that mucilage has positive effects on drought tolerance, lubrication, and nutrient uptake (Carminati et al. 2010; Zarebanadkouki et al. 2019; York et al. 2016).

Alongside the positive effects, mucilage forms a further barrier for O_2 flux to the root. Ben-Noah and Friedman (2018) stated that the restrictions of the mucilage layer on the diffusivity depend on mucilage uniformity along the root, viscosity, and the extent of the layer perpendicular to the root. Thereby, they assume a continuous mucilage layer. Nevertheless, they mentioned the recently observed formation of liquid mucilage bridges between soil particles (Carminati et al. 2017), that will impact gas diffusivity. Upon drying, the form of these liquid structures depends on mucilage content and ranges from thin filaments at low contents to interconnected surfaces at high contents (Benard et al. 2019). These various structures may favor gas diffusion compared to a uniform mucilage layer.
A further obstacle to the O_2 flux in soil is microbial colonies. In order to better withstand environmental stresses, they form biofilms by releasing EPS into the soil (Flemming and Wingender 2010). The formation of the interconnected hydro-gel like network that defines the structure of the biofilm is controlled by the EPS. EPS facilitates the adhesion of microbes to soil surfaces, anchoring them while binding bacterial cells into communities and forming aggregates (Petrova et al. 2021; Roberson and Firestone 1992). Like mucilage, the biofilm spans throughout the pore space and forms various structures between soil particles depending on EPS content (Benard et al. 2019). Both the mucilage and the EPS matrix are expected to reduce gas diffusivity in the soil. Yet, the impact of the formation of these structures on gas diffusivity remains unclear.

1.2.4. Mucilage and extracellular polymeric substances

An important process during plant growth is rhizodeposition, the release of organic compounds by the roots (Lynch and Whipps 1990). Besides others, mucilage is excreted at the root tip. It is a biopolymer that consists mainly of polysaccharides and small amounts of proteins, minerals, and lipids (Read et al. 2003; Naveed et al. 2017; Read and Gregory 1997; Nazari 2021). Mucilage behaves differently depending on its hydration status. On the one hand, when wet, it is very hydrophilic and able to absorb and hold large amounts of water (McCully and Boyer 1997; Nazari 2021). It is therefore categorized as a hydrogel by definition. On the other hand, mucilage becomes hydrophobic when dry. Even after contact with water, it remains in this state for some time and delays the rewetting of the rhizosphere (Carminati et al. 2010; Moradi et al. 2012). Besides root mucilage, mucilage extracted from seeds, mostly chia and flax seeds, is often used as an analogue because of their relatively high production

of mucilage (Rahim et al. 2024; Kroener et al. 2018; Benard et al. 2019). The physico-chemical properties of mucilage vary among plant species (Naveed et al. 2017). Nevertheless, root and seed mucilage have similar fundamental characteristics. Both increase the viscosity of the soil's liquid phase (Naveed et al. 2017; Read and Gregory 1997), decrease the surface tension at the interface between the liquid and the gas phase (Read and Gregory 1997; Naveed et al. 2019), reduce wettability by increasing contact angles at the solid-liquid interface (Zickenrott et al. 2016; Ahmed et al. 2016), and can absorb large amounts of water (Muñoz et al. 2012). When released into soil, mucilage can have different effects. Mucilage with low surface tension acts like a surfactant and exerts high swelling forces on soil particles, leading to a dispersion of the initial state, while mucilage with high viscoelastic properties acts like a glue binding particles together and increases stability (Naveed et al. 2017).
Alongside organic substances released by plant roots, a wide range of bacteria release extracellular polymeric substances. Thereby, the EPS acts as a structural component of the microbial biofilm (Flemming and Wingender 2001; Petrova et al. 2021; Roberson and Firestone 1992). EPS consist mainly of polysaccharides and fractions of proteins, lipids, and DNA (Redmile-Gordon et al. 2014; Costa, Raaijmakers, and Kuramae 2018; Or et al. 2007). Similar to mucilage, these biopolymers form a hydrate gel that helps to better withstand environmental stresses (Flemming and Wingender 2010). Furthermore, similar interconnected structures between soil particles could be observed (Zheng et al. 2018). There is a vast quantity of microorganisms that are able to form a biofilm, each producing various EPS (Sutherland 2001). Despite the enormous variety, EPS generally increases the viscosity of the liquid phase of soils (Körstgens et al. 2001; Stoodley et al. 2002; Wloka et al. 2004; Shaw et al. 2004; Lieleg et al. 2011), decreases surface tension at the interface of the gas and liquid phase (Raaijmakers et al. 2010), and can absorb large amounts of water (Roberson and Firestone 1992; Flemming et al. 2016).

A comparison between mucilage and EPS shows that they exhibit similar characteristics. Intrinsic properties and the effects on soil hydraulics of EPS, root, and seed mucilage were summarized by Benard et al. (2019) (Table 1.1). They are both biopolymers, capable of absorbing large amounts of water (Muñoz et al. 2012; McCully and Boyer 1997; Read, Gregory, and Bell 1999; Roberson and Firestone 1992; Flemming et al. 2016). They increase the viscosity of the soil solution (Naveed et al. 2017; Stoodley et al. 2002; Wloka et al. 2004) and reduce surface tension at the gas-liquid interface (Read and Gregory 1997; Raaijmakers et al. 2010). The similarities are also

reflected in their influence on hydraulic properties.

Table 1.1.: Physical properties of EPS and mucilage and their effects in soil (Table adapted from Benard et al. (2019)).

		Bacterial EPS	Root mucilage	Seed mucilage
Intrinsic properties	**Increased viscosity / Viscoelasticity**	Körstgens et al. 2001; Stoodley et al. 2002; Wloka et al. 2004; Shaw et al. 2004; Lieleg et al. 2011	Read and Gregory 1997; Naveed et al. 2019	Naveed et al. 2017
	Decreased surface tension	Raaijmakers et al. 2010 and references included	Read and Gregory 1997; Read et al. 2003	Naveed et al. 2019
	Absorption of water	Roberson and Firestone 1992; Flemming et al. 2016	McCully and Boyer 1997; Read, Gregory, and Bell 1999	Segura-Campos et al. 2014; Muñoz et al. 2012
	Reduced wettability	-	Ahmed et al. 2016; Zickenrott et al. 2016	Benard et al. 2017
Effect on soil hydraulics	**Increased soil water retention**	Roberson and Firestone 1992; Chenu 1993; Rosenzweig, Shavit, and Furman 2012; Volk et al. 2016	Benard et al. 2019	Kroener et al. 2018; Benard et al. 2019
	Slowed down evaporation from soil	Chenu 1993; Flemming 2011; Deng et al. 2015; Zheng et al. 2018; Adessi et al. 2018	-	Benard et al. 2019
	Increased relative hydraulic conductivity*	Volk et al. 2016; Zheng et al. 2018	-	Benard et al. 2019
	Induced soil water repellency	-	Ahmed et al. 2016; Carminati et al. 2010; Moradi et al. 2012	Benard et al. 2017; Benard, Zarebanadkouki, and Carminati 2018

*The relative hydraulic conductivity is defined as the hydraulic conductivity divided by the saturated hydraulic conductivity. This means changes in hydraulic conductivity during drying of soils are eased.

Due to the presence of mucilage, the physical properties of the rhizosphere differ from those of the surrounding bulk soil (Young 1995; Carminati et al. 2010; Benard et al. 2019; Zarebanadkouki, Ahmed, and Carminati 2016; Kroener et al. 2014; Hallett, Gordon, and Bengough 2003). Carminati et al. (2010) observed a higher water content during drying and a reduced wettability immediately after rewetting of the rhizosphere of lupins compared to the surrounding bulk soil. Moradi et al. (2012) confirmed these observations by measuring higher contact angles of water in the rhizosphere during

drying than in the bulk soil. A reduced wettability was also observed in the rhizosphere of maize (Ahmed et al. 2016) and for mucilage derived from chia seeds (Benard et al. 2017). Zickenrott et al. (2016) observed higher contact angles for soils mixed with mucilage and reported that the extent of the effect varies between mucilage origin and quantity. Further studies reported an increased soil water retention and a reduced saturated soil hydraulic conductivity due to presence of mucilage (Zarebanadkouki, Ahmed, and Carminati 2016; Kroener et al. 2018; Benard et al. 2019). In addition, Kroener et al. (2018) showed that the effect highly depends on the particle size distribution of the soil. Furthermore, mucilage promotes the transport of nutrients in drying soil (Zarebanadkouki et al. 2019). Besides the physical properties, studies reported that mucilage promotes aggregation and stabilizes the soil structure in the rhizosphere (Morel et al. 1991; Czarnes et al. 2000).
Carminati et al. (2017) reported the observation of liquid bridges between soil particles during drying in the presence of mucilage (Figure 1.1, left). The mucilage bridges persist longer than pure water. The authors linked the breakup of these liquid filaments to the interplay of surface tension, inertial forces, and viscosity. This correlation is expressed by the Ohnesorge number Oh (Ohnesorge 1936):

$$Oh = \frac{\mu}{\sqrt{\rho \sigma r}} \tag{1.1}$$

where μ is viscosity, ρ is density, σ is surface tension, and r is a characteristic length corresponding to the radius of the filament. For water, surface tension is the dominating force, and viscosity is low, resulting in an Ohnesorge number « 1 and consequently a faster breakage of the liquid bridge. When mucilage is added, the viscosity increases, and surface tension decreases (Table 1.1), resulting in an increase of Oh. Castrejón-Pita et al. (2012) showed that for $Oh > 1$ filaments do not break up into droplets when falling in air. For this reason, mucilage deposition around the root cannot be considered a uniform layer. Mucilage forms an interconnected network in the pore space during drying that increases stability and has a major effect on soil physical properties (Table 1.1).
In addition to their similarity in terms of intrinsic properties, the effect of EPS on soil physical properties shows a striking similarity to those of mucilage. Microscopic imaging revealed EPS structures between soil particles during drying (Figure 1.1, right). The resulting network can draw particles together and clog smaller pores, and consequently modify the soil pore size distribution (Zheng et al. 2018). A soil enriched with EPS showed an increase in soil water retention (Chenu 1993; Zheng et al. 2018;

Adessi et al. 2018; Volk et al. 2016), a slowed down evaporation (Benard et al. 2023; Zheng et al. 2018), and a decrease in soil hydraulic conductivity (Volk et al. 2016; Zheng et al. 2018).

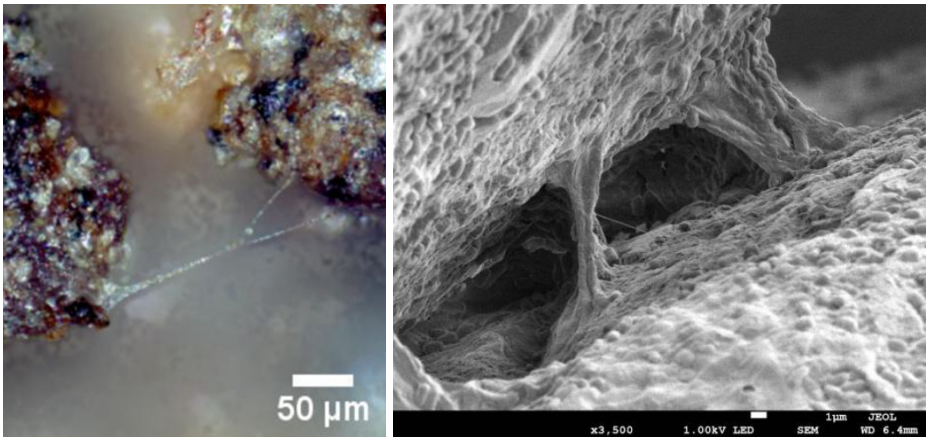

Figure 1.1.: Mucilage (*Slavia hispanica*) structures (left, Benard et al. (2019)) and EPS (*Bacillus subtilus*) structures (right, Zheng et al. (2018)) in sand.

All in all, the physical properties of the rhizosphere differ from them of the surrounding bulk soil, due to the presence of mucilage. At the same time, microbial communities affect the soil physical properties by releasing EPS. Both form interconnected structures between soil particles that span like a network throughout the pore space that maintain the connectivity of the liquid phase upon drying. Yet, there have been many studies on the effect of mucilage and EPS on soil hydraulic properties. Nevertheless, optimal plant growth needs both water and O_2 availability (Lazarovitch et al. 2018) and we still lack knowledge of how the filamentous mucilage and EPS structures affects the soil gas diffusion. The assumption of a uniform gel layer in current models highlights the necessity to elucidate the mechanisms involved on a pore-scale level.

1.2.5. Soil gas diffusion models

In a dry, porous medium, the gas diffusion coefficient D_p ($cm^2\,s^{-1}$) strongly depends on physical properties. In soil, particle size distribution and bulk density affect the pore structure, determining air-filled porosity ϵ as well as pore connectivity and tortuosity (Hamamoto et al. 2009). In coarse soils, pores are wider and less tortuous than in fine soils, resulting in higher diffusion coefficients (Thorbjørn et al. 2008).

Commonly, soil gas diffusivity is expressed as the relative diffusivity D_p/D_0, where D_0 is the diffusion coefficient of the respective gas in air at the same temperature and pressure. This normalisation means that soil gas diffusivity depends only on the properties of the air-filled pores rather than on gas properties (Allaire et al. 2008). There are several models predicting D_p/D_0. The most common models are listed in Table 1.2. The models of Buckingham (B) (1904), Penman (P) (1940), Marshall (M) (1959), Millington and Quirk (MQ) (1961) and Troeh et al. (Tr) (1982) are described as power-law functions of the soil-air content (ϵ) and serve as the foundation for models developed later: PMQ (Penman-Millington-Quirk), WLR (Water-Induced Linear Reduction), TPM (Three-Porosity Model) and SWLR (Structured Water-Induced Linear Reduction) by Moldrup et al. (1997; 2000; 2004; 2013), SAPHIR (Soil Air Phase Individual Resistances) by Thorbjørn et al. (2008) and OMF (Organic Matter Fraction) by Hamamoto et al. (2012). In general, they are a function of soil-air content ϵ and total porosity Φ and can be written as

$$\frac{D_p}{D_0} = \epsilon^X \left(\frac{\epsilon}{\Phi}\right)^\delta, \tag{1.2}$$

where δ and X are model parameters and refer to pore size, connectivity and tortuosity.

The first models developed (B, P, M) are popular for their simplicity, as they only depend on air-filled and total porosity. Advanced models (PMQ, WLR, TPM, SAPHIR) started to include parameters representing pore properties as well as a water induced reduction of soil air content and increased tortuosity. Moldrup et al. (2013) stated that models for predicting D_p/D_0 have either been developed theoretically or fitted to experimental data and that they were selected based on available input parameters rather than the actual soil conditions (repacked or undisturbed), resulting in potential prediction errors. Therefore, they developed the SWLR model and introduced a porous-media complexity factor (C_m) to cover both soil conditions. They have shown that for dry soil conditions ($\epsilon = \Phi$) $C_m = 1$ provides a good prediction of gas diffusivity. Comparison with literature data for gas diffusivity in dry porous media had shown that $C_m = 3$ represents the lower limit of D_p/D_0 models and gives a good description of pore networks with high tortuosity, like clay soils. In their study on the influence of organic matter on soil gas diffusion, Hamamoto et al. (2012) considered a percolation threshold ϵ_{th}, at which the gas-phase within pores is disconnected and gas diffusion is limited by the diffusion through the liquid phase - in water this is approximately 10^4 times lower than in air. Based on experimental data, they proposed an estimation of

Table 1.2.: Soil gas diffusivity models for effective diffusivity (D_p) depending on air-filled porosity (ϵ) (Table modified from (Ben-Noah and Friedman 2018)).

Model	$\boldsymbol{D_p/D_0}$*	**Notation**
Buckingham 1904	ϵ^2	B
Penman 1940	0.66ϵ	P
Marshall 1959	$\epsilon^{1.5}$	M
Millington and Quirk 1961	ϵ^X/Φ^δ	MQ
Troeh, Jabro, and Kirkham 1982	$[(\epsilon-\delta)/(1-\delta)]^X$	Tr
Moldrup et al. 1997	$0.66\Phi(\epsilon/\Phi)^{(12-X)/3}$	PMQ
Moldrup et al. 2000	$\epsilon^X(\epsilon/\Phi)$	WLR
Moldrup et al. 2004	$\Phi^2(\epsilon/\Phi)^X$	TPM
Thorbjørn et al. 2008	$\epsilon^{1+X+\delta\Phi}$	SAPHIR
Hamamoto et al. 2012	$(\epsilon-\epsilon_{th})^X$	OMF
Moldrup et al. 2013	$\epsilon^{[1+C_m\Phi]}(\epsilon/\Phi)$	SWLR

* D_0, diffusivity in air; Φ, soil porosity; ϵ_{th}, percolation threshold; C_m, porous media complexity factor; δ and X, fitting parameters.

the air-filled porosity threshold (ϵ_{th}) depending on the organic matter fraction (OMF):

$$\epsilon_{th} = 0.01\, exp(2.5\, OMF). \tag{1.3}$$

Consequently, the addition of organic matter results in a reduction of air-filled porosity. Since dried mucilage and EPS structures between soil particles are expected to be relatively thin (Figure 1.1), they occupy only a small fraction of the pore space and, as a result, have a minimal effect on air-filled porosity.
In conclusion, no model currently exists that effectively captures geometric alterations of the pore space induced by mucilage or EPS on soil gas diffusion. One of the main reasons for this seems to be the lack of experimental data.

1.2.6. Laboratory soil gas diffusion measurements

The key factor in studying soil gas diffusion is accurately determining the diffusion coefficient D_p ($m^2\,s^{-1}$). In their review on gas-phase diffusivity in the vadose zone,

Werner et al. (2004) compared data from in situ measurements with laboratory measurements. They came to the conclusion that both are equivalent approaches for the determination of D_p. However, data was only available from three studies. Yet, the focus of this thesis is on gas diffusion processes in the rhizosphere. Current methods have struggled to provide accurate estimates of in situ rhizodeposition, and the close relationship between root respiration, root exudation, and rhizo-microbial respiration has made it challenging to study these processes individually in natural soils (Chen et al. 2014). Soil type and structure, water content, nutrient status, microbial populations, temperature, etc., are all affecting mucilage content as well as gas diffusion processes (Chen et al. 2014; Fujikawa and Miyazaki 2005; Hamamoto et al. 2009). Even under laboratory conditions, quantification of the effects of mucilage and EPS on soil gas diffusion in natural soils remains challenging. To exclude the effect of mucilage or EPS degradation, samples need to be sterilized. Gamma irradiation and autoclaving are popular methods for soil sterilization. Nevertheless, the first is very expensive, while the latter does not ensure a complete elimination of microbial activity. Furthermore, a biologically, chemically, and physically non-reactive gas is needed to avoid intrinsic respiration. Additionally, even if samples are collected at the same site, they may vary in their physical properties. For these reasons, a laboratory study using artificial soils is the first step to quantify the effects of mucilage and EPS on soil gas diffusion.

The laboratory method to determine D_p is based on the work by Currie (1960) and follows the description of Rolston and Moldrup (2018).

The starting point for the calculation of D_p is Fick's first law. In order to be able to apply Fick's law, one of the following requirements must be met (Rolston and Moldrup 2018):

1. Diffusion of a trace gas in a binary mixture.
2. Diffusion of two gases in a closed system.
3. A three-component system, where two gases have similar diffusion coefficients and the third gas exists in trace amounts.

Assuming that one of the conditions is met and that there is a homogeneous initial distribution of the gas in the soil, diffusion is only driven by the concentration gradient along one axis, from one open end of the soil sample to the other. Thus, Fick's law can be reduced to one dimension. Additionally, if the soil is uniform with respect to the diffusion coefficient, Fick's law applies as follows

$$J = -D_p \frac{\partial C_g}{\partial x} \tag{1.4}$$

where J is the diffusion flux, the amount of gas diffusing (g gas) per cross-sectional area of the soil (m^2 soil) per unit time (s), D_p the soil gas diffusion coefficient (m^3 soil air m^{-1} soil s^{-1}), C_g the concentration in the gaseous phase (g gas m^{-3} soil air) and x the is the distance (m soil).
The basic idea of Currie's method is to establish a concentration gradient from one end of the soil core to the other. Therefore, the initial gas concentration C_0 is set at the one end of the soil core and the concentration at the other end of the soil core C_s is kept constant. A selection of possible laboratory setups to determine D_p were summarized by Allaire et al. (2008) (Figure 1.2).

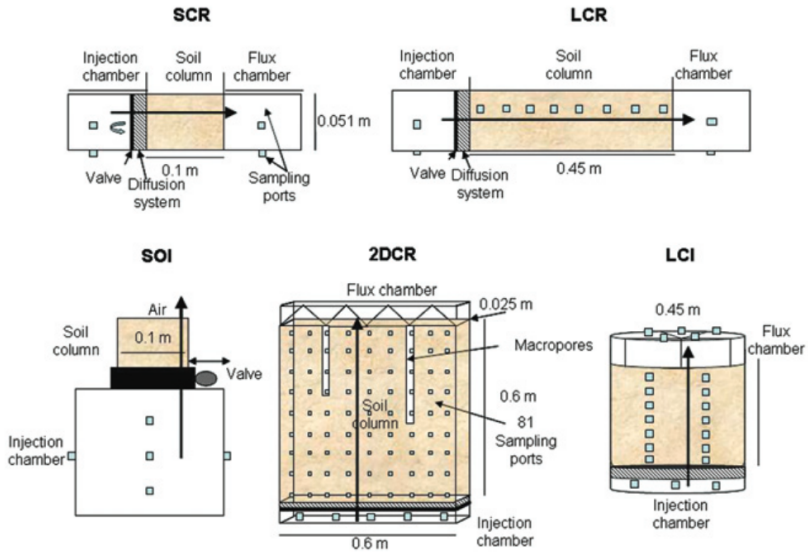

SCR: Small repacked column in a closed system; LCR: Long repacked column in a closed system; SOI/SOR: Small intact or repacked columns in an open system; 2DCR: Large 2D repacked column with macropores in a closed system; LCI: Large monoliths in a closed system.

Figure 1.2.: Selection of laboratory experimental setups to determine gas diffusion coefficient D_p (Adapted from Allaire et al. 2008).

The experimental setup used in this thesis is based on an open system approach (SOI, Figure 1.2). The initial concentration C_0 is set within the diffusion chamber.

The surrounding concentration (C_s) at the open end of the soil core remains constant. The initial concentration inside the soil core is, due to the open system setup, the same as the surrounding concentration. The gas of interest diffuses through the soil either into the diffusion chamber or out of it, depending on the direction of the concentration gradient (Figure 1.3). The rate of change of the concentration in the chamber over time is related to the soil gas diffusion coefficient.

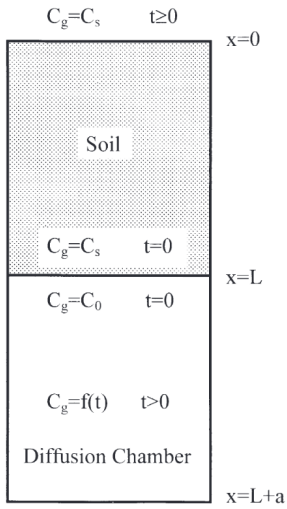

Figure 1.3.: Initial and boundary conditions for measuring soil gas diffusion coefficient (adapted from Rolsten (1986)).

Assuming that there is no intrinsic respiration, the gas that diffuses into the soil diffuses out of the soil, and the continuity equation can be applied. In free air, the continuity equation is given by

$$\nabla J + \frac{\partial C_g}{\partial t} = 0 \tag{1.5}$$

In a porous medium, such as soil, the available volume for the gas to diffuse through is limited to the air-filled porosity (ϵ). Assuming the porosity is uniform in space and time, equation (1.5) becomes:

$$\frac{\nabla J}{\epsilon} + \frac{\partial C_g}{\partial t} = 0 \tag{1.6}$$

Substituting equation 1.4 (Fick's law) in equation 1.6 (continuity equation) results in a second-order partial differential equation

$$\frac{\nabla\left(-D_p\frac{\partial C_g}{\partial x}\right)}{\epsilon}+\frac{\partial C_g}{\partial t}=0 \tag{1.7}$$

respectively

$$\frac{D_p}{\epsilon}\frac{\partial^2 C_g}{\partial x^2}=\frac{\partial C_g}{\partial t} \tag{1.8}$$

A solution to an analogue problem (thermal diffusivity in heat transfer) is given by Carslaw and Jaeger (1959, p.128) and applied to gas diffusion through a porous medium by Currie (1960). Currie's solution assumes that $C_s = 0$. With the given initial and boundary conditions (Figure 1.3), the solution of Equation (1.8) for the relative concentration in the chamber C_r is

$$C_r=\frac{C_g-C_s}{C_0-C_s}=\sum_{n=1}^{\infty}\frac{2h}{L(\alpha_n^2+h^2)+h}\exp\left(\frac{-D_p\alpha_n^2}{\epsilon}t\right) \tag{1.9}$$

where C_g is the concentration inside the chamber; C_s is the concentration in the atmosphere; C_0 is the initial concentration inside the chamber ($t = 0$); $h = \epsilon/(a\epsilon_c)$; $a = V/A$ the length of the chamber or the volume of the chamber V per area A of soil and $\epsilon_c = 1$ the air content of the chamber; L the height of the soil sample; and α_n, with $n = 1, 2, ...$, are the positive roots of $(\alpha L)tan(\alpha L) = hL$ (Table A.1). The roots are all real if $hL > 0$. The sum in Equation (1.9) has the following simplified representation

$$\sum_{n=1}^{\infty}a\frac{1}{\alpha_n^2}\exp(-b\alpha_n^2 t) \tag{1.10}$$

where $a > 0$ and $b > 0$ are constant for L, h, D_p and $\epsilon > 0$. For sufficiently large t, the first part of the term and the exponential function converge to 0, with α_n increasing for increasing n. Thus, the addends for $n \geq 2$ are negligible with respect to the first addend ($n = 1$), and Equation (1.9) reduces to

$$C_r(t)=\frac{C_g-C_s}{C_0-C_s}=\frac{2h}{L(\alpha_1^2+h^2)+h}\exp\left(\frac{-D_p\alpha_1^2}{\epsilon}t\right) \tag{1.11}$$

Applying a logarithm on both sides of Equation (1.11) results in

$$\log(C_r(t))=\log\left(\frac{2h}{L(\alpha_1^2+h^2)+h}\exp\left(\frac{-D_p\alpha_1^2}{\epsilon}t\right)\right) \tag{1.12}$$

Using the laws of logarithms, Equation (1.12) can be written as

$$\log(C_r(t)) = \log\left(\frac{2h}{L(\alpha_1^2 + h^2) + h}\right) + \frac{-D_p\alpha_1^2}{\epsilon}t \tag{1.13}$$

The right side of the equation now has the shape of a linear equation. Thus, for sufficiently large values of t, the plot of $\log(C_r)$ against t becomes linear with a slope of $-D_p\alpha_1^2/\epsilon$.

Core ideas for the diffusion apparatus were adapted from Rolston and Moldrup (2018). The final setup (Figure 1.4) consists of a desiccator (without the lid) functioning as the diffusion vessel and an acrylic plate, with an opening in the center for inserting the sample, placed on top of the desiccator and sealed airtight. O_2 was used as a tracer gas and measured with two contactless oxygen sensors (Pyroscience GmbH, Aachen, Germany). Using O_2 as a tracer had the benefit that it was contactless measurable, which reduced potential gas leaks in the setup. The setup was placed on a magnetic stirrer and a stir bar with attached flights inside the vessel. This arrangement ensured thorough mixing of the air inside the vessel during the measurement, resulting in a homogeneous O_2 distribution for accurate determination.

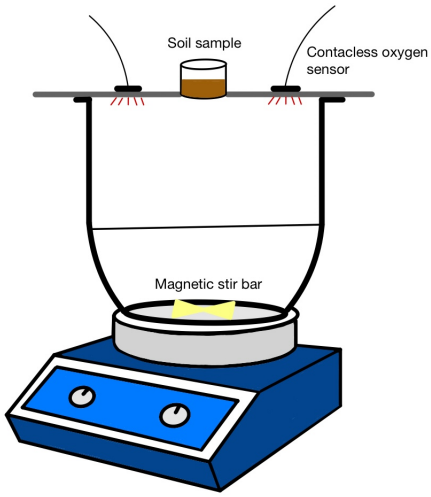

Figure 1.4.: Experimental setup for soil gas diffusion measurements based on a diffusion chamber method.

D_p is now determined as follows. First, samples are prepared, packed in cylindrical sample holders, and closed using parafilm (Amcor, Zurich, Switzerland). Then, the

diffusion vessel is flushed through the opening with N_2 until the O_2 concentration inside the diffusion chamber is close to 0. Now, the sample is placed on the opening, and the contact between holder and sample is sealed. Next, the magnetic stirrer is started. After a sufficient time, the air is well mixed, and the O_2 concentration becomes constant. This is the initial concentration C_0. To start the measurement, data logging is activated, and the parafilm is removed ($t = 0$). Figure 1.5 shows an example of the logging of O_2 concentration over time inside the chamber.

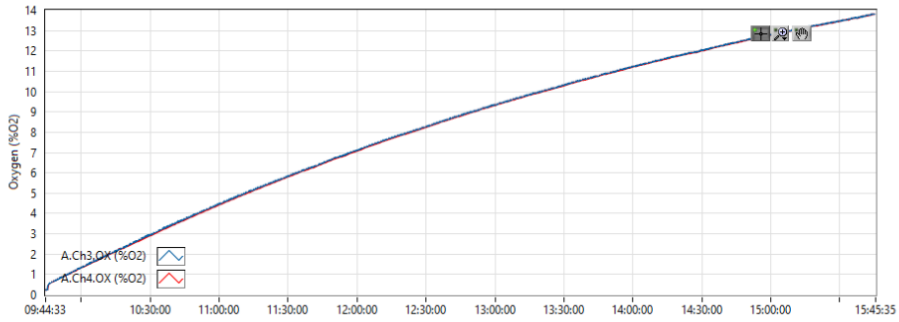

Figure 1.5.: Example data logging during a measurement.

Using O_2 as a tracer, N_2 to flush the diffusion chamber and atmospheric air, the third requirement described above is met and Fick's law can be applied to determine D_p. The diffusion coefficients of O_2 (0.231 $cm^2\,s^{-1}$) and N_2 (0.211 $cm^2\,s^{-1}$) in air are of the same order of magnitude (Wiegleb 2016), and flushing the diffusion chamber with 100 % N_2 results in similar concentration gradients for both gases. As air consists mainly of Nitrogen (78%), Oxygen (21%) and Argon (~1%) the concentration gradients of both, O_2 and N_2 are about 0.2. Thus, N_2 diffuses with the same velocity out of the chamber as O_2 diffuses into the chamber, and with only trace amounts of Ar in atmospheric air, the movement of gas is only triggered by diffusion and Fick's law can be applied.
Next, the data from Figure 1.5 can be used to plot $ln(C_r)$ against t (Figure 1.6), followed by linear regression. The slope (s) of the linear regression is given by

$$s = D_p \frac{\alpha_1^2}{\epsilon} \tag{1.14}$$

and

$$D_p = s\frac{\epsilon}{\alpha_1^2} \tag{1.15}$$

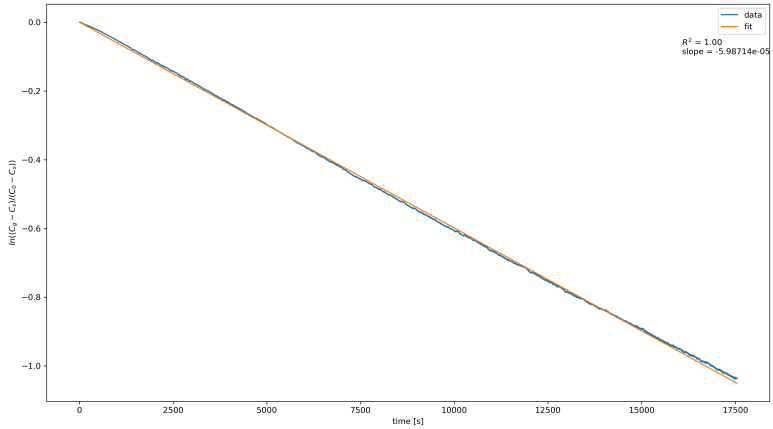

Figure 1.6.: A plot of $ln(C_r)$ against time t.

Now, D_p can be determined using Table A.1 to find the value for α_1. Finally, D_p is divided by D_0, resulting in the relative diffusion coefficient, which represents the diffusion independent of the gas used as a tracer.

There are potential errors associated with this method (Rolston and Moldrup 2018):

1. Drying of a wet soil core during measurements,
2. Convective flow,
3. Reaction of gas with the soil or chamber,
4. Diffusion of gas through chamber leaks,
5. Temperature fluctuations.

There are two possible ways to prevent the soil core from drying during the measurement. Either a water-saturated air stream is slowly passed over the sample opening, or the soil core is rewetted at certain intervals by drip irrigation. Convective flow is caused

by pressure gradients between the air in the chamber and the atmosphere. Therefore, strong air movement over the top of the sample should be avoided. Consumption or production of the tracer gas within the soil leads to an error of D_p. Especially for long measuring times, e.g. wet samples, this error can become substantial. A proper sealing of the experimental setup is needed to ensure that the gas only flows through the soil sample. Diffusion through leaks results in errors of D_p. Diffusion is sensitive to temperature fluctuations. Therefore, temperature should be monitored and kept as constant as possible during each measurement.

1.3. Outline

The primary aim of this thesis was to investigate how mucilage and EPS influence soil physical properties and how these alterations affect soil gas diffusion. More concretely, the aim was to relate the patterns of mucilage and EPS during drying to gas exchange processes in the rhizosphere. The specific questions addressed in this thesis were:

1. How do dried mucilage patterns affect soil gas diffusion and can the spatial distribution and dynamics of mucilage be described on a pore scale?

2. Does the effect of mucilage on gas diffusion in the soil depend on the particle size?

3. Does the hysteresis in soil water content during a drying-rewetting cycle affect soil gas diffusion and how does mucilage influence this effect?

4. Are the similarities between mucilage and EPS also represented in their effect on soil gas diffusion?

To achieve these goals, laboratory diffusion experiments were combined with advanced imaging techniques and numerical simulations.
In Chapter 2, a conceptual model is presented to describe gas diffusion in a dry rhizosphere. To validate the concept, gas diffusion experiments were performed on dry soil-mucilage samples. Additionally, Environmental Scanning Electron Microscopy was used to take images of dried mucilage structures in the pore space of glass beads. In a final step, simulations were performed to characterize the geometric distribution of mucilage within soil during the drying process. The hypothesis was that mucilage forms a network during drying that disconnects the gas phase, reducing soil gas diffusion. The form of mucilage structures and consequently their effect on gas diffusivity depends

on mucilage content.
In Chapter 3, the concept from Chapter 2 was expanded to various particle sizes and water contents during a drying-rewetting cycle. The aim was to gain a better understanding of gas diffusion processes in the rhizosphere by explaining the geometric alterations of the soil pore space induced by mucilage. The hypothesis was that the effect of mucilage on soil gas diffusion depends on particle size and mucilage content. In coarse soils, a higher mucilage content would be required for structures to span across larger pores, while in very fine-textured soils a reduced effect can be expected due to the higher number of potential pore throats where mucilage is deposited during drying. In addition, different distributions of water in the pore space during drying and rewetting, resulting in a hysteresis of gas diffusion, and a diminishing effect with increasing mucilage content can be expected.
Finally, the effect of microbial-derived EPS on soil gas diffusion was investigated in Chapter 4. The hypothesis was that EPS affects the physical soil properties in the same way as mucilage due to the similarity of their basic traits. It was expected that the polymeric network formed by EPS would obstruct the movement of gas and reduce soil gas diffusivity. In addition, the effect of EPS on soil gas diffusion would depend on particle size and whether the soil is drying or rewetted, resulting in a hysteresis of gas diffusion. Finally, it was hypothesized that the effect would diminish in the presence of EPS.

2. Plants control soil gas exchanges possibly via mucilage

Based on: Haupenthal, Adrian, Mathilde Brax, Jonas Bentz, Hermann F. Jungkunst, Klaus Schützenmeister, and Eva Kroener. 2021. "Plants control soil gas exchanges possibly via mucilage." Journal of Plant Nutrition and Soil Science 184 (3):320–328. DOI: 10.1002/jpln.202000496

2.1. Introduction

The availability of life-sustaining resources in the Earth's Critical Zone (National Research Council 2000) highly dependent on solute and energy transportation. Gas and water transport in air and water is quite well calculable. Gas and water transport in and out of soils is, due to the heterogeneous nature of soils, more complex. The connectivity of the pore system determines liquid and gaseous flows in the porous media soil. The basic route network for matter flow through soils is set by the solid mineral phase like soil texture. However, the tortuosity of the pore connectivity through soils is highly influenced by organic matter locking pores. Furthermore, the highly dynamic and variable liquid phase is locking pores for the gaseous flow, as gas diffusion is 10^4 times lower in water than in gas (Ferrell and Himmelblau 1967). Therefore, it remains very challenging to predict matter flow through soils like greenhouse gas emissions from soils to the atmosphere. Above all, soil is a living environment and therefore biology comes into play and the diversity of biological influences is still not yet fully understood. When growing in soil, roots create the rhizosphere. The rhizosphere is a small layer of soil particles around roots, where interactions between plants and soil take place and which is actively modified by plant root rhizodeposits and growth rate (Bais et al. 2006; Gregory 2006; Hinsinger et al. 2009). Depending on the root density, the rhizosphere frequently covers a dense layer at the interface of the soil to the atmosphere. Therefore, plants influence is decisive for all matter flow at the

interfaces soil–plant and soil–atmosphere. By releasing hydrogels, roots influence both the organic matter and the liquid phase of the soil and consequently pore tortuosity. One of the most prominent hydrogel root releases is mucilage, known to affect soil hydraulic properties (Carminati et al. 2010; Kroener et al. 2014; Kroener et al. 2018). In contact with water, it swells and is able to adsorb water up to 103 times its own weight depending on the type (Muñoz et al. 2012). During drying mucilage forms liquid bridges between soil particles, filling larger parts of the pore space (Albalasmeh and Ghezzehei 2014; Carminati et al. 2017; Benard, Zarebanadkouki, and Carminati 2018).

The movement of gas is triggered by concentration gradients that develop due to autotrophic (mainly plants) and heterotrophic (microbes) respiration in the rhizosphere between soil and atmosphere and by concentration gradients within the soil. Soil-gas diffusion is controlled by soil gas diffusion coefficient D_p which is mostly affected by the soil structure, air-filled porosity, bulk density, and pore connectivity and tortuosity (Fujikawa and Miyazaki 2005; Hamamoto et al. 2009). The main barriers for gas movement in soil is altered pore structure due to compaction, water saturation and organic matter fraction (Xu, Nieber, and Gupta 1992; Moldrup et al. 2000; Thorbjørn et al. 2008; Hamamoto et al. 2009, 2012).

The composition of soil gas is affected by atmospheric diffusion and respiration of roots and microorganisms (Fujikawa and Miyazaki 2005). During respiration oxygen is used by heterotrophic organisms producing carbon dioxide. Other gases like methane and nitrous oxide are produced and used as well. At high soil moisture there is a limited availability of oxygen in soil pore-space leading to hypoxia (Badri and Vivanco 2009). As a result of hypoxia respiration change from aerobic to anaerobic leading to an accumulation of ethanol, lactic acid and alanine at phytotoxic levels (Rivoal and Hanson 1994). It is reported that roots protect themselves from toxication by secreting exudates from their roots (Xia and Roberts 1994). Thus, the process of diffusion in soil close to the roots is a key aspect in the survival of plants.

Despite several studies on the effect of physical properties and organic matter on soil gas diffusion, it is still unknown how mucilage affects gas movement in soils. Benard et al. (2019) showed that during drying maize mucilage and extracellular polymeric substances (EPS) form filaments and twodimensional interconnected structures, which span across multiple pores. Due to a higher viscosity and a lower surface tension of mucilage and EPS compared to water, these structures will not break up easily. As a result, the formed network enhances water retention, keeps the liquid phase connected

during drying, and decreases vapour diffusivity and local drying rates. They expect that mucilage and EPS layers limit the diffusion of gases. However, we still lack both, measurements and models of the effect of rhizodeposits on gas diffusion in soil.
In this study, we examined the effect of mucilage on soil gas diffusion coefficient during drying. Our hypothesis is that during drying mucilage forms a network that disconnects the gas phase, reducing soil gas diffusion. We present experimental data and a conceptual model with pore scale simulations of simplified drying scenarios. For the experiments, we mixed a sandy soil with chia seed mucilage at various concentrations and given bulk density, dried the samples and measured gas diffusion coefficient.

2.2. Material and Methods

2.2.1. Theory and conceptual model

Mucilage and organic matter dependent gas diffusion models

Diffusion models to predict gas diffusivity depending on soil porosity, pore tortuosity and water content, as well as organic matter are presented in Chapter 1.2.5. When mucilage is added to the soil, we assume a blocking effect. However, we assume that, unlike organic matter, mucilage blocks diffusion pathways without affecting air-filled porosity. Oleghe et al. (2019) recognized that adding mucilage can result in an increase of soil water retention without bulk porosity being affected by chia seed mucilage and thus suggested that pores got clogged by mucilage. It is very straightforward to postulate that hydrogel is clogging pores, so the challenge now lies in conceptualizing the effects of soil gas exchanges when mucilage (hydrogel) is drying or has dried out. The addition of mucilage results in an increase of viscosity of the liquid phase which leads to a formation of mucilage bridges between soil particles during drying (Albalasmeh and Ghezzehei 2014; Benard, Zarebanadkouki, and Carminati 2018; Benard et al. 2019). At low concentrations of mucilage within soil (mass of dry mucilage per mass of dry soil) the bridges between particles are shaped like thin filaments. With higher concentrations the amount of mucilage per soil increases and instead of filaments, hollow structures or even interconnected surfaces of dry mucilage are formed which are spanning across the pore space (Fig. 2.1). Similar to a foil, these very thin layers break the connectivity of the gas phase and we expect that gas diffusion may get strongly reduced. Due to its low volumetric content, dry mucilage

does not affect total air-filled porosity in sandy soils significantly. We hypothesize that, in dry soils, mucilage increases the tortuosity of gas diffusion pathways until disconnecting the gas phase which results in a reduction of the gas diffusion coefficient (Fig. 2.1).

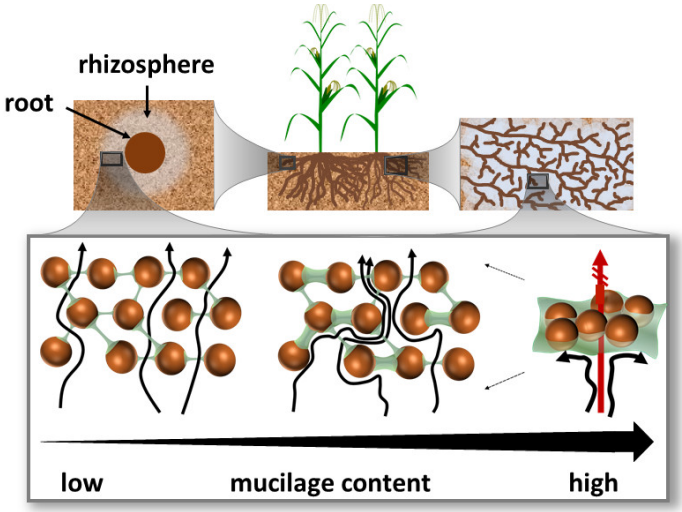

Figure 2.1.: Schematic of increasing mucilage content at constant dry soil condition for (left) the rhizosphere of a single root and (right) a soil with many roots coated with mucilage. Depending on mucilage concentration, liquid bridges form thin filaments (low), hollow structures or interconnected surfaces (high) between soil particles.

Since dry mucilage does not affect air-filled porosity significantly, models such as the OMF model (1.2) by Hamamoto et al. (2012) considering a reduction of air-filled porosity due to organic matter cannot serve as a suitable model to predict D_p in the rhizosphere. There is the possibility to adjust the complexity factor C_m of the model of Moldrup et al. (2013) to represent the complexity of the air-filled pore network. However, in Moldrup et al. (2013) C_m is supposed to be related to total porosity — a parameter that is, in our case, not significantly affected by mucilage.
The described models may serve as a first rough approximation to predict the influence of mucilage on soil gas diffusion. But, these models are developed for organic matter in general instead of mucilage. To develop more suitable models an understanding of underlying pore scale processes affecting gas phase connectivity is needed.

Pore scale model of mucilage distribution during drying

To simulate the effect of mucilage on gas phase connectivity, a model is required that describes pore scale spatial distribution and dynamics of mucilage. At low concentrations of mucilage, i.e., when there are large distances between polymers (Fig. 2.2a, left), mucilage behaves like a liquid, having a viscosity that increases with polymer concentration. Polymer chains start to build cross-links to create a network as mucilage dries out and the concentration of polymers increases (Fig. 2.2a, right).

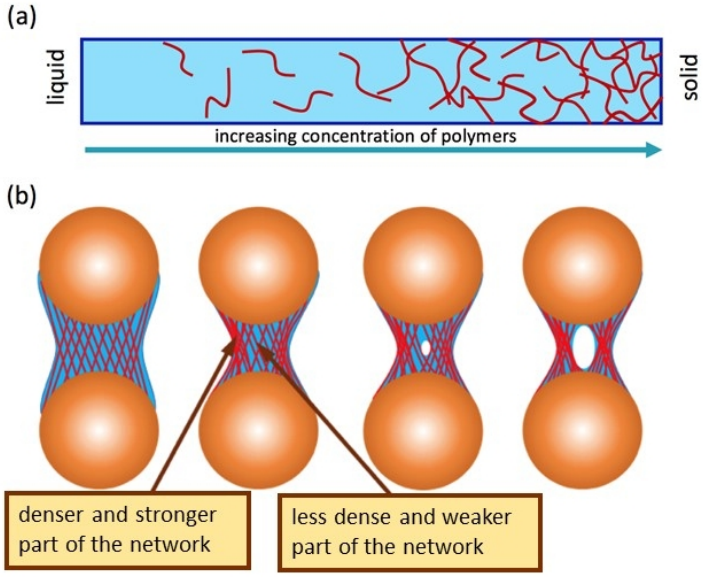

Figure 2.2.: Conceptual idea of mucilage drying: (a) transition from low to high concentrated mucilage (i.e., transition from high to low water content) corresponds to a transition from a liquid with large distances between polymers to a solid network where long chained polymers are connected via cross-links, (b) when mucilage is at high mucilage concentrations, during drying, its polymeric web shrinks, becomes denser and thus stronger at its outer parts and may break at its weakest parts in the centre forming a hollow structures.

Mucilage transforms from a liquid to a solid made of an elastic hydrogel that spans a three-dimensional solid web between the mineral soil particles. To properly simulate those drying processes at the pore scale, a description of the smooth transition from the rather liquid to the rather solid state is required. Here, we present a simplified case

study. Simulations of the two extremes, the liquid and the solid network, only, without a transition between the two states. Lattice–Boltzmann methods are a suitable tool to simulate the pore scale dynamics of liquids (Sukop and Or 2004; Tuller and Or 2004; Pot et al. 2015; Richefeu, Radjai, and Delenne 2016). To simulate dynamics of the highly concentrated, rather solid mucilage, we applied the discrete element method which is a common tool to describe deformation and rupture processes of solids (Munjiza, Owen, and Bicanic 1995; Bobet et al. 2009) and has also been used to simulate fracture of hydrogels (Kimber, Kazarian, and Štěpánek 2012; Yang et al. 2018). Using the description of highly concentrated mucilage as a network spanning across the pore space, one can explain the formation of hollow cylinders between particles (Fig. 2.2b). Upon drying the volume of water decreases, surface tension together with the attractive forces between polymers and water induce a tension on the network: it shrinks and as a result the density of polymers may locally increase near to the outer parts and strengthen the network there. Upon further tension the network may break at its weakest point which may be in the centre. Here, this concept is presented just in two dimensions. However, in the more complex three-dimensional pore space geometry this concept may not only describe the formation of hollow bridges between two particles but also the formation of connected surfaces of mucilage spanning across many pores (Fig. 2.1, right) and disconnecting the gas phase.

Setup of the simulations

For both simulations of the distribution of mucilage during drying (either as a liquid or as a polymeric network) we assume a slow drying process, i.e., the system is assumed to be in a quasi-steady state in which viscosity and momentum do not need to be considered. For the liquid case, we implemented the Shan–Chen type multiphase lattice Boltzmann model (Shan and Chen 1993) using the LBM simulation tool Yantra (Patel, Perko, and Jacques 2017). For each drying step, a certain water content is chosen and its equilibrium distribution is simulated assuming a contact angle of the soil surface close to 0°. The model is based on the D2Q9 method: this means for each cell of the regular 2D-lattice, interactions with its eight neighbouring cells and the cell itself are considered to calculate streaming and collision at this step. These steps are repeated until equilibrium can be assumed, i.e., changes in the liquid distribution are smaller than a certain threshold value. In each equilibrium state, the liquid–air interface adjusts such that its curvature is constant (compare Young–Laplace equation where interface curvature is related to surface tension and pressure difference). Upon

further drying, i.e., reduced water content, the negative curvature of the liquid phase becomes more and more negative.
In the highly concentrated case, mucilage is described as a polymeric network (Fig. 2.3) which consists of many nodes. These nodes are connected to their neighbouring nodes via springs of a certain stress-strain relation which represent the attractive forces. In our model, the stress-strain relation is represented by a simple linear relation between the elongation of the spring and the force F on the spring:

$$F(r) = -k \times (R_{equ} - r), \tag{2.1}$$

where k is a constant, and the elongation $(R_{equ} - r)$ is the difference between length of the spring R_{equ} in equilibrium and its current extension r. If a node gets close to the soil surface, it connects also to the soil surface via a spring, representing the attractive force towards the soil particle. During the drying process, each quasi-steady-state spatial distribution of the network is simulated stepwise: in each step, each node moves one step into the direction of the total force and proportional to the total force acting on it. If the tension on a spring gets larger than its breaking point, then the nodes get disconnected. Equilibrium is assumed when each node becomes stationary, i.e., the forces on all the springs connected to this node sum up to approximately zero.

The next quasi-steady state of the drying process, i.e., a reduced water content of the mucilage phase, is obtained by decreasing the equilibrium distance R_{equ} of the stress-strain relation of each spring. This way, the decreased equilibrium distance is related to the tension on the network induced by the reduced water content, i.e., a reduced pore volume available for polymers.

To sum up, important parameters that need to be defined for the simulation are: k, the critical tension at which a connection breaks, the distance between two nodes at which a new connection can form between both nodes, the maximum number of springs one node can connect with, and the density of network nodes which may be related to the concentration of mucilage. An extensive analysis of the effect of each of these parameters exceeds the purpose of this viewpoint paper, here we only want to present qualitative results describing spatial structures that are created by hydrogel dynamics. Our two-dimensional simulations serve as a proposition of possible modelling tools to describe the observed pore space distributions of mucilage. For a quantitative analysis of these complex pore space dynamics, further advanced three-dimensional models, a transition between the two cases (low and high concentration of mucilage in the liquid phase) and knowledge of the changes of physico-chemical properties of the specific

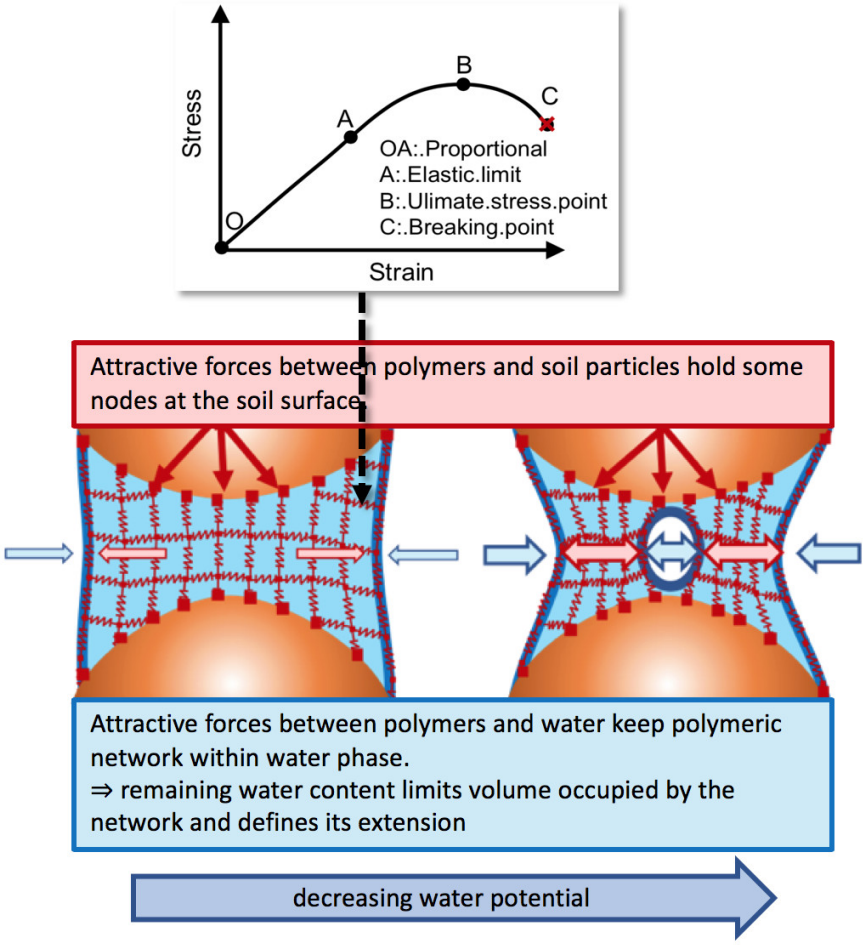

Figure 2.3.: Setup of the simulation of drying dynamics at high concentrations using the discrete element methods.

mucilage type during the drying process will be needed.

2.2.2. Mucilage collection

Mucilage was collected from chia seeds. Chia seed mucilage is easily available in large amounts and widely used as a model for plant mucilage. Its physical properties are similar to those of plant mucilage (McCully and Boyer 1997; Read and Gregory 1997; Naveed et al. 2017), but there are still differences, e.g., a relatively high content of polysaccharides and a higher viscosity of chia seeds compared to barley mucilage or maize mucilage which contain more organic acid (Naveed et al. 2017; Veelen et al. 2018). Mucilage was extracted from chia seeds according to the method of Kroener et al. (2018). The gel–water mixture was frozen and freeze-dried to obtain dry mucilage which was then pulverized.

2.2.3. Sample preparation

As an analogue of the rhizosphere, a soil–mucilage mixture was chosen to test the effect of mucilage on soil gas diffusion coefficient. Sand (soil) of particle sizes of 500–630 µm was mixed with chia mucilage to concentrations of 0, 0.1, 0.3 and 0.6 % (w/w dry mucilage/dry soil). Dry mucilage was diluted with water and kept in a closed container for 15 min to swell. We set the amount of water for the gel–water mixture so that the volumetric water content was equal to the porosity. In this way, porosity was not affected during drying for all samples. Soil was mixed with wet mucilage, packed and allowed to dry for 48 h at 20 °C ± 1 °C. After drying, gravimetric water content of the samples was <1 %. While the simulations describe the effect of mucilage on pore scale dynamics of the liquid phase during drying, the following experiments were performed on already dried samples.

2.2.4. Environmental Scanning Electron Microscopy

Glass beads (0.2 mm) were mixed with chia seed mucilage at various concentrations and dried in the oven at 30 °C for 24 h. ESEM images were taken with a FEI Quanta 250 ESEM (FEI Company Hillsboro, United States) under low vacuum with chamber pressures between 60 Pa and 80 Pa. A large field detector was used with an acceleration voltage between 12.5 kV and 15 kV.

2.2.5. Gas diffusion measurements

To examine the effect of mucilage on gas diffusion in a dried sandy soil and to determine the diffusion coefficient D_p, a diffusion chamber experiment as described in Chapter 1.2.6 was conducted (Fig. 1.4). D_p was measured as a function of mucilage concentration. For each concentration three replicates were prepared. Samples were repacked in 5.77 cm^3 soil cores, with a height of 0.6 cm, a cross section of 9.62 cm^2 and a weight of 10 g. Oxygen was used as a tracer gas with a gas diffusion coefficient in free air of $D_0 = 0.231\,cm^2\,s^{-1}$ (Wiegleb 2016). All measurements were performed at room temperature of 20 °C ± 1 °C.

2.3. Results

2.3.1. Gas diffusion measurements

Measurements of the diffusion coefficient D_p/D_0 for a dry sandy soil (500–630 µm) as a function of mucilage concentration show that with increasing mucilage concentration the relative diffusion coefficient D_p/D_0 decreases. Gas diffusion was reduced by about 50 % as can be seen in Fig. 2.4.
Throughout all measurements bulk density ($(1.737 \pm 0.002)\,g\,cm^{-3}$) and porosity ($(0.343 \pm 0.002)\,cm^3\,cm^{-3}$) were not affected. Dry weight of mucilage per sample ranged depending on concentration (0.1–0.6 % gravimetric concentrations) from 0.01 g to 0.06 g. Assuming a mucilage density of roughly $1\,g\,cm^{-3}$ leads to a volumetric mucilage fraction of 0.17 % to 1.04 %. Thus, the volume occupied by mucilage is ≤1.04 % of the volume of bulk soil and the effect of dry mucilage on air-filled porosity is negligible.

2.3.2. Environmental Scanning Electron Microscopy

The conceptual model (Fig. 2.1) is supported by images created using an environmental scanning electron microscope. Fig. 2.5 shows the formation of mucilage structures in glass beads after drying. At a concentration of 0.16 % thin mucilage filaments spanning across various pores are shown (Fig. 2.5a, d), at intermediate concentration of 0.25 % hollow cylinders emerge (Fig. 2.5b, e), and at high concentration of 0.49 % mucilage forms interconnected surfaces throughout the pore space (Fig. 2.5c, f).

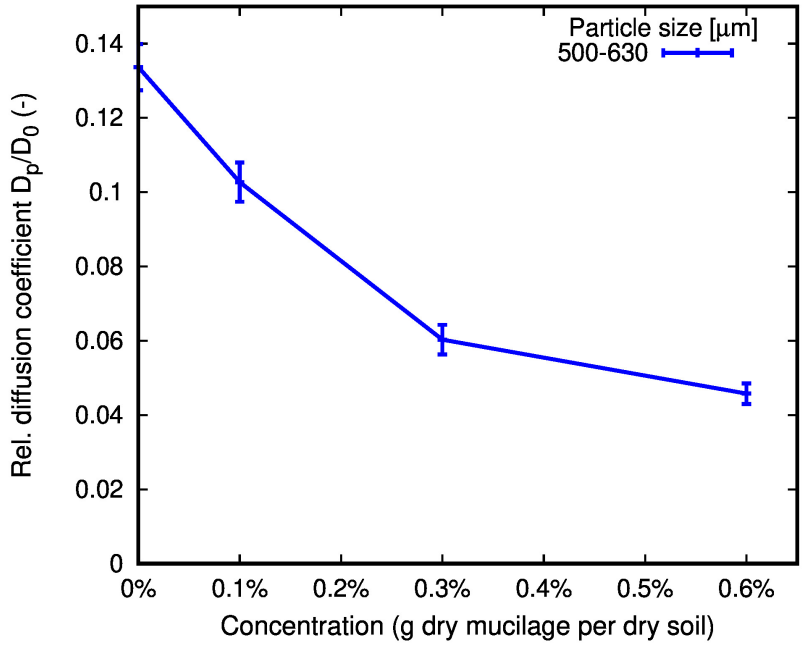

Figure 2.4.: Relative diffusion coefficient D_p/D_0 as a function of mucilage concentration for a sandy soil with particle size of 500–630 µm.

2.3.3. Simulation of mucilage distribution during drying

Simulations of two simplified two-dimensional scenarios (either liquid or elastic network) can indeed reproduce pore scale dynamics observed for water and highly concentrated mucilage, respectively. For the liquid case (Fig. 2.6, left), simulations create the typical geometry of water bridges that break at low water contents. For the case of an elastic network (Fig. 2.6, right), simulations indeed show the formation of hollow structures between two particles upon drying. Here, the simulations are not meant to quantitatively describe processes, but they are rather a qualitative illustration of how interactions of polymer-like nanostructures may create the observed porescale distributions, e.g., hollow cylinders, of mucilage which very much differ from those structures of water bridges.

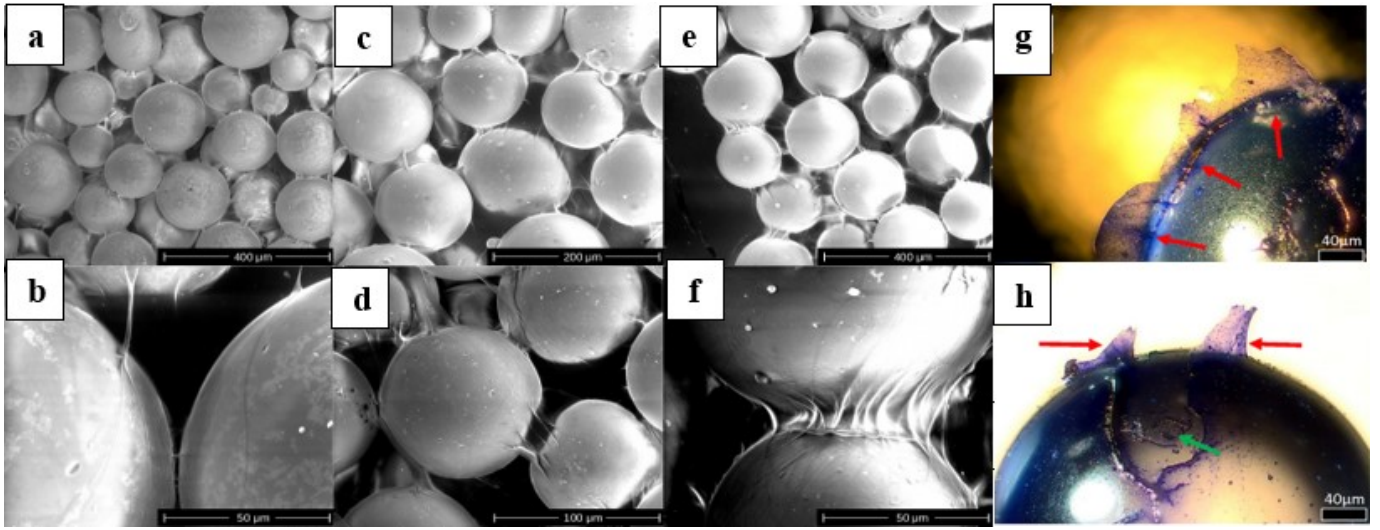

Figure 2.5.: Environmental Scanning Electron Microscope (a–f) and Light Microscope (g, h) images of mucilage-based structures within the pore space of glass beads (0.2 mm diameter). Increasing concentration from left to right (0.16 %, 0.25 % and 0.49 %). (a–f) Various structures can be seen depending on mucilage concentration (thin filaments, hollow cylinders, interconnected surfaces). (g, h) remains of broken mucilage filaments (red arrows) and former interparticle contact (green arrow) show that dry mucilage forms hollow structures during drying.

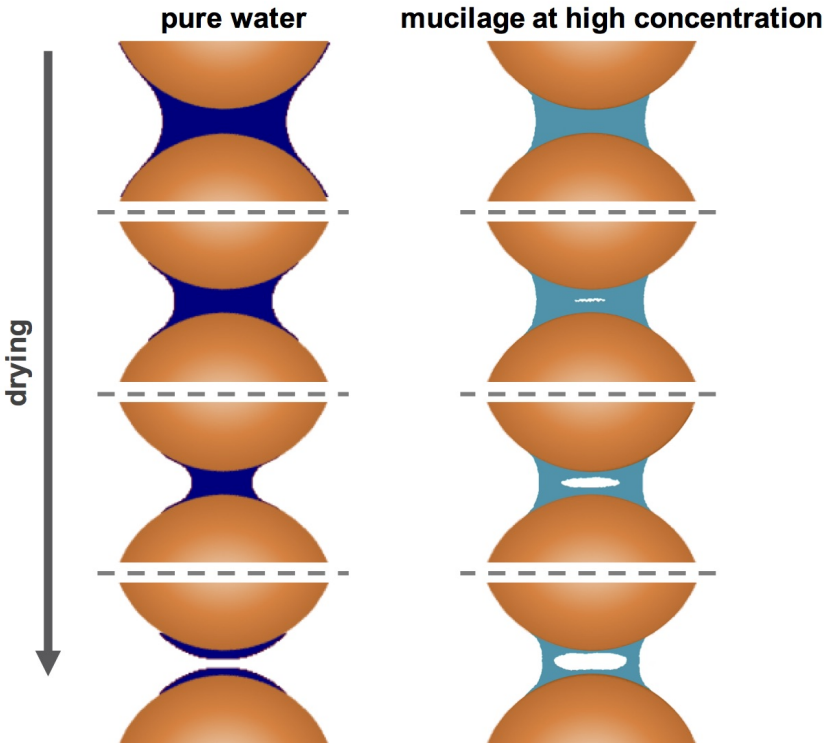

Figure 2.6.: Simulated pore scale dynamics during a slow drying process of a liquid between two particles. In each step, the steady state spatial distribution of the liquid phase is simulated in each case at a certain water content.

2.4. Discussion

Gas diffusion measurements of dry soil (Fig. 2.4) confirmed the hypothesis of the conceptual model (Fig. 2.1): mucilage decreases the gas diffusion coefficient in dry soil without significantly affecting air-filled porosity. This can be explained by the formation of a mucilage dry surface spanning throughout the pore-space as imaged using Environmental Scanning Electron Microscopy (Fig. 2.5). These are in agreement with the observations by Carminati et al. (2017) and Benard et al. (2019), who discovered mucilage forming liquid bridges throughout the pore space during drying. The mucilage-based structures between neighbouring particles are able to disconnect the gas phase. This leads to an increased air-filled pore tortuosity and longer diffusion pathways resulting in a lower diffusion coefficient.

In their review on root respiration, Ben-Noah and Friedman (2018) presented a model to describe diffusion in a soil–mucilage layer. They assumed a homogeneous mucilage layer of a certain diffusion coefficient and thickness around the root. But neglecting the complex mucilage structures and considering mucilage as a uniform layer coating the root, is a simplification that might have a huge impact on predictions of gas diffusion through a soil–mucilage layer. We show that the pore scale dynamics of mucilage are more complex. Therefore, it is necessary to regard a more intricate spatial arrangement of mucilage within the pore-space.

Existing models (Tab.1.2) describe gas diffusion processes in soil and how this is affected by water content and organic matter in general, but they are not designed to describe how mucilage alters gas diffusion. As a consequence, the predicted values of these models [$D_p/D_0 = 0.22$, 0.22 and 0.28 using Eq. (1.2), OMF model*, respectively MQ model** (Tab. 1.2)] when applied to our soil samples are much higher compared to our measured data. More flexible models, like the SWLR model [Tab. 1.2] allow a better description of gas diffusion processes. Considering literature references of $C_m = 2$ ($D_p/D_0 = 0.163$), respectively $C_m = 3$ ($D_p/D_0 = 0.114$) allow a closer prediction of gas diffusion coefficient for a dry sandy soil with 0 % ($D_p/D_0 = 0.134$) and 0.1 % ($D_p/D_0 = 0.103$) mucilage concentration used in this study. However, a complexity factor of $C_m = 2$ provides a good estimation of gas diffusion coefficient for a variety of natural soils, while $C_m = 3$ gave a good description for specifically clay minerals (Moldrup et al. 2013). An adaption of the complexity factor on measured results only allows a comparison between gas diffusion coefficient of a sandy soil affected by mucilage and gas diffusion coefficient of soils with different soil texture. Since, in dry soil, air-filled porosity is not significantly affected by mucilage concentrations, these models would not predict an effect of dry mucilage on the relative diffusion coefficient. A reduction of the relative diffusion coefficient by a factor of 0.5 which we measured at 0.3 % mucilage concentration could be predicted by the OMF model (Tab. 1.2) only if air-filled porosity was reduced from 34 % to 11.4 % opposed to our experiment where air-filled porosity was not significantly affected.

A better description of pore scale processes of the spatial formation of liquid mucilage bridges and surfaces is needed to create more appropriate gas diffusion models. Further experimental, theoretical and numerical studies may help to understand and describe the effect of mucilage on gas diffusion also at further water contents and soil conditions.

*$X = 0.4 + 2.9\Phi$ and $\epsilon_{th} = 0.11\Phi^4$

**$X = 10/4$ and $\delta = 2$

Although mucilage membranes reduce gas diffusion at dry soil conditions these structures may prevent roots from a deficiency of oxygen during a heavy rain fall event after drought: when dry, a hydrophobic mucilage surface that disconnects the pore space may prevent the pore space around the root from being completely filled with water while rewetting. In this way it may allow a better aeration of roots at the critical conditions close to saturation.
This results in a deceleration of gas movement in soil and by extending the pathway through the soil it may enhance possible redox reactions. Therefore, we hypothesize that it will affect soil–rhizosphere biogeochemistry and in consequence also the biogeochemical exchange between soil and atmosphere. Using greenhouse gases as a topic example, plants most likely may have a so far unaccounted biophysical effect on N_2O and CH_4 emissions. Both gases are highly reactive in the soil–rhizosphere being sources of energy for soil microbes. A decelerated diffusion through the soil increases the probability that N_2O will be denitrified to N_2 and CH_4 oxidized to CO_2 which reduces the climate warming feedback effect from soils. Additionally, soils and therefore plants will lose less water because water vapour will not move as fast to the open atmosphere. Since root exudates play a significant role in shaping rhizosphere bacterial community (Haichar et al. 2008; Dennis, Miller, and Hirsch 2010), a next step would be to investigate the interactions with the microbial communities which may alter additionally our view on how plants control soil gas exchanges.
Our study does not only advance our understanding of gas diffusion in soil, but gas diffusion measurements may also be a useful tool to learn about the conditions at which mucilage forms connected surfaces in the pore space. In this way we want to contribute to further interdisciplinary rhizosphere research combining hydrology, gas transport and microbial activity as controlled by plant roots.

2.5. Conclusion

This study shows that plant derived mucilage increases air-filled pore tortuosity in soils by partly locking pores even when dry. During drying mucilage forms a polymeric network spanning throughout the pore space. Existing soil gas diffusion models (e.g., Hamamoto et al. 2012; Moldrup et al. 2013) cannot provide a proper estimation of the influence of mucilage on soil gas diffusion, since mucilage increases pore tortuosity without affecting air-filled porosity. Most of these gas diffusion models do not have such a flexible tortuosity factor implemented. Therefore, a key to predict the effect of

rhizodeposition on soil gas diffusion is at first to find a way to estimate tortuosity in rhizosphere soils and secondly to adjust gas diffusion models to consider a tortuosity factor. Such a decoupling of tortuosity from total porosity and air-filled porosity may help predicting the influence of rhizodeposition on soil gas diffusion. In summary, this study supports the concept that plants are capable of altering soil physical properties to their advantage.

3. A root mucilage analogue from chia seeds reduces soil gas diffusivity

Based on: Haupenthal, Adrian, Patrick Duddek, Pascal Benard, Mathilde Knott, Andrea Carminati, Hermann F. Jungkunst, Eva Kroener, and Nicolas Brüggemann. 2024. "A root mucilage analogue from chia seeds reduces soil gas diffusivity." European Journal of Soil Science 75 (5): e13576. DOI: 10.1111/ejss.13576

3.1. Introduction

Gas exchange between roots and soil is essential as the O2 supply from the aerial parts of plants is often insufficient for satisfactory root growth (Gardner, Laryea, and Unger 1999) and the accumulation of toxic substances like ethanol and lactic acid near roots can be harmful (Rivoal and Hanson 1994). Therefore, maintaining gas exchange within the root-rhizosphere-bulk soil system is advantageous for biota in soils.
The movement of gas through soil occurs mainly by diffusion (Gliński and Stępniewski 1985). Gradients in concentration force gas to move from areas with high concentration to areas with low concentration. This process is controlled by the distribution and connectivity of air-filled pores, and this soil-specific property is represented by the effective diffusion coefficient D_p (Fujikawa and Miyazaki 2005; Hamamoto et al. 2009). Several studies quantified the effect of soil compaction, water saturation, organic matter and mucilage on gas diffusion and discussed their potential implications (Hamamoto et al. 2012; Haupenthal et al. 2021; Moldrup et al. 2000; Thorbjørn et al. 2008; Xu, Nieber, and Gupta 1992). Wesseling et al. (1957) stated that a volumetric soil air content of 10% seems to be a threshold for gas diffusion.
Aside from the quantity of water in the soil, its distribution in the pore space affects the connectivity of air-filled pores. Non-uniformity of the pores, entrapped air and a difference in contact angle between the pore water and the interface of soil particles during drying and rewetting, affect the distribution of water, resulting in an effect

known as hysteresis (Cooper et al. 2017; Haines 1930; Wen, Shao, and Guo 2021). This phenomenon results in differences in water content at the same water potential and thus in water and air-filled pore connectivity between the drainage and the wetting branches of the soil water retention curve (Haines 1930; Likos, Lu, and Godt 2014). Further, it explains observations of Hamamoto et al. (2022) who reported differences in gas diffusion coefficients at the same air-filled porosity during a wetting-drying cycle.

Plant roots actively modify the physical properties of the soil in their vicinity by secreting mucilage (Benard et al. 2019; Carminati et al. 2016; Haupenthal et al. 2021; Kroener et al. 2018). Lazarovitch et al. (2018) stated that optimal plant growth requires a balance between water and O_2 contents. Mucilage may be a plant's tool to maintain this balance. The physico-chemical properties of root mucilage (e.g., water holding capacity, viscosity and surface tension) vary between plant species. Seed mucilage (e.g., from chia or flax seeds), which has similar physico-chemical properties, is often used as an analogue in experimental studies (Brax et al. 2020; Naveed et al. 2019). Studies have shown that mucilage has a strong impact on soil hydraulic properties (Benard, Zarebanadkouki, and Carminati 2019; Carminati et al. 2010; Kroener et al. 2018), solute diffusion (Holz et al. 2019; Zarebanadkouki et al. 2019) and gas diffusion (Haupenthal et al. 2021) in soil. Due to its hydrogel-like behavior, mucilage has the capacity to absorb water up to 600 times its own dry weight (Nazari 2021). Furthermore, Benard et al. (2018) showed that the contact angle at the soil-water interface increased with mucilage content. Kroener et al. (2018) found that the effect of mucilage on saturated soil hydraulic conductivity and water retention depended on soil particle size. Mucilage reduced the hydraulic conductivity of fine sand by several orders of magnitude, whereas its effect was negligible in clay. Moreover, mucilage increased water content at low matric potentials in all soils. However, in coarse soils a comparably high mucilage content was needed to induce an increase in soil water retention.

High viscosity of mucilage leads to the formation of characteristic bridges between soil particles during soil drying (Albalasmeh and Ghezzehei 2014; Benard, Zarebanadkouki, and Carminati 2019). Carminati et al. (2017), Benard et al. (2018) and Haupenthal et al. (2021) observed various types of structures in different porous media. The shape of these bridges depends on mucilage content. Thin filaments are formed at low content. With increasing content, hollow cylinders were observed and at high mucilage content, 2D interconnected surfaces reaching through the pore space are formed. Benard et

al. (2017) observed, that for particles with a high surface roughness more mucilage is needed to create bridges similar sized compared to particles with a smooth surface. It is, therefore, reasonable to postulate that the interaction of mucilage with the soil matrix alters the connectivity of air-filled pores in soil.

A conceptual model to describe the effect of mucilage on gas movement in soil under a drying-rewetting cycle for a given water content is shown in Figure 3.1. The shape of mucilage structures in soil and their effect on gas diffusion depends on mucilage content. An increase in mucilage content results in larger structures, hence a decrease in connectivity of air-filled pores, thereby limiting gas diffusion. The distribution of water in the pore space depends on whether the soil has been dried or rewetted. The main drivers for a different water distribution are air entrapment, an ink-bottle effect and a contact angle hysteresis (Likos, Lu, and Godt 2014; Diamantopoulos et al. 2013). In coarse soils with large average pore diameter the amount of potential pore throats is rather low. Therefore, not many bottleneck effects can be expected, resulting in a quite similar water distribution and consequently a comparable gas diffusivity between wetting and drying of the soil. With a decreasing particle size, the specific surface area of the particles increases and with it surface roughness, leading to a higher amount of potential pore throats. As a consequence, a bottleneck effect can occur more frequently. Therefore, a less connected air-filled porosity during drying compared to rewetting can be expected in fine soils. Hence, gas diffusion is higher during rewetting at the same water content. However, in clay the amount of pores and potential pore throats is so high that water cannot be present in every pore throat during drying, therefore not affect air-filled pore connectivity and consequently gas diffusivity. In contact with water, mucilage starts to swell and to expand throughout the pore space (Brax, Buchmann, and Schaumann 2017). As mucilage dries, persistent liquid bridges between particles can draw them together (Williams et al. 2021). Both processes can cause an alteration of the geometry of the soil by rearranging the particles and pores. In coarse soils with large pores, mucilage will swell into the pore space without affecting pore structure. At low mucilage content, only a few mucilage bridges can be formed between soil particles, which do not affect gas diffusion. With increasing content, mucilage will be able to span across larger pores (Carminati et al. 2017), disconnecting the gas phase and reducing gas diffusivity. Furthermore, mucilage is able to displace soil particles and change the structure of the soil (Hallett et al. 2022). In a fine-textured soil, the swelling of mucilage results in the formation of large pores. During drying, water is no longer present within these large pores, and at low mucilage content the

Figure 3.1.: Conceptual model of gas movement in soil as a function of mucilage content and particle size at a constant low water content. The distribution of water and mucilage depends on whether the soil is dried or rewetted. Mucilage content increases from left to right and particle size increases from bottom to top. Water and mucilage are clogging pores reducing gas diffusivity, indicated by extended diffusion pathways. Note that for fine sand swelling of mucilage displaces particles (red circles) without affecting porosity, resulting in large pores where mucilage at low contents is no longer able to span across a pore, leaving the pore open for gas to diffuse. This effect is neglected for clay since swollen mucilage would change the porosity of the soil, which would make the soils incomparable.

pores are too wide for mucilage bridges to be formed. This process opens up pores for gas to diffuse through which increases diffusion. However, at high mucilage contents wider pores will be clogged again (Benard et al. 2021) and diffusivity decreases. In clay soils, swelling of mucilage is supposed to have the highest impact. Not only a change in soil structure is to be expected, but also a change in total porosity, respectively bulk density, resulting in an increase of the soil volume (Kroener et al. 2018). For simplification, the effect of mucilage swelling in clay soils is neglected. Therefore, as with clay soil without mucilage, the gas diffusivity during drying and rewetting will not differ. Despite progress in conceptualizing the interactions between soil particles and mucilage, the impact of particle size and soil water content in the context of gas diffusion remain unclear.

The approach of using X-ray computed tomography (CT) to quantify soil structure has been established in recent years. It has been used in several studies for visualization and quantification of pore connectivity (Koestel, Larsbo, and Jarvis 2020; Lucas et al. 2021; Renard and Allard 2013; Vogel 1997), as well as pore alteration induced by roots (Aravena et al. 2011). Hamamoto et al. (2022) used X-ray CT to visualize differences in water distribution during a wetting-drying cycle. Common parameters to quantify the connectivity of the pore system are the Euler-Poincaré Characteristic (EPC) χ and the Gamma ($\Gamma-$) indicator. Whilst χ describes the connectivity of the pore space characterized by its geometrical topology (Vogel 1997), Γ represents the probability of finding a continuous path through the pore system (Lucas et al. 2021; Renard and Allard 2013). Hence, the $\Gamma-$indicator is more sensitive to global connectivity of a soil, whilst χ is independent of the size of pore clusters.

In this study, we investigated the effect of a root mucilage analogue on soil gas diffusion in the soil of different particle sizes and at different water contents for drying and rewetting conditions. Gas diffusion coefficients were determined experimentally at various mucilage contents during a drying-rewetting cycle. The experimental data were supported by X-ray CT and environmental scanning electron microscopy (ESEM) images. Our hypothesis was that the effect of mucilage on air-filled pore connectivity depends on particle size. We expected a substantial decrease in soil gas diffusivity with an increase in mucilage content as mucilage structures increase in size, thereby reducing the cross section of available pathways for gas diffusion. In coarse soils, a higher mucilage content would be required for structures to form which reach across big pores. In very fine-textured soils, we expected a reduced effect due to the number of potential pore throats where mucilage deposits and structures are formed during

soil drying. In addition, we assumed a hysteresis in gas diffusion coefficient during a drying-rewetting cycle caused by non-uniformity of interconnected pores. Finally, we hypothesized that the effect would diminish with increasing mucilage content as the structures formed during drying would attract water during rewetting and redistribute it to larger pores.

3.2. Material and Methods

3.2.1. Mucilage collection

Chia seed mucilage was used as an analogue for root exudates. A detailed description of the extraction process is given by Kroener et al. 2018. After the extraction, mucilage was frozen, then freeze-dried and ball-milled.

3.2.2. Gas diffusion measurements

A detailed description of the experimental setup (Figure 1.4) and the procedure to determine D_p is given in Chapter 1.2.6.

A soil-mucilage mixture was used as a model of the rhizosphere. We mixed soils of various particle sizes (800–1000, 500–800, 200–500, 63–200, 20–63 and <20 µm) with different amounts of chia seed mucilage to achieve specific mucilage content in soil (0, 0.5, 1, 2.5 and 5 mg g^{-1} dry mucilage/dry soil). Coarse sandy soil (800–1000 and 500–800 µm, Quarzwerk WOLFF & MÜLLER, Haida, Germany), medium and fine sand, silty and clay soil (Quarzwerke Frechen, Frechen, Germany; organic matter content below detection limit) were used. Three replicates of each combination of particle size and mucilage content were prepared at a dry bulk density of (1.51 ± 0.05) g cm^{-3}. Soil-mucilage mixtures were packed in PVC tubes with a diameter of 3.6 cm and a height of (0.60 ± 0.01) cm. Air-filled porosity was derived from bulk density, particle density (2.65 g cm^{-3}) and volumetric water content, and ranged from (0.430 ± 0.015) cm^3 cm^{-3} (total porosity) for dry samples to (0.230 ± 0.015) cm^3 cm^{-3} for the highest water content. Mucilage was diluted in water. The amount of water for dilution was determined by setting the volumetric water content (Φ_V) equal to the porosity of the sample. Thereby, saturating the sample but not exceeding soil porosity. Silt and clay samples were slightly compacted during the drying process by using a stamp to counteract swelling of the samples and maintain the original soil volume. Samples were air-dried ((22 ± 1) °C) and the weight was monitored to determine gravimetric and volumetric

water content, seeking Φ_V of $0.1\,cm^3\,cm^{-3}$, $0.15\,cm^3\,cm^{-3}$ and $0.2\,cm^3\,cm^{-3}$ for testing. For rewetting, the amount of water corresponding to predefined Φ_V was applied by drip irrigation using a pipette. Before measurements, the samples were closed with parafilm (Amcor, Zurich, Switzerland) and stored at 4 °C for at least 4 h to ensure equilibration of the water content across depth while limiting microbial activity. During drying, the evaporation rate was monitored. To maintain the desired water content during diffusion measurements, water was resupplied to the soil surface every 30 minutes based on the recorded evaporative loss. The measurements were performed at room temperature ((22 ± 1) °C).

3.2.3. X-ray CT-imaging

Sand (Carlo Bernasconi AG, Zurich, Switzerland) was sieved (200 µm–500 µm) and mixed with wet mucilage to achieve a range of mucilage content in soil ($0\,mg\,g^{-1}$, $1\,mg\,g^{-1}$ and $2.5\,mg\,g^{-1}$), and air-dried, respectively wetted via capillary rise, to Φ_V of $0.1\,cm^3\,cm^{-3}$, $0.15\,cm^3\,cm^{-3}$ and $0.2\,cm^3\,cm^{-3}$. Sample holders were sealed with parafilm in order to avoid evaporative losses and stored at 4 °C for 4 h to reach equilibrium in matric potential before imaging. Immediately after rewetting and sealing the samples, additional CT scans were performed. X-ray CT-images were taken with a GE Phoenix V|tome|x s micro-CT scanner (General Electric Company, Boston, MA, United States) with a tube voltage of 140 kV and a tube current of 70 µA. An actual pixel size of 11×11 µm^2 was achieved at a scan time of 17 min. Images were reconstructed from 2000 projections using the Phoenix datos|x CT Data Acquisition Software. Reconstructed images (consisting of 1012 slices) were analyzed using the analysis software Avizo (Thermo Fisher Scientific, Waltham, MA USA). For preprocessing, the following steps in corresponding order were performed: (i) Since concave and convex deformations occurred at the top and bottom of the samples, respectively, during sample preparation, the total number of slices was reduced to 700 during image preprocessing, removing the upper- and lowermost layers from the processed image. This resulted in a consistent cylindrical shape of the CT images, allowing for accurate comparisons of the different treatments, but also in minor changes in water content calculated from the CT image analysis. (ii) Images were converted from 16 to 8 bit and, to reduce noise, a non-local means as well as an unsharp masking filter were applied. (iii) The diameter of the sample holder was 1 cm; images were cut cylindrically with a diameter of 0.89 cm to match the sample geometry and to minimize edge effects at the cylinder wall. (iv) A grayscale value histogram was created

to determine the markers of the solid, liquid and gaseous phase, which were required as input for the watershed transformation. Therefore, a rolling window calculation was applied at each grayscale with a center labeled window of size 5 to determine the mean of the values within the window. This resulted in a smooth curve over the data, which was then used to find the peak values, corresponding to each phase. To have a standardized procedure, the interval of grayscale values defining each phase was evaluated at a relative height of 0.5 be-tween the height of the peak itself and the lowest contour line. At this height, the width of the curve determines the threshold values for the respective phase. (v) Afterwards, markers derived from the histogram analysis were used as input for a marker-based watershed transformation (Beucher and Meyer 1992) to segment the different phases (soil, water and air). (vi) Finally, a morphological opening with a sphere of radius 2 px as the structuring element was applied to account for features with a volume below the spatial resolution limit. An exemplary cross section of the segmented result is shown in Figure 3.2.

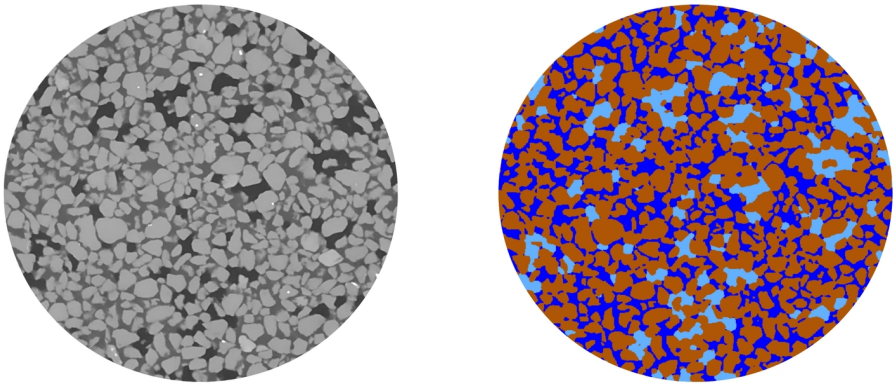

Figure 3.2.: Exemplary cross section of a raw and corresponding segmented X-ray CT-image with water (dark blue), air (light blue) and soil (brown).

The connectivity of the gas phase, was estimated based on the EPC χ and the Γ-indicator. Calculation of χ was done by applying a label analysis based on the Avizo inbuilt EPC measure using a 26-neighborhood algorithm. χ is related to the topology of the pore space, dimensionless, and is based on the number of unconnected clusters (N), the number of redundant connections (C) and number of completely enclosed cavities (H) (Vogel 2002):

$$\chi = N - C + H. \tag{3.1}$$

For a network of pores in soil, H is negligible. The larger the χ, the lower is the connectivity of the pore system. Typically, χ is highly negative in soils, indicating a high connectivity of the pore space. However, a negative χ does not imply the presence of a percolating path connecting top and bottom of a soil sample (Lucas et al. 2021). Another metric to describe pore connectivity is the Γ-indicator. The Γ-indicator is a measure of probability for two voxels belonging to the same cluster, and consequently being connected. For soil-water-air samples it can be calculated from the total number of all air-filled pore voxels ($N_{p_{air}}$), the number of all air clusters k_{air} ($N_{k_{air}}$) and the number of air-filled pore voxels p_{air} contained in each cluster k_{air} ($n_{p_{k_{air}}}$). $\Gamma(p_{air})$ is defined as (Renard and Allard 2013):

$$\Gamma(p_{air}) = \begin{cases} \frac{1}{N_{p_{air}}^2} \sum_{k=1}^{N_{k_{air}}} n_{p_{k_{air}}}^2 & p_{air} \neq 0 \\ 0 & p_{air} = 0 \end{cases} \tag{3.2}$$

A Γ value of one indicates that all air-filled pore voxels are connected and consequently belong to the same, single cluster. In contrast, a value close to zero indicates the presence of many unconnected air-filled pore clusters.
However, both measures do not provide information on the volume of the connected pore clusters and whether there is a percolating path from the bottom to the top of the sample (Koestel, Larsbo, and Jarvis 2020).

3.2.4. Environmental scanning electron microscopy

Samples packed with the same soil textures and mucilage contents as for diffusion measurements were scanned using ESEM. Samples were dried for 48 h at room temperature ((22 ± 1) °C). Prior to the measurements, samples were coated with gold using a Quorum Q 150R S Rotary Pumped Coater (Quorum Technologies, Judges House, Lewes Road, Laughton, East Sussex, UK). ESEM images were taken with a FEI Quanta 250 ESEM (FEI Company, Hillsboro, OR, United States) under low vacuum with chamber pressures between 60 Pa and 80 Pa. A large field detector was used with an acceleration voltage of 30 kV.

3.3. Results

3.3.1. Gas diffusion measurements

The amount of mucilage per sample ranged from 0.495 mg g^{-1} to 5.1 mg g^{-1} dry mucilage/dry soil, depending on initial mucilage content. Assuming a mucilage density of roughly 1 g cm^{-3}, the volumetric mucilage fraction would be roughly 0.9 %. Thus, the volume occupied by pure mucilage would be <1 % of the volume of the bulk soil. Therefore, the effect of dry mucilage on air-filled porosity was assumed negligible.

In Figure 3.3, the relative diffusion coefficient D_p/D_0 is plotted as a function of water content for various particle sizes and mucilage content during a drying-rewetting cycle. A comprehensive presentation of the results differentiated by mucilage content and particle size can be found in the supplemental material (Figure A.1). Generally, D_p/D_0 decreased with increasing water content and increasing mucilage content (Table 3.1). The effect of mucilage on gas diffusion was highly dependent on the particle size. The reduction in medium sandy soil (200 µm–500 µm) was six times larger than the reduction in silty and clay soil. For untreated samples, a hysteresis in D_p/D_0 during the drying-rewetting cycle was observed. The extent of the hysteresis depended on particle size. While the coarse soils showed no difference, D_p/D_0 was significantly lower during drying in fine soils. This effect diminished with increasing mucilage content. At the highest water content (20%), diffusivity changed only slightly with increasing mucilage content.

Table 3.1.: Relative diffusion coefficient (D_p/D_0) for dry samples without mucilage and the reduction of D_p/D_0 caused by mucilage and water.

	Particle size [μm]					
Parameter	**800 – 1000**	**500 – 800**	**200 – 500**	**63 – 200**	**< 40**	**< 20**
D_p/D_0 for control soil	0.137	0.129	0.127	0.12	0.124	0.142
Reduction factor caused by mucilage (5 mg g^{-1})	3.66	3.08	6.68	4.24	1.01	1.08
Reduction factor caused by water (0.2 cm^3 cm^{-3} drying)	3.91	2.93	5.08	6.9	5.39	8.88
Reduction factor caused by water (0.2 cm^3 cm^{-3} rewetting)	2.49	2.58	4.23	4.29	3.54	3.38

Note: The reduction caused by mucilage was highest for 200 – 500 μm particle size. For silt (< 40 μm) and clay (< 20 μm) no reduction could be observed. The reduction caused by water was higher during drying compared to rewetting.

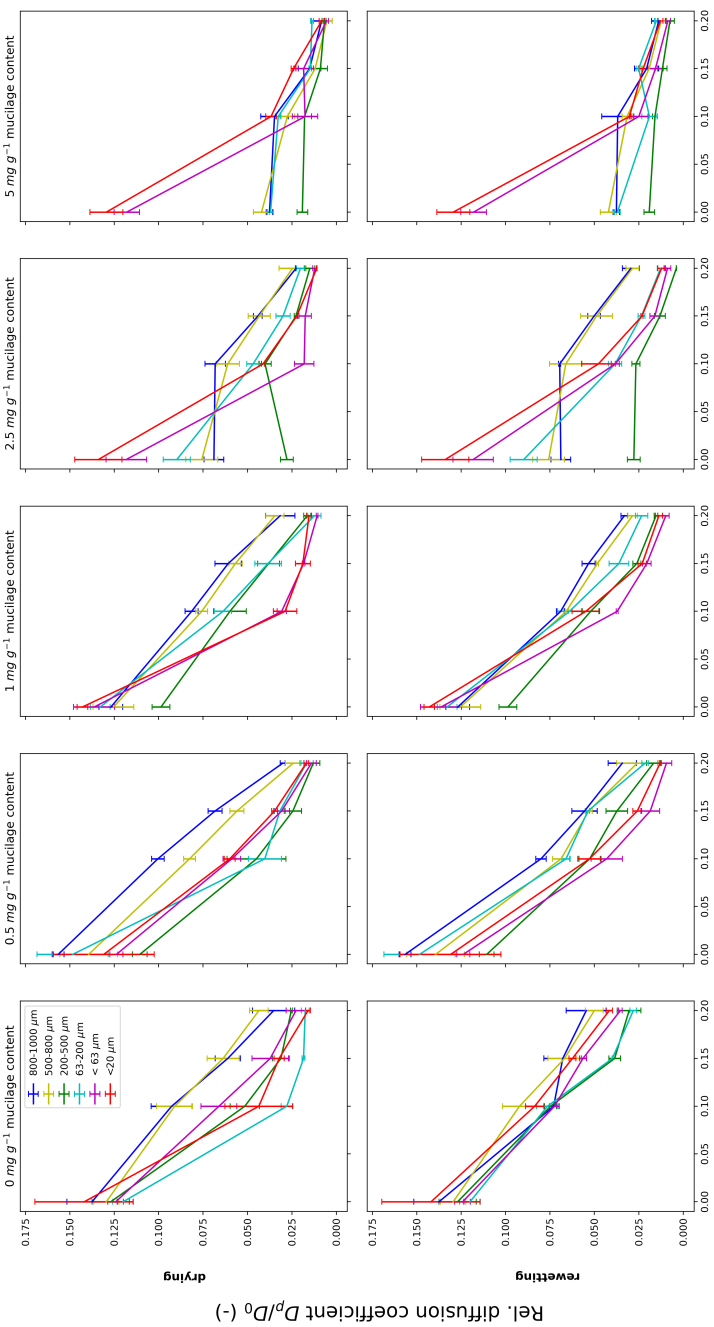

Figure 3.3.: Relative diffusion coefficient D_p/D_0 depending on water content and mucilage content during drying (top row) and rewetting (bottom row). Results indicate a hysteresis for control treatments which diminished with increase in mucilage content.

3.3.2. X-ray CT-Imaging

The EPC χ for the gas phase decreased for all contents with decreasing water content, while for the liquid phase χ decreased for increasing water content for all mucilage contents (Figure 3.4). Φ_V values were lower than initially set due to image processing, during which the top and bottom of the image stack were cut off. Due to drying from evaporation and wetting from capillary rise, more volume of water than volume of air was removed. This resulted in a reduced calculated soil moisture content. Results for samples without mucilage indicated a hysteresis behavior for the gas phase. Values for during rewetting were slightly smaller compared to drying for water contents above 10 %. However, for the liquid phase no differences in χ during drying and rewetting, and consequently no hysteresis was observed for all mucilage contents.

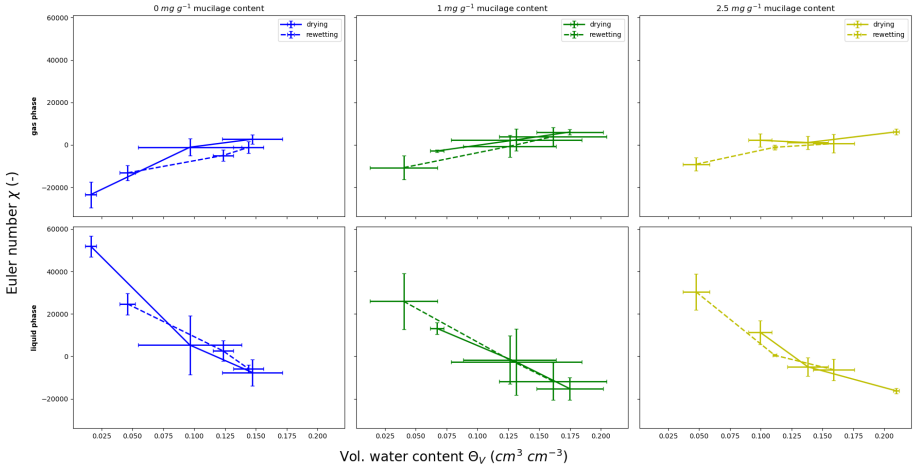

Figure 3.4.: Euler-Poincaré characteristic χ for the gas (top) and liquid phase (bottom) depending on water content and mucilage content.

Results for χ immediately after rewetting and after 4 h showed no significant differences, indicating that the topology of the air-water-mucilage phase equilibrates quickly (Figure 3.5).

The Γ-indicator of the gas phase decreased with increasing water content in all treatments (Figure 3.6). In contrast to diffusion coefficient measurements, no significant difference between drying and rewetting could be observed. Overall, values for all mucilage contents were in the same range at their corresponding water content. For the liquid phase, values increased with increasing water content. Values for various

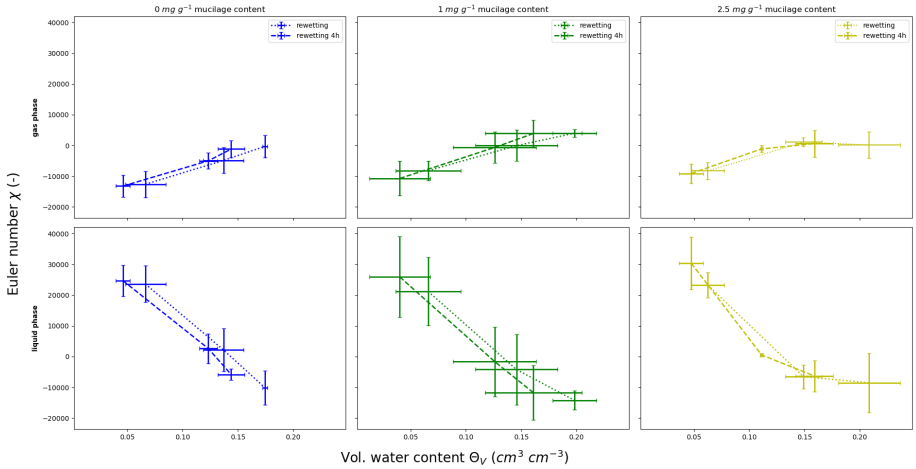

Figure 3.5.: Euler-Poincaré characteristic χ immediately after rewetting and 4 hours after rewetting. The connectivity of the liquid phase improved over time while the connectivity of the gas phase decreased. The effect seems to diminish with increasing mucilage content.

mucilage contents did not differ significantly. Also, no major differences between drying and rewetting could be observed. Furthermore, values immediately after rewetting and after 4 h showed no significant difference (Figure 3.7). As with the EPC, this showed a quick equilibration of the air-water-mucilage phase.

Comparison of the percolating gas phase cluster for various mucilage and water contents indicates a reduction of the connectivity throughout the sample with increasing mucilage and water content (Figure A.2).

3.3.3. Environmental scanning electron microscopy

The ESEM images reveal various dried mucilage structures in the dried soil samples depending on mucilage content. These structures ranged from thin filaments at low mucilage content, membrane-like structures and hollow cylinders at intermediate content up to interconnected surfaces spanning throughout the pore space at high content (Figure 3.8). While at low content, mucilage deposits preferentially in pores with small diameters, mucilage bridges span across larger pores with increasing content. However, even at low content interconnected surfaces were observed, while with increasing content the size of these surfaces increased.

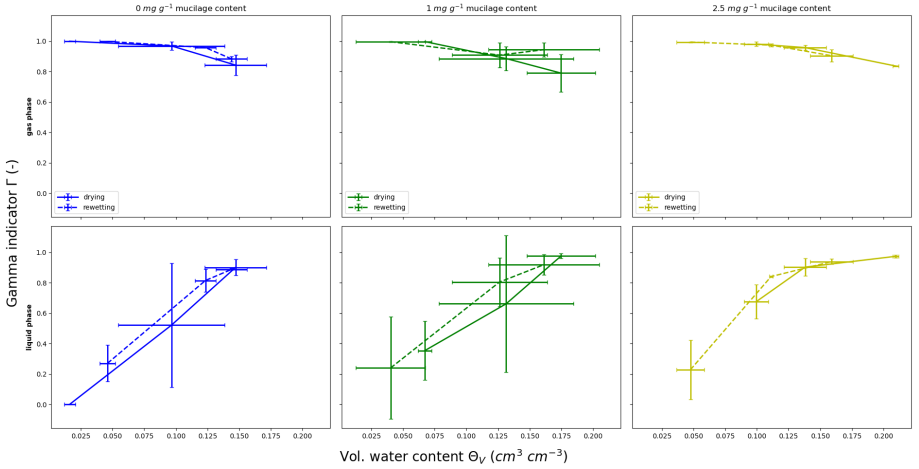

Figure 3.6.: Gamma indicator for the gas and liquid phase depending on water content and mucilage content.

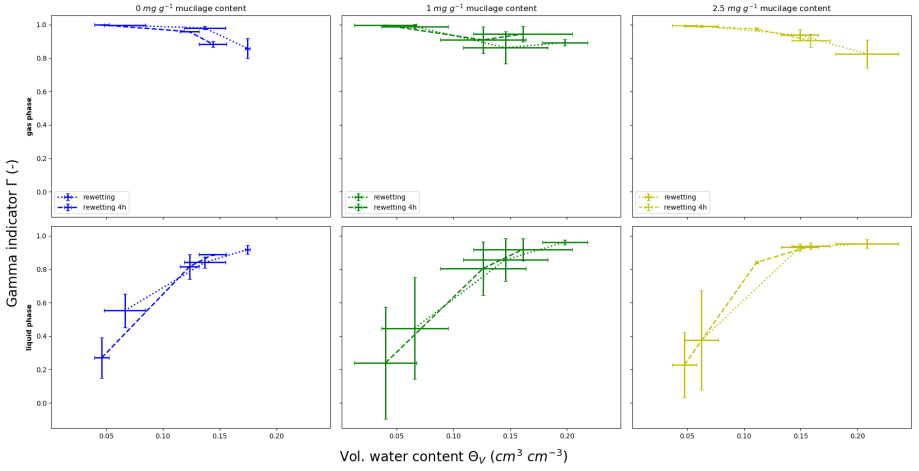

Figure 3.7.: Gamma indicator for the gas and liquid phase depending on water content and mucilage content immediately after rewetting and 4 h after rewetting.

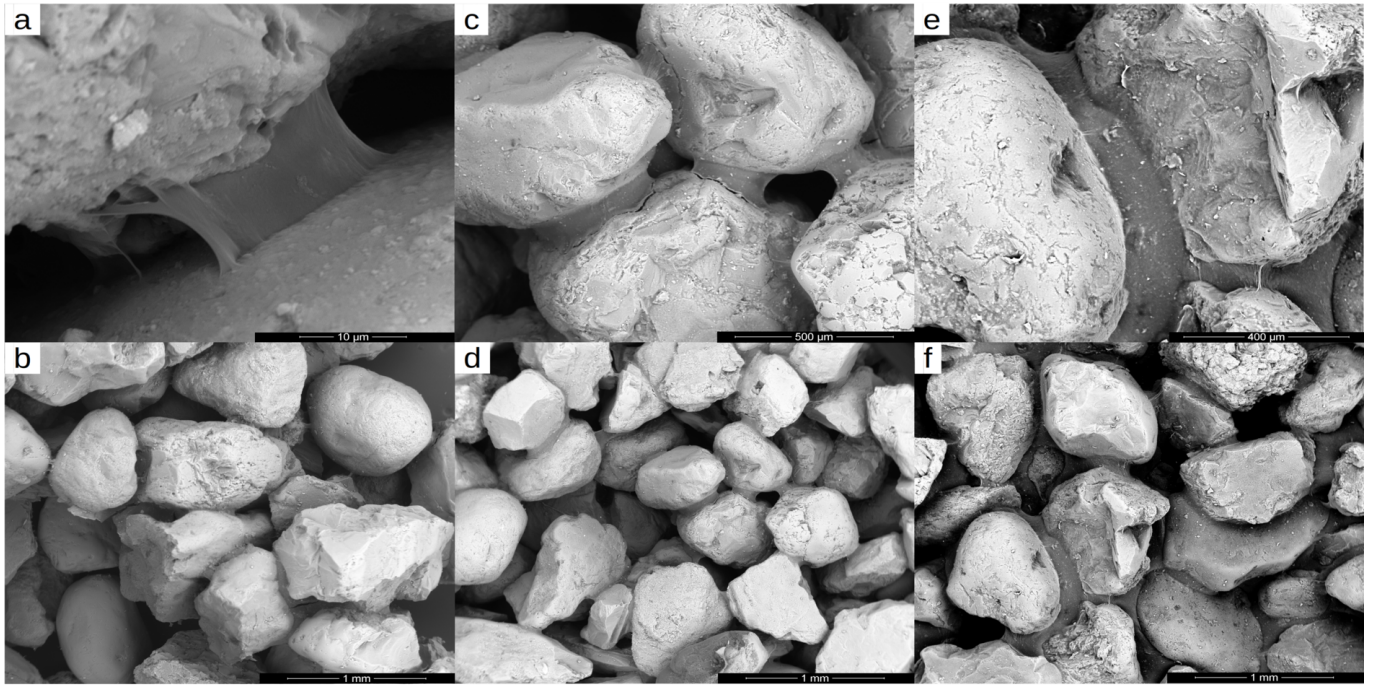

Figure 3.8.: ESEM images of mucilage deposits in the pore space of coarse sandy soil with 500–800, respectively 800–1000 particle size. Mucilage content increases from left to right (a, b $1\,\mathrm{mg\,g^{-1}}$, c, d $2.5\,\mathrm{mg\,g^{-1}}$, e, f $5\,\mathrm{mg\,g^{-1}}$). Various mucilage concentration-dependent structures are visible in the images: (a, b) Thin filaments and membrane-like structures are dominant, but also small connected surfaces are visible. (c, d) Cylindrical structures became visible with increasing mucilage content. (e, f) At highest content, interconnected surfaces span across multiple pores.

3.4. Discussion

The gas diffusion measurements of soils with various particle size and mucilage content under a drying-rewetting cycle supports the conceptual model (Figure 3.1). In dry soils, the effect of mucilage on gas diffusion depends on soil texture and mucilage content (Figure 3.3). At low mucilage contents ($0.5\,\mathrm{mg\,g^{-1}}$ to $1\,\mathrm{mg\,g^{-1}}$), only minor reduction in D_p/D_0 could be observed. With mucilage content increasing ($0.5\,\mathrm{mg\,g^{-1}}$ to $1\,\mathrm{mg\,g^{-1}}$), gas diffusivity was reduced for the coarse, medium and fine sandy soils, while for silt and clay no reduction could be observed. In general, when mucilage caused a reduction of D_p/D_0 in dry soils, it did not affect air-filled porosity. At the same water content, the diffusivity differed between dried and rewetted soils. However, the diffusion always depended on mucilage content (Figure 3.3). Thorbjorn et al. (2008) proposed a conceptual model in which gas diffusivity depends on particle size. However, no significant differences in diffusion coefficient depending on particle size for dry samples without mucilage could be observed in our study (Table 3.1). All samples were prepared to have the same bulk density. Furthermore, the density of the soil particles was the same, thus air-filled porosity was the same between the differently textured soils. Liu et al. (2006) reported that for an artificial macropore network (pores smaller than ~100 μm are assumed to be blocked) no universal relationship between diffusion coefficient and porosity exists. Local porosity heterogeneities could lead to deviations in gas diffusivity. Furthermore, tortuosity is related to the weighted length of diffusion pathways. The soil samples used in this study were very thin (0.6 cm), consequently, the effect of porosity fluctuations and tortuosity can be assumed negligible, which could explain the similar gas diffusivity for all textures. The driest samples showed the biggest reduction in D_p/D_0 for medium sandy soil mixed with mucilage compared to the untreated medium sand samples. At $0\,\mathrm{cm^3\,cm^{-3}}$ water content and mucilage content of $2.5\,\mathrm{mg\,g^{-1}}$, the diffusion coefficient of the untreated samples was reduced by a factor of 5, and increased to a factor of 6.68 for $5\,\mathrm{mg\,g^{-1}}$ (Table 3.1). Mucilage structures observed via ESEM seem to disconnect the gas phase significantly, and the ratio between pore size and the amount of potential pore throats seems to be optimal in medium sand (200 µm–500 µm) for mucilage to span across many pores and have a significant effect on gas diffusivity. In coarse sandy soil (500 µm–800 µm and 800 µm–1000 µm) and fine sandy soil (63 µm–200 µm) the effect is smaller. In coarse soil, the average pore seems to be too large for mucilage to span across, while in fine sand, and even more so in silty and clayey soil, the number of potential pore throats

is higher, and mucilage would not be present in every pore. Therefore, mucilage likely accumulates in certain regions of the pore space, leaving others available for gas diffusion. Furthermore, the higher surface roughness of silt and clay particles compared to sand might lead to more, but smaller mucilage structures as observed by Benard et al. (2018). As a result, no reduction in gas diffusivity could be observed for silt and clay. A similar particle size-dependent effect was observed by Kroener et al. (2018), where mucilage had no effect on the saturated hydraulic conductivity of clay soil. Note that since the physicochemical properties differ among mucilage from different plants and environmental conditions, it is reasonable to assume that their effect on gas diffusion is also variable.

Furthermore, our results confirm the findings of Hamamoto et al. (2022), who also observed a hysteresis in gas diffusion coefficient during a drying-rewetting cycle. The hysteresis was more distinct in fine soils. These observations are in good agreement with the concept of an ink bottle, small bottle throat diameter and broad bottle body diameter, caused by non-uniformity of interconnected pores, as well as the concept of differences in solid-liquid contact angles during wetting and drying (Haines 1930; Likos, Lu, and Godt 2014). During drying, narrow parts of interconnected pores are able to hold water and increase the length of diffusion pathways. During rewetting, water might not reach the narrow parts of the pore, leaving space for gas to diffuse. Additionally, lower contact angles between the soil and water during drying lead to less connected air-filled pores resulting in a lower gas diffusivity. However, if mucilage is added this effect diminishes with increasing mucilage content. With mucilage, liquid bridges persist under drying. As they dry further, they are likely to draw particle together, enhancing local soil aggregation (Williams et al. 2021). As mucilage rewets, it starts to absorb water and swells. Both processes are likely to create preferential diffusion pathways, increasing gas diffusivity and reducing the hysteresis effect. Despite this, mucilage can increase the contact angle at the soil–water interface, especially under dry conditions (Benard et al. 2017). This results in more similar water–soil contact angles during drying and wetting, reducing the hysteresis effect in the water retention, and consequently leading to a diminishing hysteresis in gas diffusivity during a drying–rewetting cycle. In our conceptual model for fine sand, the ability of mucilage to absorb large amounts of water and to swell can cause an alteration of the soil structure. Swelling mucilage exerts stress on soil particles. Changes in soil structure were reported in studies with super-absorbing polymers mixed with soil (Misiewicz et al. 2020; Saha, Sekharan, and Manna 2022). Results for

D_p/D_0 in medium (200 µm–500 µm) and fine soil (63 µm–200 µm) showed a distinct increase in gas diffusion at low mucilage content during drying compared to untreated samples. Swollen mucilage created larger pores by displacing soil particles. With increasing diameter, the capillary forces in the pore decrease and water can no longer be retained. At the same time as the soil dries, mucilage at low contents can no longer bridge the enlarged pores, and gas can now diffuse through the pore. A similar effect can be expected, when drying liquid bridges draw particles together. However, at high mucilage contents, D_p/D_0 decreased in both scenarios, i.e., drying and rewetting. At increasing content, mucilage can extend even across larger pores, and diffusion pathways are blocked again. Furthermore, connected mucilage bridges that were formed during drying turn hydrophilic after some time (Zickenrott et al. 2016) and draw water during rewetting to areas that otherwise would not have been reached by water. Results for coarse sand indicate no distinct change in soil structure. Large particles might be too heavy to be displaced by the mucilage, instead mucilage tends to swell into empty pore space during wetting or liquid bridges break during drying. In the experiments, a visible swelling of the silt and clay soil samples was observed. Since the swelling mucilage caused an increase in the height of the samples, we suppressed that effect to maintain soil porosity. Therefore, D_p/D_0 decreased in both cases even at low mucilage contents.

The EPC χ and the Γ-indicator revealed a better-connected gas phase at low water contents and an increased liquid phase connectivity with increasing water content. While χ values of the gas phase for samples without mucilage were higher for rewetted samples compared to dried samples, the effect diminished for the samples with mucilage. The variations in water distribution between drying and rewetting lead to a hysteresis effect in the connectivity of the gas phase. This hysteresis during a drying-rewetting cycle, as well as its reduction with increasing mucilage content, is in good agreement with results from gas diffusion measurements (Figure 3.3), where diffusivity was higher during rewetting for samples without mucilage. However, the hysteresis was not as distinct as expected based on gas diffusion measurements. Furthermore, dry mucilage can be temporarily water repellent (Moradi et al. 2012; Zickenrott et al. 2016). Therefore, it is expected that immediately after rewetting, water preferentially saturates pores which are unaffected by mucilage, additionally disconnecting the gas phase. As a result, a less connected gas phase compared to a state when mucilage has turned hydrophilic and absorbed the water is likely. However, in our study χ and Γ measurements showed no such differences. This might be a consequence of the

limitation in spatial and temporal image resolution, due to which it was not possible to detect mucilage directly. As a consequence, mucilage structures (Figure 3.8), which may have disconnected the gas phase, could not be explicitly considered resulting in an overestimation of the connectivity of the gas phase in treated soils. Furthermore, parts from the top and bottom of the image stack of each sample were removed during image processing. This altered the soil moisture content, which may have also impacted the connectivity of the liquid and gaseous phase.

3.5. Conclusion

This study showed the effects of mucilage on soil gas diffusion processes at the pore scale depended on basic physical soil properties. It indicates that by secreting mucilage from roots, plants can help mitigate changes in gas diffusivity induced by soil moisture fluctuations. Results show that dry mucilage reduced soil gas diffusion without affecting air-filled porosity. The effect of mucilage on soil diffusivity depended highly on particle size and mucilage content. While the biggest effect could be observed in medium sand, no differences were observed in silt and clay soils. During a drying-rewetting cycle, hysteresis in the gas diffusion coefficient and gas phase connectivity could be observed in samples without mucilage. With increasing mucilage content this effect diminished. Results indicate that swelling mucilage can alter the structure of the soil, especially in soils with fine particles. Yet, a quantitative description of the influence of mucilage on soil structure is missing. This study supports the hypothesis that plants actively try to maintain stable physical conditions in the soil around the root and that they balance oxygen and water content by secreting mucilage.

4. Extracellular Polymeric Substances (EPS) decrease soil gas diffusion coefficient

*This chapter includes contributions from Thomas Konjetzko and Nick Wierckx from IBG-1, Forschungszentrum Jülich**

4.1. Introduction

Microorganisms in soil usually live in colonies. In order to better withstand environmental stress factors, these colonies can form a so-called biofilm (Flemming and Wingender 2010). The formation of this biofilm is controlled by extracellular polymeric substances (EPS) produced by the microbes, which form a hydrogel-like, three-dimensional matrix that determines the structure of the biofilm (Petrova et al. 2021; Flemming and Wingender 2001; Roberson and Firestone 1992). Although there are many studies investigating the effect of this EPS matrix on soil hydraulic properties, e.g. increased water retention (Chenu 1993; Zheng et al. 2018; Adessi et al. 2018), reduced saturated hydraulic conductivity (Volk et al. 2016; Zheng et al. 2018), and reduced evaporation (Benard et al. 2023; Zheng et al. 2018), it is still unclear how this three-dimensional architecture of the biofilm affects the connectivity and tortuosity of the air-filled soil pore system and consequently gas diffusion.

EPS are natural biopolymers produced by microbes and consist mainly of polysaccharides, but might contain other biopolymers such as proteins, lipids, and DNA (Redmile-Gordon et al. 2014; Costa, Raaijmakers, and Kuramae 2018; Or, Phutane, and Dechesne 2007). Extracellular bacterial polysaccharides are important for biofilm

*T.K. produced and harvested the EPS, wrote the first draft of section 4.2.1, reviewed and edited section 4.1; N.W. reviewed and edited section 4.1 and 4.2.1

formation (Schmid, Sieber, and Rehm 2015). The produced EPS network expands the microenvironment of the microbes, leading to increased resilience against environmental stress factors and improved nitrogen fixation (Schimel 2018). The oxygen-dependent production of these hydrogel-like substances demands a significant energy input from the microbes. Nevertheless, the advantages it offers, including protection, hydration, anchoring, and more, outweigh the energy expenditure (Flemming and Wingender 2010; Costa, Raaijmakers, and Kuramae 2018; Or et al. 2007). Due to its large water holding capacity (up to 20 times its own weight), EPS maintain liquid connectivity, thereby protecting the microbes against desiccation and improving their survivability (Chenu 1993; Redmile-Gordon et al. 2014; Roberson and Firestone 1992). Furthermore, the interconnected polymer chains of the network attach to the surface of the soil particles, binding them together, anchoring the microbial colonies in the pore space, stabilizing the soil, and forming microaggregates (Chenu 1993; Or et al. 2007). As a result, the alteration of the microbial microenvironment by the production of EPS not only affects the microbes themselves but also has a major effect on the physical properties of the soil.

Microbial growth in the rhizosphere results in symbiosis between microbes and plants. On the one hand, plant roots provide organic carbon by releasing mucilage; on the other hand, microbial EPS promote soil aggregation, increase root adhering soil, protect the rhizosphere against drying and fluctuations in water potential, stimulate root exudation, increase nutrient uptake, and are capable of nitrogen fixation and phosphate solubilization (Costa, Raaijmakers, and Kuramae 2018; Alami et al. 2000; Bezzate et al. 2000; Roberson, Chenu, and Firestone 1993; Jeong et al. 2019; Mahdi et al. 2020). In their study on plant mucilage and microbial EPS, Nazari et al. (2022) reported similarities in their chemical composition and physical properties. Specifically, the viscosity and surface tension of mucilage and EPS showed almost no difference. Therefore, they suggested that mucilage can also function as a biofilm matrix. Furthermore, studies showed similar effects of EPS on soil hydraulic properties as mucilage (Benard et al. 2019). The polymer network produced by mucilage spans throughout the pore space, forming interconnected structures, which alter pore connectivity and porosity by clogging them. Haupenthal et al. (2021) observed a reduction in gas diffusivity in soil mixed with mucilage even at low water contents and related it to the formation of interconnected mucilage structures within the pore space. It is therefore straightforward to postulate an identical effect of EPS structures on gas diffusivity. However, measurements of the effect of EPS on gas diffusion in soil are still lacking.

In this study, the effect of EPS produced by *Paenibacillus polymyxa* DSM 365 and *Bacillus licheniformis* DSM 13 on soil gas diffusivity was examined for soils with specific particle size ranges and at different water contents during a drying-rewetting cycle. We postulated that the polymeric network formed by EPS obstructs gas flow by clogging pores, leading to changes in connectivity and tortuosity, thereby reducing gas diffusivity. Furthermore, we expected that this effect would depend on soil particle size distribution, with higher EPS concentrations needed in coarse soils to clog the pores than in fine-textured soils, while in fine-textured soils the EPS network would not be able to span throughout the whole pore space and therefore would only have minor effects on gas diffusion. To test our hypothesis, EPS was mixed with artificial soils of different particle sizes, which were then progressively dried and rewetted with the gas diffusion coefficient quantified at each stage.

4.2. Material and Methods

4.2.1. Production and harvesting of EPS

P. polymyxa and *B. lichenirofmis* are both Gram-positive, non-pathogenic, and plant growth-promoting soil bacteria (Mahdi et al. 2020; Jeong et al. 2019). They were selected for their natural occurrence in soil, high potential for biofilm formation, and production of EPS.

A cryogenic culture of *P. polymyxa* DSM 365 was streaked onto petri dishes filled with solidified lysogeny broth (LB) medium containing 1.5 % (w/v) agar and incubated overnight at 30 °C. The next day, one single colony was picked and cultivated in 15 mL test tubes with a cultivation volume of 3 mL liquid LB medium at 30 °C shaking at 200 rpm overnight as a pre-culture. Four 500 mL shake flasks were filled each with 50 mL EPS medium (33 g L^{-1} glucose monohydrate, 5 g L^{-1} peptone from casein, 0.05 g L^{-1} $CaCL_2 \cdot 2\,H_2O$, 1.67 g L^{-1} KH_2PO_4, 1.33 g L^{-1} $MgSO_4 \cdot 7\,H_2O$, 2.5 g L^{-1} $FeSO_4 \cdot 7\,H_2O$, 2.1 g L^{-1} $C_4H_4Na_2O_6 \cdot 2\,H_2O$, 1.8 g L^{-1} $MnCl_2 \cdot 2\,H_2O$, 0.075 g L^{-1} $CoCl_2 \cdot H_2O$, 0.031 g L^{-1} $CuSO_4 \cdot 5\,H_2O$, 0.258 g L^{-1} H_3BO_3, 0.023 g L^{-1} $Na_2MoO_4 \cdot 2\,H_2O$, 0.021 g L^{-1} $ZnCl_2$, and 10 mL L^{-1} 100x concentrated RPMI 1640 vitamins solution from Sigma Aldrich) and inoculated to an OD_{600} of 0.1 from the pre-culture. The main cultures were cultivated for 48 h at 30 °C, shaking at 200 rpm. After 48 h, the cultures were diluted 1:8 with ddH_2O due to high viscosity. The diluted culture broth was centrifuged for 30 min at maximum speed (25000 rpm)

in an ultracentrifuge. For EPS extraction, the resulting supernatant was mixed 1:2 with 2-propanol (≥98 %), leading to EPS precipitate formation, which could be easily collected. The EPS were dried under the fume hood for 48 h and for further 24 h in a 60 °C incubator.
The procedure was the same for EPS obtained from *B. licheniformis* DSM 13, with the difference that the cultivation temperature was 37 °C instead of 30 °C for this strain, and the main cultures were cultivated in Okonkwo medium modified by Tsigoriyna et al. (2021) (100 g L^{-1} sucrose, 0.5 g L^{-1} $(NH_4)_2SO_4$, 13.38 g L^{-1} yeast extract, 6.41 g L^{-1} peptone from casein, 2.1 g L^{-1} K_2HPO_4, 1.75 g L^{-1} KH_2PO_4, 0.316 g L^{-1} $MgSO_4 \cdot 7\,H_2O$, 1.25 g L^{-1} ammonium acetate, 1.75 mg L^{-1} $CaCl_2 \cdot 2\,H_2O$, 2.5 mg L^{-1} $FeSO_4 \cdot 7\,H_2O$, 2.1 mg L^{-1} sodium tartrate $\cdot 2\,H_2O$, 1.8 mg L^{-1} $MnCl_2 \cdot 2\,H_2O$, 75 µg L^{-1} $CoCl_2 \cdot 6\,H_2O$, 31 µg L^{-1} $CuSO_4 \cdot 5\,H_2O$, 258 µg L^{-1} H_3BO_3, 23 µg L^{-1} $Na_2MoO_4 \cdot 2\,H_2O$, 21 µg L^{-1} $ZnCl_2$, and 10 mL L^{-1} 100x concentrated RPMI 1640 vitamins solution from Sigma Aldrich). Finally, both EPS were freeze-dried and ball-milled.

4.2.2. Gas diffusion measurements

A soil-EPS mixture was used to test the effect of EPS on soil gas diffusion coefficient. Therefore, D_p/D_0 was determined for soils with various particle sizes and 1 mg g^{-1} EPS content produced by *P. polymyxa* DSM 365 and *B. licheniformis* DSM 13 during a drying-rewetting cycle. The setup and the procedure of the experiment are described in Chapter 1.2.6. The soil, the sample preparation, as well as the experimental procedure and setup (Figure 1.4) are the same as in Chapter 3, allowing to compare the effect of EPS and mucilage on soil gas diffusion.

4.3. Results

The effect of dry EPS on air-filled porosity was assumed to be negligible. The dry weight of the EPS per sample was (1.0 ± 0.1) mg g^{-1} dry EPS/dry soil. Assuming that EPS has a density of roughly 1 g cm^{-3}, the volume fraction would be approximately 0.16 % and thus, less than 0.2 % of the volume of the bulk soil would be occupied by EPS.

The relative diffusion coefficient D_p/D_0 as a function of water content for various particle sizes and 1 mg g^{-1} of EPS produced by *P. polymyxa* DSM 365 and *B. licheniformis* DSM 13 during a drying-rewetting cycle is shown in Figure 4.1. Figure A.3

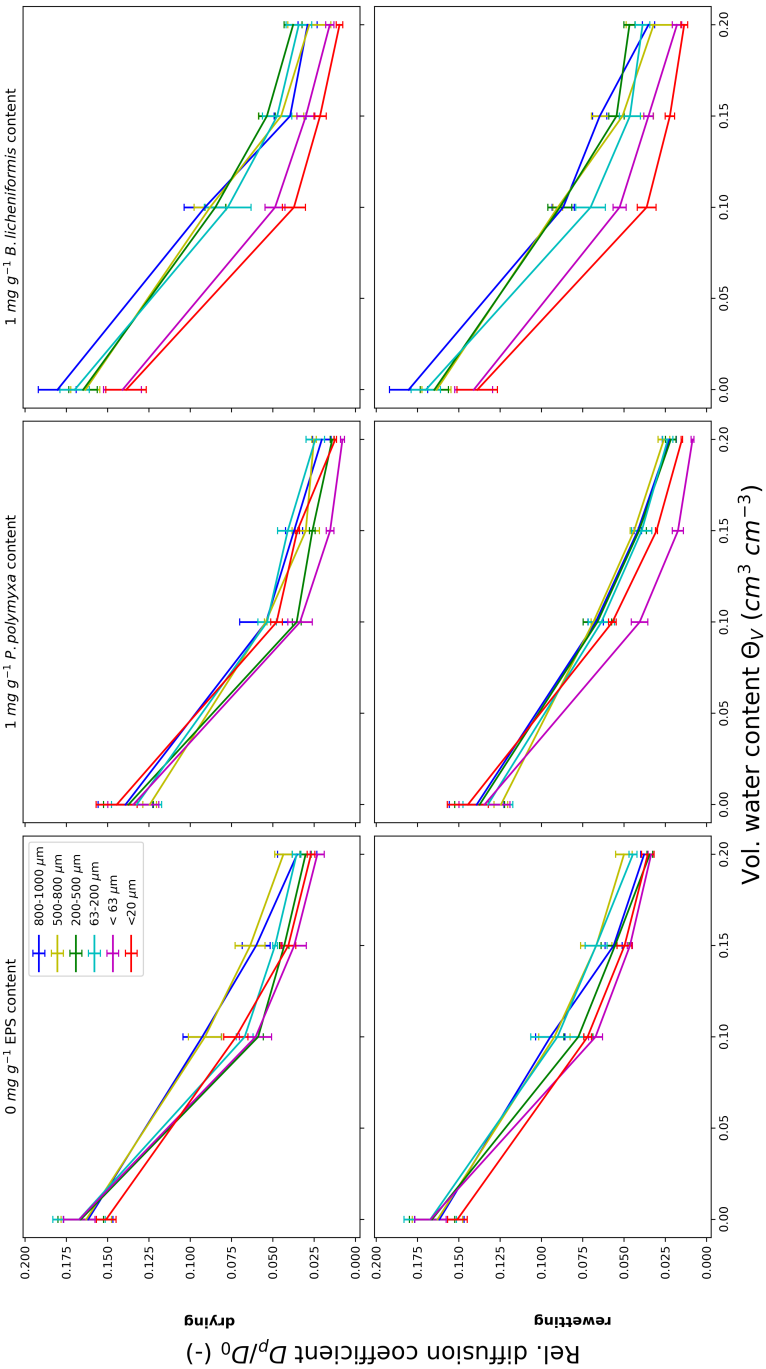

Figure 4.1.: Relative diffusion coefficient D_p/D_0 depending on water content for 1 mg g^{-1} *P. polymyxa* DSM 365 (middle) and *B. licheniformis* DSM 13 (right) EPS content during drying (top row) and rewetting (bottom row). Results indicate a hysteresis for control treatments which diminished with the addition of EPS.

Table 4.1.: Relative diffusion coefficient (D_p/D_0) for dry samples without EPS and the reduction of D_p/D_0 caused by EPS and water.

	Particle size [μm]					
Parameter	**800 – 1000**	**500 – 800**	**200 – 500**	**63 – 200**	**< 40**	**< 20**
D_p/D_0 for control soil	0.162	0.163	0.166	0.167	0.167	0.151
Reduction factor caused by *P. polymyxa* ($1\,\mathrm{mg\,g^{-1}}$)	1.16	1.31	1.21	1.27	1.25	1.05
Reduction factor caused by *B. licheniformis* ($1\,\mathrm{mg\,g^{-1}}$)	0.9	1	1.01	0.99	1.18	1.09
Reduction factor caused by water ($0.2\,\mathrm{cm^3\,cm^{-3}}$ drying)	4.59	4.93	5.53	4.69	7.26	5.59
Reduction factor caused by water ($0.2\,\mathrm{cm^3\,cm^{-3}}$ rewetting)	4.28	4.85	4.88	3.71	4.64	4.19

Note: The reduction caused by EPS was higher for EPS produced by *P. polymyxa*. For EPS produced by *B. licheniformis* only silt (< 40 μm) and clay (< 20 μm) showed a reduction in D_p/D_0. The reduction caused by water was higher during drying compared to rewetting.

shows a comparison between drying and rewetting for each EPS type and control samples as well as each particle size distribution of the artificial soil mixtures. In general, D_p/D_0 decreased with increasing water content. The addition of 1 mg EPS per g soil resulted in a decrease in D_p/D_0 for samples mixed with EPS of *P. polymyxa* DSM 365. For samples mixed with EPS produced by *B. licheniformis*, only silt and clay samples showed a reduction in D_p/D_0 (Table 4.1). Differences in the reduction of D_p/D_0 between drying and rewetting could be observed for untreated samples, resulting in a hysteresis. The extent of the hysteresis varied with the particle size. This effect diminished with the addition of EPS. However, for medium sand samples (200 µm–500 µm) mixed with EPS of *P. polymyxa*, the effect could still be observed. At the highest water content ($0.2\,\mathrm{cm^3\,cm^{-3}}$), D_p/D_0 changed only slightly with the addition of EPS.

4.4. Discussion

Gas diffusion measurements for a soil-EPS mixture with various particle sizes under a drying-rewetting cycle also support the conceptual model developed in Chapter 3 (Figure 3.1). Intrinsic properties of EPS and mucilage (Table 1.1) and their effect on soil gas diffusion are astoundingly similar. This allows us to draw the same conclusions as in Chapter 3. Microbially produced EPS shows a hydrogel-like behavior that is similar to mucilage exuded by plant roots (Nazari et al. 2022). Like mucilage, EPS

form liquid structures between soil particles during drying (Zheng et al. 2018), reducing gas diffusivity by increasing diffusion pathways without affecting air-filled porosity.
In dry soils, the addition of EPS caused only a minor reduction of D_p/D_0 (Figure 4.1). The reduction of D_p/D_0 caused by EPS was not accompanied by a change in air-filled porosity. Compared to untreated samples, EPS derived from *P. polymyxa* showed the highest reduction in sandy soils, where it reduced D_p/D_0 by a factor of 1.31, while *B. licheniformis* EPS reduced D_p/D_0 only in silt (factor 1.18) and clay (factor 1.09) soil samples (Table 4.1). The small sample height (0.6 cm) suggests that fluctuations of porosity and tortuosity were negligible, while no differences in gas diffusion could be observed for the various particle sizes. In general, the addition of water caused a reduction in gas diffusivity. The biggest reduction was observed for silty soil at $0.2\,\mathrm{cm^3\,cm^{-3}}$, where D_p/D_0 was reduced by a factor of 7.26 (Table 4.1). Furthermore, the results confirm the findings of Hamamoto et al. (2022) and of Chapter 3, where also a hysteresis in D_p/D_0 during a drying-rewetting for untreated samples could be observed. Likewise, the extent of the hysteresis depends on particle size and was more distinct in fine-textured soil mixtures. With the addition of EPS, the hysteresis effect diminished. The ink-bottle effect and differences in soil-liquid contact angle can explain the hysteresis effect and the dependence on particle size (Haines 1930; Likos, Lu, and Godt 2014). As for mucilage (Chapter 3), the reduction of the hysteresis effect is caused by the liquid EPS network, which is able to attract water into pores that would not be reached by water during rewetting. In addition, the ability of EPS to swell and push soil particles, as well as EPS bridges between particles that are able to draw particles together during drying, are likely to create preferential diffusion pathways, which reduce the hysteresis effect. An aggregation of sand particles mixed with EPS, indicating that the particles were drawn together, was observed by Zheng et al. (2023).
Benard et al. (2019) developed a conceptual model to describe the persistence of mucilage and EPS structures. They showed that the viscosity of the liquid and the pore diameter play a dominant role in the durability of the structures against drying. Higher viscosity and smaller pore diameter result in more persistent structures. The diffusion measurement results suggest that chia seed mucilage (Chapter 3) and EPS produced by *P. polymyxa* seem to have a similar viscosity, resulting in comparable structures, while EPS produced by *B. licheniformis* seems to be less viscous. Consequently, the structures formed by *B. licheniformis* are less persistent, and the reduction of D_p/D_0 is lower. Nevertheless, the EPS in this study were first produced and harvested, and

afterwards mixed with soil. It remains still unclear how microbial EPS would affect soil gas diffusion if the EPS had been released after incubation of the bacteria in the soil.

4.5. Conclusion

The present study demonstrated the effects of microbially produced EPS on soil gas diffusion processes at the pore scale. Results showed that the addition of EPS reduced soil gas diffusivity, with the effect depending on particle size distribution and the type of EPS. A hysteresis in the gas diffusion coefficient during a drying-rewetting cycle was observed, with the most distinct effect occurring in fine-textured soil mixtures, which was attenuated by the addition of EPS. The findings of this study indicate that microbial activity can impede the movement of gases within soil. Produced EPS accumulate in the pore space, forming structures during drying that are able to clog pores and extend gas diffusion pathways. This process results in a reduction of the gas phase connectivity and consequently in a reduction of soil gas diffusivity. The results of this study emphasize the similarities between mucilage and EPS identified to date and support the hypothesis that microbial communities try to maintain stable physical conditions in the soil in their vicinity by balancing oxygen and water content through EPS production and biofilm formation. Furthermore, gas diffusion measurements prove to be a helpful indicator for geometrical alterations of the pore space induced by hydrogels. This way, we pave the way for further rhizosphere research, since water and gas transport may not only be controlled by plant roots but more by an interplay between plants and microbial communities.

5. Synopsis

5.1. Summary

Gas flow from the soil towards the root and vice versa needs to pass the rhizosphere, a thin layer around the root whose physical properties are actively modified by root growth and rhizodeposition. Besides root exudates, microbes colonising the rhizosphere are capable of modifying soil physical properties by releasing EPS. Both form a net-like structure throughout the pore space during drying, that acts as a barrier for the gas flow.

To describe the effect of mucilage on soil gas exchange, we performed gas diffusion experiments on samples of dry sandy soil mixed with mucilage and took images of glass beads mixed with mucilage to visualize the formation of mucilage bridges after drying, using Environmental Scanning Electron Microscopy. Finally, we set up simulations to characterize the geometric distribution of mucilage within soil during the drying process. Measurements of gas diffusion showed that mucilage decreased the gas diffusion coefficient in dry soil without significantly altering bulk density and porosity. Electron microscopy indicated that mucilage forms filaments and interconnected structures throughout the pore space during drying, thereby reducing the gas phase connectivity. The evolution of these geometric structures was explained via pore scale modelling based on identifying the elastic strength of rhizodeposition during soil drying.

Next, we quantified the effect of a root mucilage analogue collected from chia seeds on oxygen diffusion in various artificial soil textures with no intrinsic respiratory activity at different water contents during drying-rewetting cycles in a diffusion chamber experiment. Quantification of oxygen diffusion showed that mucilage decreased the gas diffusion coefficient in dry soil without affecting air-filled porosity. Without mucilage, a hysteresis of the gas diffusion coefficient during a drying-rewetting cycle was observed. The effect depended on particle size and diminished with increasing mucilage content. X-ray computed tomography (CT) imaging indicated a hysteresis in

the connectivity of the gas phase during a drying-rewetting cycle for samples without mucilage. This effect was attenuated with increasing mucilage content. Furthermore, electron microscopy showed that mucilage structures formed in drying soil increase with mucilage content, thereby progressively reducing the connectivity of the gas phase. We found that the effect of mucilage on soil gas diffusion highly depends on soil texture and mucilage content. The decreasing hysteresis with the addition of mucilage suggests that plants balance oxygen availability and water content even under fluctuating moisture conditions by secreting mucilage.
Finally, we performed gas diffusion experiments to quantify the effect of EPS produced by *Paenibacillus polymyxa* DSM 365 and *Bacillus lechiniformis* DSM 13 on oxygen diffusion for various soil textures at different water contents during a drying-rewetting cycle. We found that in dry soil EPS from *Paenibacillus polymyxa* DSM 365 decreased soil gas diffusivity without affecting air-filled porosity, while EPS from *Bacillus lechiniformis* DSM 13 reduced gas diffusivity only in silt and clay. A hysteresis of the gas diffusion coefficient could be observed for control samples without EPS and depended on soil texture. The decreasing hysteresis effect with the addition of EPS suggests that, as for plants, microbial communities modify the physical properties of the soil to their advantage.

5.2. Synthesis

The objective of this thesis was to quantify the effect of mucilage and EPS on soil gas diffusion. Recently observed net-like structures, that mucilage and EPS form in the pore space of soil during drying seem to favor gas diffusion compared to a uniform layer (Carminati et al. 2017; Ben-Noah and Friedman 2018). Despite the beneficial effects of mucilage and EPS on soil hydraulics, e.g. soil moisture content, root water and nutrient uptake (Table 1.1), they represent an additional barrier for gas movement in soil. However, knowledge to what extent mucilage and EPS structures affect soil gas diffusivity is still lacking.
In Chapter 2, we developed a conceptual model to describe the effect of mucilage on soil gas diffusion under dry conditions and tested it in a gas diffusion experiment with sandy soil. While the most common soil gas diffusion models use air-filled porosity as a parameter to associate barriers for gas movement, e.g. water or organic matter, with reduced gas diffusivity, we have shown that mucilage structures reduce gas diffusivity without affecting air-filled porosity under dry conditions. The reduction in

gas diffusivity can be associated with the different structures mucilage forms depending on its content in the soil. Carminati et al. (2017) observed thin mucilage filaments at low contents and larger structures with increasing content using light transmission microscopy. We could confirm this observations in the pore space of glass beads using environmental scanning electron microscopy. The results confirmed our hypothesis that at low mucilage contents, thin mucilage filaments predominate and have only little effect on gas diffusion in the soil, as the gas can easily diffuse past them. With increasing mucilage content the number of cylindrical structures and interconnected surfaces increases, which are able to clog pores and disconnect the gas phase, resulting in distinct reduction of soil gas diffusivity. In addition, our simulations were able to reproduce the observed cylindrical structures with the addition of mucilage and the broken structures without mucilage (pure water) between two soil particles during drying. In this way, we were able to describe the development of these structures and explain that the cylindrical mucilage structures are hollow inside. All in all, the results of this study show that the different structures have different effects on gas diffusion in soil, at least under dry conditions. Thin filaments allow for relatively unimpeded diffusion of gas, whereas cylindrical structures and interconnected surfaces disrupt the continuity of the gas phase, thereby reducing gas diffusivity. This indicates that mucilage cannot be treated as a uniform layer for modelling gas exchange processes in the rhizosphere and that the mucilage-induced reduction in gas diffusivity is not a factor of air-filled porosity. Due to the formation of thin structures capable of clogging pores and increasing the tortuosity of diffusion pathways, models predicting the impact on gas diffusion in soil require a flexible tortuosity factor to allow for a reasonable estimation of the gas diffusion coefficient.

Based on the results of Chapter 2, we expanded our conceptual model for soil gas diffusion under dry conditions to include various soil textures and water contents during a drying-rewetting cycle (Chapter 3). The results have shown that the effect of mucilage on gas diffusion under dry conditions is strongly dependent on soil texture. While the addition of mucilage in coarse, medium and fine sandy soils led to reduced gas diffusivity, it had no effect in silt and clay soils. A similar effect was observed by Kroener et al. (2018) where the saturated hydraulic conductivity in silt and clay was not affected by mucilage, while it was reduced for coarse, medium and fine sand. It is most likely, that the ratio of average pore diameter and number of potential pore throats is an important factor. In silt and clay, with many small pores, mucilage is unable to settle in every pore, leaving enough pores open for gas

to diffuse through. However, in coarse soils the number of pores is lower, they are broader than in fine-textured soils and mucilage clogs most of them, resulting in a reduction in gas diffusion. Furthermore, Benard et al. (2017) observed that in soils with a high surface roughness, e.g. silt and clay, mucilage structures are smaller compared to structures in soils with low surface roughness at the same mucilage content. A combination of both explains the observed texture-dependent effect of mucilage under dry conditions. Measurements at different water contents during a drying-rewetting cycle revealed a hysteresis effect in gas diffusivity for samples without mucilage. We measured a lower gas diffusion coefficient during drying compared to rewetting at the same water content. This confirms the findings of Hamamoto et al. (2022) who observed a hysteresis in gas diffusion for a sandy soil. The effect is closely related to observed hysteresis in water retention (Haines 1930). Non-uniformity of the pores, entrapped air and different contact angles at liquid-solid interface for drying and rewetting are the factors responsible for the effect. As a result, during drying, narrow parts of interconnected pores are able to hold water and increase the length of diffusion pathways. During rewetting, water might not reach the narrow parts of the pore, leaving space for gas to diffuse. However, the effect diminished with increasing mucilage content. Moreover, to our surprise we observed an increase in diffusion coefficient at low mucilage contents during drying. This suggests that mucilage not only settles in the pore space but also swells and pushes particles during rewetting and draws particles together during drying, thereby affecting soil structure and creating larger pores for preferential gas diffusion. In addition, connectivity measurements of the liquid and the gas phase using X-ray CT also showed a hysteresis effect. However, we were not able to find differences in the connectivity of the two phases between measurements after immediate rewetting and after 4 hours. This indicated a quick equilibrium of the topology of the air-water-mucilage phase. Nevertheless, limitations in voxel resolution and cutting of the images to have comparable samples might have had a large effect on the results, i.e. thin mucilage structures were probably not detectable and most of the water was likely at the bottom of the samples. Finally, we could visualize various mucilage structures depending on mucilage content in the pore space of a coarse sand. Compared to almost perfectly spherical glass beads, mucilage bridges span across the edges of the surface of the soil particles, forming rather membrane-like structures than thin filaments. Furthermore, mucilage structures could be found more frequently in the narrow parts of two or more particles.
The effect of EPS on soil gas diffusion was similar to that of mucilage (Chapter 4).

Their comparable intrinsic properties and similar impacts on soil hydraulics were also reflected in gas diffusion measurements. The results showed a reduction in gas diffusivity in samples containing EPS, with the extent of this effect depending on soil texture. As observed in Chapter 3, a hysteresis in the gas diffusion coefficient was evident in fine-textured soils without EPS, while the addition of EPS reduced this effect. The non-uniformity of pores, entrapped air, and differing contact angles at the liquid-solid interface during drying and rewetting are the key factors responsible for hysteresis. EPS, like mucilage, reduces these effects through the same mechanism as mentioned above. These findings indicate that microbially produced EPS can reduce gas diffusivity, further highlighting the inadequacy of treating EPS or mucilage as uniform layers in models predicting gas diffusion. Nevertheless, additional experimental data across a range of EPS contents are needed to refine our understanding of this effect. The results of this study suggest that both mucilage and EPS influence soil gas diffusion processes. This implies that water and gas transport in soil may be governed not solely by plant roots but also by the interactions between plants and microbial communities.

5.3. Conclusions and outlook

Accurate prediction of soil gas diffusion is critical for optimizing resource utilization, irrigation strategies, and crop performance. Current models often assume mucilage exists as uniform layers surrounding the root (Ben-Noah and Friedman 2018). However, the findings of this thesis demonstrate that upon drying, mucilage forms reticular structures within the pore space, enhancing gas diffusivity compared to a uniform layer. Furthermore, the results indicate that dried mucilage structures reduce gas diffusivity without affecting the soil's air-filled porosity. This highlights the necessity of adapting models to predict gas diffusivity, as current models rely on air-filled porosity as the primary variable controlling changes in soil gas diffusion (Table 1.2). Experiments with EPS reveal that it behaves similarly to mucilage. Incorporating an additional tortuosity factor is essential to improve predictions in soils containing mucilage or EPS. Although mucilage and EPS are generally assumed to settle in the pore space and alter the soil's physical properties, the findings of this thesis suggest that they also modify the soil structure, thereby influencing gas movement. Further research is required to quantify these structural changes and their impact on soil physical properties.
The experiments conducted in this thesis were carried out under simplified conditions;

chia seed mucilage, EPS produced outside of the soil and artificial soils. Therefore, further research is needed to fully understand the impact of mucilage and EPS on soil physical properties, improving our understanding of the complex interactions between crops and soils, which have great implications for root uptake of water and nutrients, gas transport, biogeochemical turnover processes in the soil, and ultimately for crop performance as well as nutrient and water use efficiency. The following additional experiments and improvements are suggested:

- Undisturbed soil samples. Measurements of mucilage and EPS in undisturbed environments.
- Although they have similar physical properties, a shift from a seed mucilage (chia seeds) to a root mucilage (e.g. from maize roots) could help to improve our understanding of the effect of mucilage.
- Measurements with EPS released after incubation of the bacteria in the soil could improve our understanding of the geometrical alterations of the pore space induced by EPS.
- In-situ measurements: At this point, we still lack measurement techniques to perform in-situ rhizosphere experiments. However, diffusion measurements using ^{18}O as a tracer and the development of micro-electrodes capable of functioning in unsaturated soil environments are promising approaches.
- Modeling the evolution of mucilage structures: A shift from perfect spherical soil particles to particles with a higher surface roughness could help to improve our understanding of the various shapes of mucilage structures and represent them more accurately.
- Gas diffusion models: Since the dried mucilage and EPS structures do not affect air-filled porosity, an additional tortuosity factor might be needed to accurately predict the effect of mucilage or EPS on soil gas diffusion.
- CT imaging with a higher resolution than used in this thesis (e.g. synchrotron-based X-ray CT) might help to identify dried mucilage structures, resulting in more accurate connectivity measurements.
- Effects of mucilage and EPS on soil structure: Observed increases in gas diffusivity under certain scenarios lead to the conclusion that mucilage and EPS not only

settles in the pore space. Their ability to swell and shrink might lead to an alteration of the soil structure that seems to benefit gas diffusion. High resolution CT imaging could help to quantify these alterations in soil structure.

A. Appendix

A.1. Supplemental material for chapter 1

Table A.1.: The first six roots, αL, of $(\alpha L)\tan(\alpha L) = hL$. The roots of this equation are all real if $hL > 0$ (Adapted from (Rolston and Moldrup 2018)).

hL	$\alpha_1 L$	$\alpha_2 L$	$\alpha_3 L$	$\alpha_4 L$	$\alpha_5 L$	$\alpha_6 L$
0	0	3.1416	6.2832	9.4248	12.5664	15.7080
0.001	0.0316	3.1419	6.2833	9.4249	12.5665	15.7080
0.002	0.0447	3.1422	6.2835	9.4250	12.5665	15.7081
0.004	0.0632	3.1429	6.2838	9.4252	12.5667	15.7082
0.006	0.0774	3.1435	6.2841	9.4254	12.5668	15.7083
0.008	0.0893	3.1441	6.2845	9.4256	12.5670	15.7085
0.01	0.0998	3.1448	6.2848	9.4258	12.5672	15.7086
0.02	0.1410	3.1479	6.2864	9.4269	12.5680	15.7092
0.04	0.1987	3.1543	6.2895	9.4290	12.5696	15.7105
0.06	0.2425	3.1606	6.2927	9.4311	12.5711	15.7118
0.08	0.2791	3.1668	6.2959	9.4333	12.5727	15.7131
0.1	0.3111	3.1731	6.2991	9.4354	12.5743	15.7143
0.2	0.4328	3.2039	6.3148	9.4459	12.5833	15.7207
0.3	0.5218	3.2341	6.3305	9.4565	12.5902	15.7270
0.4	0.5932	3.2636	6.3461	9.4670	12.5981	15.7344
0.5	0.6533	3.2923	6.3616	9.4775	12.6060	15.7397
0.6	0.7051	3.3204	6.3770	9.4879	12.6139	15.7360
0.7	0.7506	3.3477	6.3923	9.4983	12.6218	15.7524
0.8	0.7910	3.3744	6.4074	9.5087	12.6296	15.7587
0.9	0.8274	3.4003	6.4224	9.5190	12.6375	15.7650
1.0	0.8603	3.4256	6.4373	9.5293	12.6451	15.7713
1.5	0.9882	3.5422	6.5097	9.5801	12.6841	15.7945
2.0	1.0769	3.6436	6.5783	9.6296	12.7223	15.8164
3.0	1.1925	3.8088	6.7040	9.7240	12.7966	15.8945
4.0	1.2646	3.9352	6.8140	9.8119	12.8592	15.9536
5.0	1.3138	4.0336	6.9096	9.8928	12.9135	15.9998
6.0	1.3496	4.1116	6.9924	9.9667	12.9988	16.0654
7.0	1.3766	4.1746	7.0640	10.0339	13.0584	16.1175
8.0	1.3978	4.2264	7.1263	10.0949	13.1141	16.1675
9.0	1.4149	4.2694	7.1806	10.1496	13.1664	16.2153
10.0	1.4289	4.3058	7.2281	10.2003	13.2142	16.2594
15.0	1.4729	4.4255	7.3398	10.3898	13.4078	16.4478
20.0	1.4961	4.4915	7.4954	10.5117	13.5420	16.5864
30.0	1.5202	4.5615	7.6057	10.6540	13.7058	16.7584
40.0	1.5325	4.5979	7.6647	10.7334	13.8048	16.8794
50.0	1.5400	4.6202	7.7012	10.7833	13.8666	16.9519
60.0	1.5451	4.6335	7.7259	10.8172	13.9094	17.0028
80.0	1.5541	4.6543	7.7573	10.8609	13.9644	17.0686
100.0	1.5552	4.6658	7.7764	10.8871	13.9981	17.1068
∞	1.5708	4.7124	7.8540	10.9956	14.1372	17.2788

A.2. Supplemental material for chapter 3

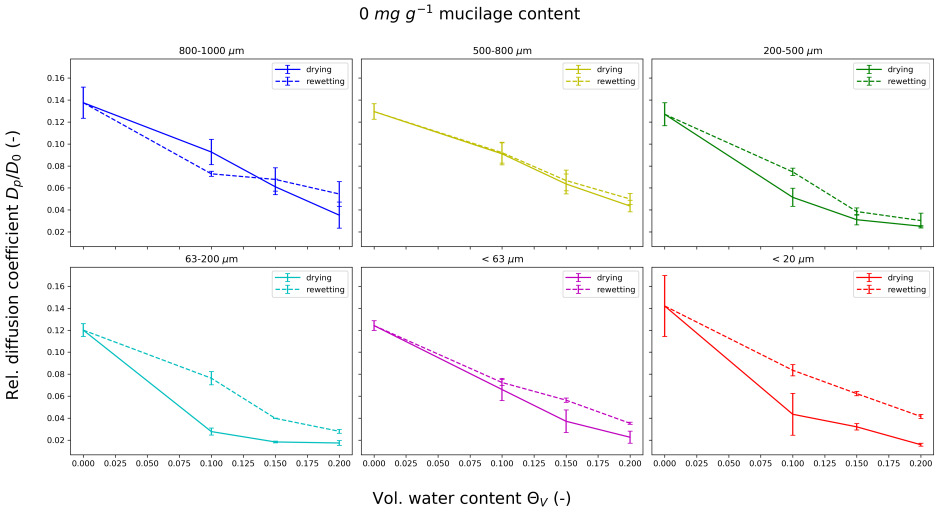

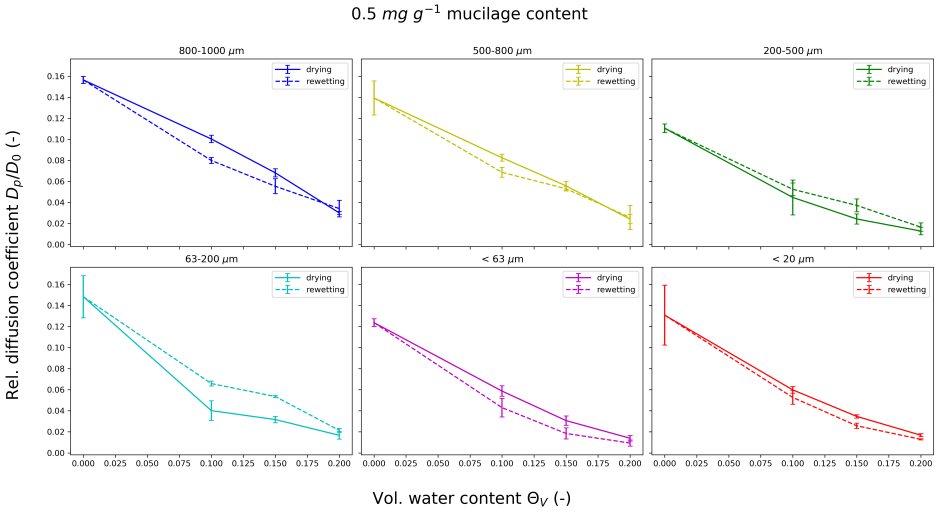

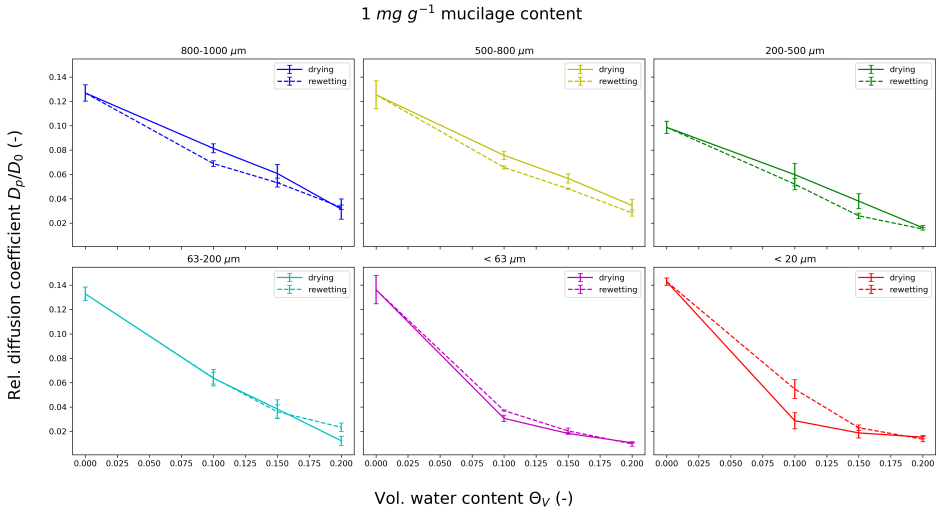
1 mg g^{-1} mucilage content
800-1000 µm
500-800 µm
200-500 µm
63-200 µm
< 63 µm
< 20 µm
drying
rewetting
Rel. diffusion coefficient D_p/D_0 (-)
Vol. water content Θ_V (-)

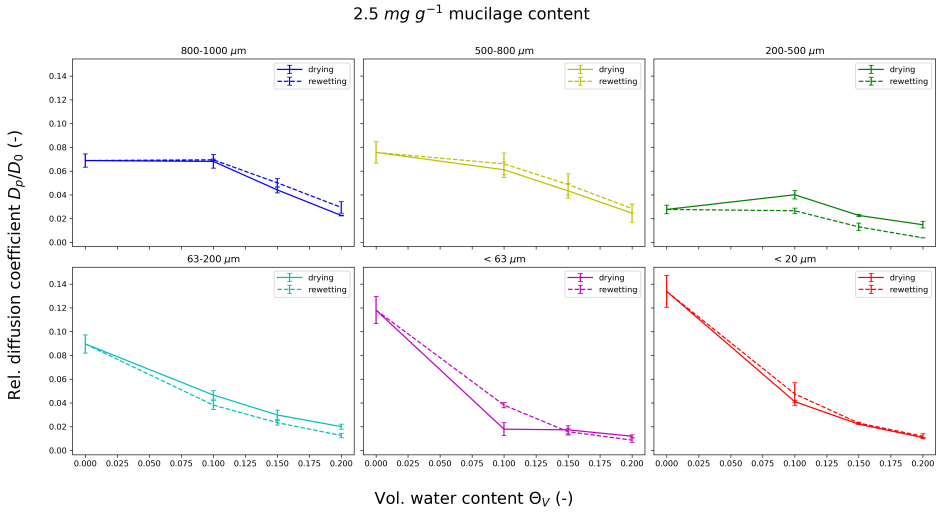
2.5 mg g^{-1} mucilage content
800-1000 µm
500-800 µm
200-500 µm
63-200 µm
< 63 µm
< 20 µm
drying
rewetting
Rel. diffusion coefficient D_p/D_0 (-)
Vol. water content Θ_V (-)

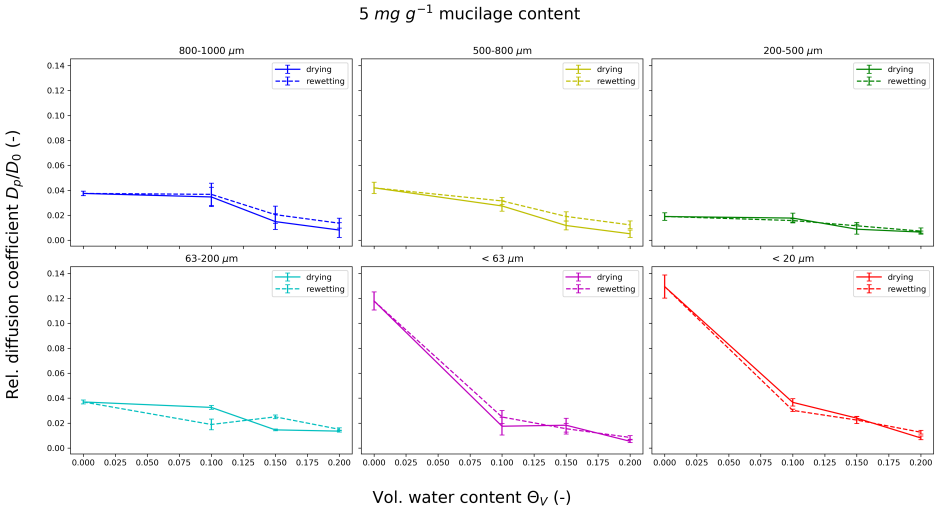

Figure A.1.: Gas diffusion coefficient D_p/D_0 depending on water content for each mucilage content and particle size.

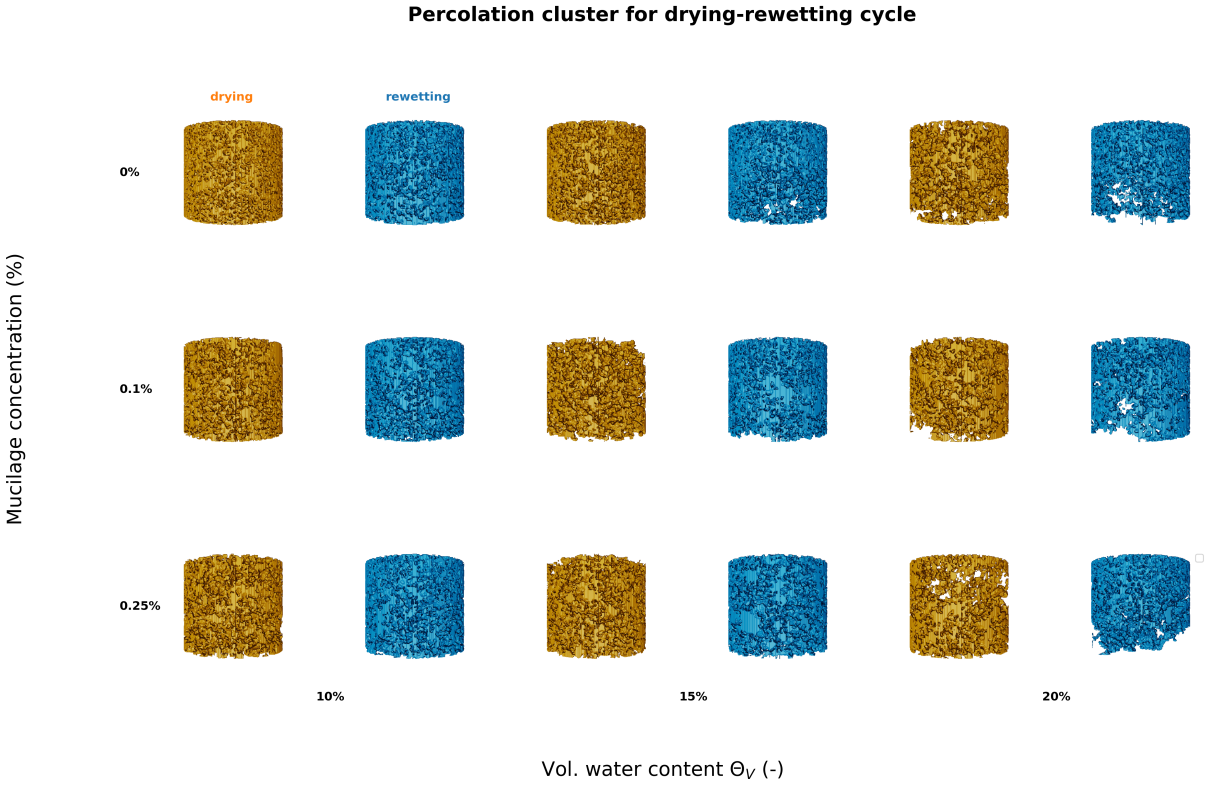

Figure A.2.: Gas phase percolation clusters depending on mucilage content and water content during a drying-rewetting cycle. Images indicate a reduction in the connectivity with increasing mucilage content and water content.

A.3. Supplemental material for chapter 4

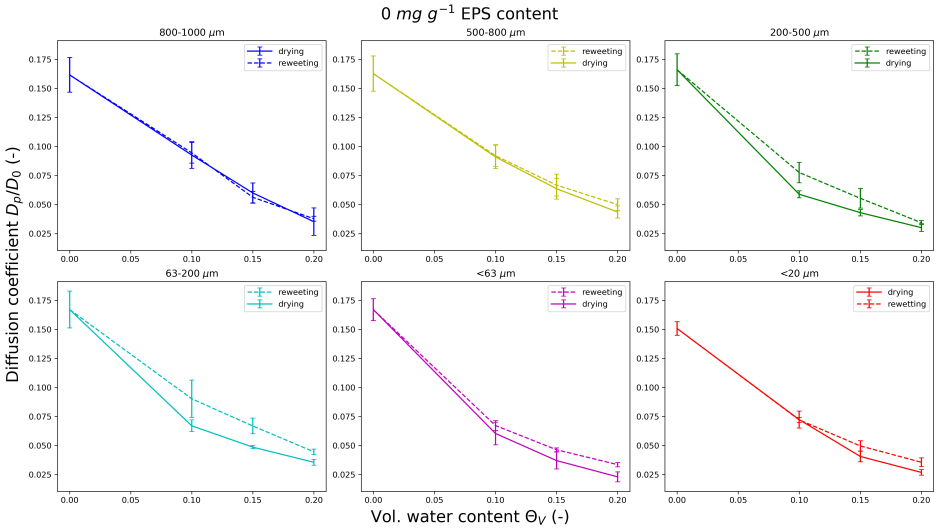

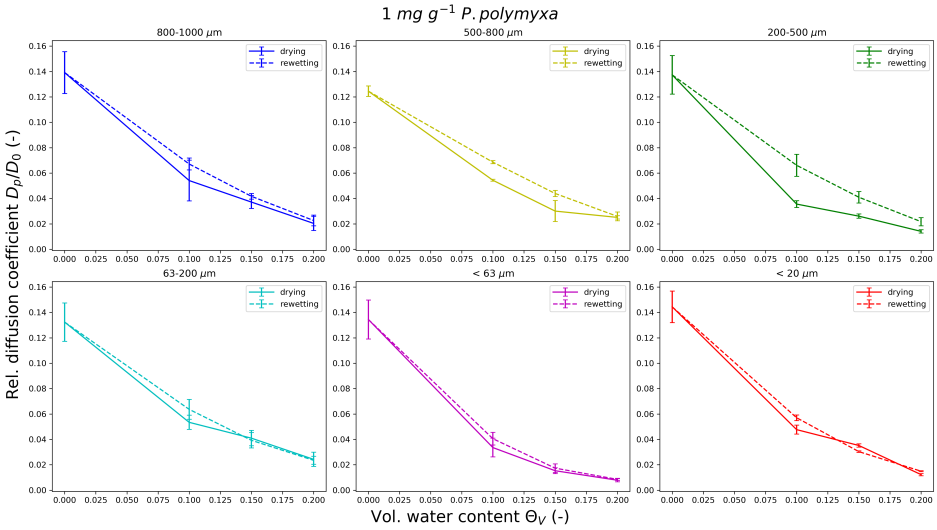

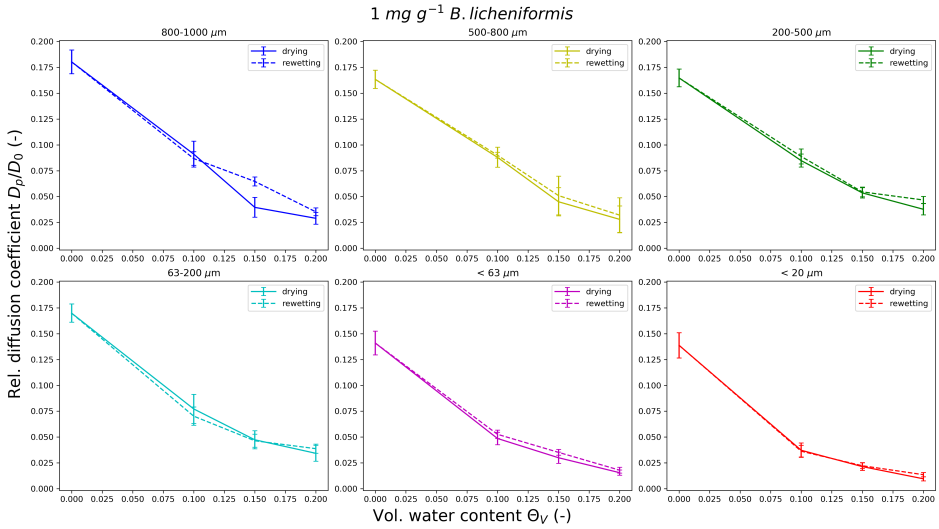

Figure A.3.: Gas diffusion coefficient D_p/D_0 depending on water content for each EPS type and particle size.

References

Adessi, Alessandra, Ricardo Cruz de Carvalho, Roberto De Philippis, Cristina Branquinho, and Jorge Marques da Silva. "Microbial extracellular polymeric substances improve water retention in dryland biological soil crusts." 2018. *Soil Biology and Biochemistry* 116 (January 1, 2018): 67–69. https://doi.org/10.1016/j.soilbio.2017.10.002.

Ahmed, Mutez Ali, Eva Kroener, Pascal Benard, Mohsen Zarebanadkouki, Anders Kaestner, and Andrea Carminati. "Drying of mucilage causes water repellency in the rhizosphere of maize: measurements and modelling." 2016. *Plant Soil* 407 (1): 161–171. https://doi.org/10.1007/s11104-015-2749-1.

Alami, Younes, Wafa Achouak, Christine Marol, and Thierry Heulin. "Rhizosphere Soil Aggregation and Plant Growth Promotion of Sunflowers by an Exopolysaccharide-Producing Rhizobiumsp. Strain Isolated from Sunflower Roots." 2000. *Applied and Environmental Microbiology* 66 (8): 3393–3398. https://doi.org/10.1128/AEM.66.8.3393-3398.2000.

Albalasmeh, Ammar A., and Teamrat A. Ghezzehei. "Interplay between soil drying and root exudation in rhizosheath development." 2014. *Plant Soil* 374 (1-2): 739–751. https://doi.org/10.1007/s11104-013-1910-y.

Allaire, Suzanne, Jonathan Lafond, Alexandre Cabral, and S.F. Lange. "Measurement of gas diffusion through soils: Comparison of laboratory methods." 2008. *J. Environ. Monit.* 10:1326–36. https://doi.org/10.1039/b809461f.

Amthor, Jeffrey S. "The McCree–de Wit–Penning de Vries–Thornley Respiration Paradigms: 30 Years Later." 2000. *Annals of Botany* 86, no. 1 (July 1, 2000): 1–20. https://doi.org/10.1006/anbo.2000.1175.

Aravena, Jazmín E., Markus Berli, Teamrat A. Ghezzehei, and Scott W. Tyler. "Effects of Root-Induced Compaction on Rhizosphere Hydraulic Properties - X-ray Microtomography Imaging and Numerical Simulations." 2011. *Environ. Sci. Technol.* 45 (2): 425–431. https://doi.org/10.1021/es102566j.

Armstrong, W. "Aeration in Higher Plants." 1980. In *Advances in Botanical Research,* edited by H. W. Woolhouse, 7:225–332. Academic Press, January 1, 1980. https://doi.org/10.1016/S0065-2296(08)60089-0.

Badri, Dayakar V., and Jorge M. Vivanco. "Regulation and function of root exudates." 2009. *Plant, Cell Environ.* 32 (6): 666–681. https://doi.org/10.1111/j.1365-3040.2009.01926.x.

Bais, Harsh P., Tiffany L. Weir, Laura G. Perry, Simon Gilroy, and Jorge M. Vivanco. "The Role of Root Exudates in Rhizosphere Interactions with Plants and Other Organisms." 2006. *Annu. Rev. Plant Biol.* 57 (1): 233–266. https://doi.org/10.1146/annurev.arplant.57.032905.105159.

Ben-Noah, Ilan, and Shmulik P. Friedman. "Review and Evaluation of Root Respiration and of Natural and Agricultural Processes of Soil Aeration." 2018. *Vadose Zone J.* 17 (1): 170119. https://doi.org/10.2136/vzj2017.06.0119.

Benard, Pascal, Samuel Bickel, Anders Kaestner, Peter Lehmann, and Andrea Carminati. "Extracellular polymeric substances from soil-grown bacteria delay evaporative drying." 2023. *Advances in Water Resources* 172:104364. https://doi.org/10.1016/j.advwatres.2022.104364.

Benard, Pascal, J. R. Schepers, M. Crosta, M. Zarebanadkouki, and A. Carminati. "Physics of Viscous Bridges in Soil Biological Hotspots." 2021. *Water Resources Research* 57 (11): e2021WR030052. https://doi.org/10.1029/2021WR030052.

Benard, Pascal, M. Zarebanadkouki, C. Hedwig, M. Holz, M. A. Ahmed, and A. Carminati. "Pore-Scale Distribution of Mucilage Affecting Water Repellency in the Rhizosphere." 2017. *Vadose Zone J.* 17 (1): 170013. https://doi.org/10.2136/vzj2017.01.0013.

Benard, Pascal, Mohsen Zarebanadkouki, Mathilde Brax, Robin Kaltenbach, Iwan Jerjen, Federica Marone, Estelle Couradeau, Vincent J. M. N. L. Felde, Anders Kaestner, and Andrea Carminati. "Microhydrological Niches in Soils: How Mucilage and EPS Alter the Biophysical Properties of the Rhizosphere and Other Biological Hotspots." 2019. *Vadose Zone J.* 18 (1): 180211. https://doi.org/10.2136/vzj2018.12.0211.

Benard, Pascal, Mohsen Zarebanadkouki, and Andrea Carminati. "Impact of Pore-Scale Wettability on Rhizosphere Rewetting." 2018. *Front. Environ. Sci.* 6. https://doi.org/10.3389/fenvs.2018.00016.

Benard, Pascal, Mohsen Zarebanadkouki, and Andrea Carminati. "Physics and hydraulics of the rhizosphere network." 2019. *J. Plant Nutr. Soil Sci.* 182 (1): 5–8. https://doi.org/10.1002/jpln.201800042.

Beucher, S., and F. Meyer. "The Morphological Approach to Segmentation: The Watershed Transformation." 1992. In *Mathematical Morphology in Image Processing.* CRC Press.

Bezzate, Samira, Stéphane Aymerich, Régis Chambert, Sonia Czarnes, Odile Berge, and Thierry Heulin. "Disruption of the Paenibacillus polymyxa levansucrase gene impairs its ability to aggregate soil in the wheat rhizosphere." 2000. *Environmental Microbiology* 2 (3): 333–342. https://doi.org/10.1046/j.1462-2920.2000.00114.x.

Bobet, A., A. Fakhimi, S. Johnson, J. Morris, F. Tonon, and M. Ronald Yeung. "Numerical Models in Discontinuous Media: Review of Advances for Rock Mechanics Applications." 2009. *J. Geotech. Geoenviron. Eng.* 135 (11): 1547–1561. https://doi.org/10.1061/(ASCE)GT.1943-5606.0000133.

Brax, Mathilde, Christian Buchmann, Kilian Kenngott, Gabriele Ellen Schaumann, and Dörte Diehl. "Influence of the physico-chemical properties of root mucilage and model substances on the microstructural stability of sand." 2020. *Biogeochemistry* 147 (1): 35–52. https://doi.org/10.1007/s10533-019-00626-w.

Brax, Mathilde, Christian Buchmann, and Gabriele Ellen Schaumann. "Biohydrogel induced soil–water interactions: how to untangle the gel effect? A review." 2017. *Journal of Plant Nutrition and Soil Science* 180 (2): 121–141. https://doi.org/10.1002/jpln.201600453.

Buckingham, Edgar. *Contributions to Our Knowledge of the Aeration of Soils.* 1904. U.S. Government Printing Office.

Carlslaw, HS, and JC Jaeger. "Conduction of Heat in Solids, Oxford." 1959.

Carminati, Andrea, Pascal Benard, Mutez A. Ahmed, and Mohsen Zarebanadkouki. "Liquid bridges at the root-soil interface." 2017. *Plant Soil* 417 (1): 1–15. https://doi.org/10.1007/s11104-017-3227-8.

Carminati, Andrea, Ahmad B. Moradi, Doris Vetterlein, Peter Vontobel, Eberhard Lehmann, Ulrich Weller, Hans-Jörg Vogel, and Sascha E. Oswald. "Dynamics of soil water content in the rhizosphere." 2010. *Plant Soil* 332 (1): 163–176. https://doi.org/10.1007/s11104-010-0283-8.

Carminati, Andrea, M. Zarebanadkouki, E. Kroener, M. A. Ahmed, and M. Holz. "Biophysical rhizosphere processes affecting root water uptake." 2016. *Ann Bot* 118 (4): 561–571. https://doi.org/10.1093/aob/mcw113.

Castrejón-Pita, Alfonso A., J. R. Castrejón-Pita, and I. M. Hutchings. "Breakup of Liquid Filaments." 2012. *Physical Review Letters* 108, no. 7 (February 17, 2012): 074506. https://doi.org/10.1103/PhysRevLett.108.074506.

Chen, Shutao, Jianwen Zou, Zhenghua Hu, Haishan Chen, and Yanyu Lu. "Global annual soil respiration in relation to climate, soil properties and vegetation characteristics: Summary of available data." 2014. *Agricultural and Forest Meteorology* 198-199:335–346. https://doi.org/10.1016/j.agrformet.2014.08.020.

Chenu, Claire. "Clay- or sand-polysaccharide associations as models for the interface between micro-organisms and soil: water related properties and microstructure." 1993. *Geoderma,* International Workshop on Methods of Research on Soil Structure/Soil Biota Interrelationships, 56 (1): 143–156. https://doi.org/10.1016/0016-7061(93)90106-U.

Cooper, L. J., K. R. Daly, P. D. Hallett, M. Naveed, N. Koebernick, A. G. Bengough, T. S. George, and T. Roose. "Fluid flow in porous media using image-based modelling to parametrize Richards' equation." 2017. *Proceedings of the Royal Society A: Mathematical, Physical and Engineering Sciences* 473, no. 2207 (November 22, 2017): 20170178. https://doi.org/10.1098/rspa.2017.0178.

Costa, Ohana Y. A., Jos M. Raaijmakers, and Eiko E. Kuramae. "Microbial Extracellular Polymeric Substances: Ecological Function and Impact on Soil Aggregation." 2018. *Frontiers in Microbiology* 9.

Currie, J A. "Gaseous diffusion in porous media Part 1. - A non-steady state method." 1960. *Br. J. Appl. Phys.* 11 (8): 314–317. https://doi.org/10.1088/0508-3443/11/8/302.

Czarnes, S., P. D. Hallett, A. G. Bengough, and I. M. Young. "Root- and microbial-derived mucilages affect soil structure and water transport." 2000. *Eur. J. Soil Sci.* 51 (3): 435–443. https://doi.org/10.1046/j.1365-2389.2000.00327.x.

Deng, Jinzi, Erika P. Orner, Jessica Furrer Chau, Emily M. Anderson, Andrea L. Kadilak, Rebecca L. Rubinstein, Grant M. Bouchillon, Reed A. Goodwin, Daniel J. Gage, and Leslie M. Shor. "Synergistic effects of soil microstructure and bacterial EPS on drying rate in emulated soil micromodels." 2015. *Soil Biology and Biochemistry* 83 (April 1, 2015): 116–124. https://doi.org/10.1016/j.soilbio.2014.12.006.

Dennis, Paul G., Anthony J. Miller, and Penny R. Hirsch. "Are root exudates more important than other sources of rhizodeposits in structuring rhizosphere bacterial communities?" 2010. *FEMS Microbiol. Ecol.* 72 (3): 313–327. https://doi.org/10.1111/j.1574-6941.2010.00860.x.

Diamantopoulos, E., W. Durner, A. Reszkowska, and J. Bachmann. "Effect of soil water repellency on soil hydraulic properties estimated under dynamic conditions." 2013. *Journal of Hydrology* 486:175–186. https://doi.org/https://doi.org/10.1016/j.jhydrol.2013.01.020.

Dinar, Ariel, Amanda Tieu, and Helen Huynh. "Water scarcity impacts on global food production." 2019. *Global Food Security* 23:212–226. https://doi.org/10.1016/j.gfs.2019.07.007.

Drew, Malcolm C. "OXYGEN DEFICIENCY AND ROOT METABOLISM: Injury and Acclimation Under Hypoxia and Anoxia." 1997. *Annual Review of Plant Biology* 48 (Volume 48, 1997 1997): 223–250. https://doi.org/10.1146/annurev.arplant.48.1.223.

FAO. “Soils, where food begins: how can soils continue to sustain the growing need for food production in the current fertilizer crisis?” 2023. Edited by Food and Agricultural Organization of the United Nations. *ITPS Soil Letters* 6:7.

Ferrell, Ralph T., and David M. Himmelblau. “Diffusion coefficients of nitrogen and oxygen in water.” 1967. *J. Chem. Eng. Data* 12 (1): 111–115. https://doi.org/10.1021/je60032a036.

Flemming, Hans-Curt. “The perfect slime.” 2011. *Colloids and Surfaces B: Biointerfaces* 86, no. 2 (September 1, 2011): 251–259. https://doi.org/10.1016/j.colsurfb.2011.04.025.

Flemming, Hans-Curt, and Jost Wingender. “Relevance of microbial extracellular polymeric substances (EPSs) - Part I: Structural and ecological aspects.” 2001. *Water Science and Technology* 43 (6): 1–8. https://doi.org/10.2166/wst.2001.0326.

Flemming, Hans-Curt, and Jost Wingender. “The biofilm matrix.” 2010. *Nat Rev Microbiol* 8 (9): 623–633. https://doi.org/10.1038/nrmicro2415.

Flemming, Hans-Curt, Jost Wingender, Ulrich Szewzyk, Peter Steinberg, Scott A. Rice, and Staffan Kjelleberg. “Biofilms: an emergent form of bacterial life.” 2016. *Nature Reviews Microbiology* 14, no. 9 (September): 563–575. https://doi.org/10.1038/nrmicro.2016.94.

Fujikawa, Tomonori, and Tsuyoshi Miyazaki. “Effects of Bulk Density and Soil Type on the Gas Diffusion Coefficient in Repacked and Undisturbed Soils:” 2005. *Soil Science* 170 (11): 892–901. https://doi.org/10.1097/01.ss.0000196771.53574.79.

Gardner, Catriona MK, Kofi Budu Laryea, and Paul W. Unger. *Soil physical constraints to plant growth and crop production.* 1999. Vol. 11. Citeseer.

Gerten, D., J. Heinke, H. Hoff, H. Biemans, M. Fader, and K. Waha. “Global Water Availability and Requirements for Future Food Production.” 2011. *Journal of Hydrometeorology* 12 (5): 885–899. https://doi.org/10.1175/2011JHM1328.1.

Gliński, Jan, and Witold Stępniewski. *Soil Aeration and Its Role for Plants.* 1985. Boca Raton: CRC Press. https://doi.org/10.1201/9781351076685.

Gregory, P. J. “Roots, rhizosphere and soil: the route to a better understanding of soil science?” 2006. *Eur. J. Soil Sci.* 57 (1): 2–12. https://doi.org/10.1111/j.1365-2389.2005.00778.x.

Haichar, Feth el Zahar, Christine Marol, Odile Berge, J. Ignacio Rangel-Castro, James I. Prosser, Jérôme Balesdent, Thierry Heulin, and Wafa Achouak. "Plant host habitat and root exudates shape soil bacterial community structure." 2008. *The ISME Journal* 2 (12): 1221–1230. https://doi.org/10.1038/ismej.2008.80.

Haines, William B. "Studies in the physical properties of soil. V. The hysteresis effect in capillary properties, and the modes of moisture distribution associated therewith." 1930. *The Journal of Agricultural Science* 20 (1): 97–116. https://doi.org/10.1017/S002185960008864X.

Hallett, P. D., D. C. Gordon, and A. G. Bengough. "Plant influence on rhizosphere hydraulic properties: direct measurements using a miniaturized infiltrometer." 2003. *New Phytol.* 157 (3): 597–603. https://doi.org/10.1046/j.1469-8137.2003.00690.x.

Hallett, Paul D., Maria Marin, Gary D. Bending, Timothy S. George, Chris D. Collins, and Wilfred Otten. "Building soil sustainability from root–soil interface traits." 2022. *Trends in Plant Science,* Special issue: Climate change and sustainability I, 27 (7): 688–698. https://doi.org/10.1016/j.tplants.2022.01.010.

Hamamoto, Shoichiro, Per Moldrup, Ken Kawamoto, and Toshiko Komatsu. "Effect of Particle Size and Soil Compaction on Gas Transport Parameters in Variably Saturated, Sandy Soils." 2009. *Vadose Zone Journal* 8 (4): 986–995. https://doi.org/10.2136/vzj2008.0157.

Hamamoto, Shoichiro, Per Moldrup, Ken Kawamoto, and Toshiko Komatsu. "Organic Matter Fraction Dependent Model for Predicting the Gas Diffusion Coefficient in Variably Saturated Soils." 2012. *Vadose Zone Journal* 11 (1). https://doi.org/10.2136/vzj2011.0065.

Hamamoto, Shoichiro, Yushi Ohko, Yutaka Ohtake, Per Moldrup, and Taku Nishimura. "Water- and air-filled pore networks and transport parameters under drying and wetting processes." 2022. *Vadose Zone Journal* n/a (n/a): e20205. https://doi.org/10.1002/vzj2.20205.

Hanson, P.J., N.T. Edwards, C.T. Garten, and J.A. Andrews. "Separating root and soil microbial contributions to soil respiration: A review of methods and observations." 2000. *Biogeochemistry* 48 (1): 115–146. https://doi.org/10.1023/A:1006244819642.

Haupenthal, Adrian, Mathilde Brax, Jonas Bentz, Hermann F. Jungkunst, Klaus Schützenmeister, and Eva Kroener. "Plants control soil gas exchanges possibly via mucilage." 2021. *Journal of Plant Nutrition and Soil Science* 184 (3): 320–328. https://doi.org/10.1002/jpln.202000496.

Haupenthal, Adrian, Patrick Duddek, Pascal Benard, Mathilde Knott, Andrea Carminati, Hermann F. Jungkunst, Eva Kroener, and Nicolas Brüggemann. "A root mucilage analogue from chia seeds reduces soil gas diffusivity." 2024. *European Journal of Soil Science* 75 (5): e13576. https://doi.org/10.1111/ejss.13576.

Hinsinger, Philippe, A. Glyn Bengough, Doris Vetterlein, and Iain M. Young. "Rhizosphere: biophysics, biogeochemistry and ecological relevance." 2009. *Plant Soil* 321 (1): 117–152. https://doi.org/10.1007/s11104-008-9885-9.

Hocke, Klemens. "Oxygen in the Earth System." 2023. *Oxygen* 3, no. 3 (September): 287–299. https://doi.org/10.3390/oxygen3030019.

Holz, Maire, Mohsen Zarebanadkouki, Andrea Carminati, Jan Hovind, Anders Kaestner, and Marie Spohn. "Increased water retention in the rhizosphere allows for high phosphatase activity in drying soil." 2019. *Plant Soil* 443 (1): 259–271. https://doi.org/10.1007/s11104-019-04234-3.

Jensen, Creighton R., and Don Kirkham. "Labeled Oxygen: Increased Diffusion Rate through Soil Containing Growing Corn Roots." 1963. *Science* 141 (3582): 735–736. https://doi.org/10.1126/science.141.3582.735.

Jeong, Haeyoung, Soo-Keun Choi, Choong-Min Ryu, and Seung-Hwan Park. "Chronicle of a Soil Bacterium: Paenibacillus polymyxa E681 as a Tiny Guardian of Plant and Human Health." 2019. *Frontiers in Microbiology* 10.

Kimber, James A., Sergei G. Kazarian, and František Štěpánek. "Modelling of pharmaceutical tablet swelling and dissolution using discrete element method." 2012. *Chem. Eng. Sci.* 69 (1): 394–403. https://doi.org/10.1016/j.ces.2011.10.066.

Koestel, J., M. Larsbo, and N. Jarvis. "Scale and REV analyses for porosity and pore connectivity measures in undisturbed soil." 2020. *Geoderma* 366:114206. https://doi.org/10.1016/j.geoderma.2020.114206.

Körstgens, V., H.-C. Flemming, J. Wingender, and W. Borchard. “Influence of calcium ions on the mechanical properties of a model biofilm of mucoid Pseudomonas aeruginosa.” 2001. *Water Science and Technology* 43, no. 6 (March 1, 2001): 49–57. https://doi.org/10.2166/wst.2001.0338.

Kroener, Eva, Maire Holz, Mohsen Zarebanadkouki, Mutez Ahmed, and Andrea Carminati. “Effects of Mucilage on Rhizosphere Hydraulic Functions Depend on Soil Particle Size.” 2018. *Vadose Zone J.* 17 (1): 170056. https://doi.org/10.2136/vzj2017.03.0056.

Kroener, Eva, Mohsen Zarebanadkouki, Anders Kaestner, and Andrea Carminati. “Nonequilibrium water dynamics in the rhizosphere: How mucilage affects water flow in soils.” 2014. *Water Resour. Res.* 50 (8): 6479–6495. https://doi.org/10.1002/2013WR014756.

Kuzyakov, Yakov, and Evgenia Blagodatskaya. “Microbial hotspots and hot moments in soil: Concept & review.” 2015. *Soil Biology and Biochemistry* 83:184–199. https://doi.org/10.1016/j.soilbio.2015.01.025.

Lambers, Hans, Eveliene Steingröver, and Gerard Smakman. “The Significance of Oxygen Transport and of Metabolic Adaptation in Flood-Tolerance of Senecio Species.” 1978. *Physiologia Plantarum* 43 (3): 277–281. https://doi.org/10.1111/j.1399-3054.1978.tb02578.x.

Lazarovitch, Naftali, Jan Vanderborght, Yan Jin, and Martinus Van Genuchten. “The Root Zone: Soil Physics and Beyond.” 2018. *Vadose Zone J.* 17. https://doi.org/10.2136/vzj2018.01.0002.

Lieleg, Oliver, Marina Caldara, Regina Baumgärtel, and Katharina Ribbeck. “Mechanical robustness of Pseudomonasaeruginosa biofilms.” 2011. *Soft Matter* 7, no. 7 (March 22, 2011): 3307–3314. https://doi.org/10.1039/C0SM01467B.

Likos, William J., Ning Lu, and Jonathan W. Godt. “Hysteresis and Uncertainty in Soil Water-Retention Curve Parameters.” 2014. *J. Geotech. Geoenviron. Eng.* 140 (4): 04013050. https://doi.org/10.1061/(ASCE)GT.1943-5606.0001071.

Liu, Gang, Baoguo Li, Kelin Hu, and M. Th. van Genuchten. “Simulating the Gas Diffusion Coefficient in Macropore Network Images: Influence of Soil Pore Morphology.” 2006. *Soil Science Society of America Journal* 70 (4): 1252–1261. https://doi.org/10.2136/sssaj2005.0199.

Lucas, Maik, Doris Vetterlein, Hans-Jörg Vogel, and Steffen Schlüter. "Revealing pore connectivity across scales and resolutions with X-ray CT." 2021. *European Journal of Soil Science* 72 (2): 546–560. https://doi.org/10.1111/ejss.12961.

Lynch, J. M., and J. M. Whipps. "Substrate flow in the rhizosphere." 1990. *Plant and Soil* 129, no. 1 (December 1, 1990): 1–10. https://doi.org/10.1007/BF00011685.

Lynch, Jonathan P., and Kathleen M. Brown. "New roots for agriculture: exploiting the root phenome." 2012. *Philosophical Transactions of the Royal Society B: Biological Sciences* 367 (1595): 1598–1604. https://doi.org/10.1098/rstb.2011.0243.

Mahdi, Ismail, Nidal Fahsi, Mohamed Hafidi, Abdelmounaaim Allaoui, and Latefa Biskri. "Plant Growth Enhancement using Rhizospheric Halotolerant Phosphate Solubilizing Bacterium Bacillus licheniformis QA1 and Enterobacter asburiae QF11 Isolated from Chenopodium quinoa Willd." 2020. *Microorganisms* 8 (6): 948. https://doi.org/10.3390/microorganisms8060948.

Marshall, T. J. "The Diffusion of Gases Through Porous Media." 1959. *J. Soil Sci.* 10 (1): 79–82. https://doi.org/10.1111/j.1365-2389.1959.tb00667.x.

McCully, M. E., and J. S. Boyer. "The expansion of maize root-cap mucilage during hydration. 3. Changes in water potential and water content." 1997. *Physiol. Plant.* 99 (1): 169–177. https://doi.org/10.1111/j.1399-3054.1997.tb03445.x.

Millington, R. J., and J. P. Quirk. "Permeability of porous solids." 1961. *Trans. Faraday Soc.* 57 (0): 1200–1207. https://doi.org/10.1039/TF9615701200.

Misiewicz, Jakub, Arkadiusz Głogowski, Krzysztof Lejcuś, and Daria Marczak. "The Characteristics of Swelling Pressure for Superabsorbent Polymer and Soil Mixtures." 2020. *Materials* 13 (22): 5071. https://doi.org/10.3390/ma13225071.

Moldrup, Per, T.k.k. Chamindu Deepagoda, Shoichiro Hamamoto, Toshiko Komatsu, Ken Kawamoto, Dennis E. Rolston, and Lis Wollesen de Jonge. "Structure-Dependent Water-Induced Linear Reduction Model for Predicting Gas Diffusivity and Tortuosity in Repacked and Intact Soil." 2013. *Vadose Zone Journal* 12 (3): vzj2013.01.0026. https://doi.org/10.2136/vzj2013.01.0026.

Moldrup, Per, T. Olesen, J. Gamst, P. Schjønning, T. Yamaguchi, and D.e. Rolston. "Predicting the Gas Diffusion Coefficient in Repacked Soil Water-Induced Linear Reduction Model." 2000. *Soil Science Society of America Journal* 64 (5): 1588–1594. https://doi.org/10.2136/sssaj2000.6451588x.

Moldrup, Per, T. Olesen, D. E. Rolston, and T. Yamaguchi. "MODELING DIFFUSION AND REACTION IN SOILS: VII. PREDICTING GAS AND ION DIFFUSIVITY IN UNDISTURBED AND SIEVED SOILS." 1997. *Soil Science* 162, no. 9 (September): 632.

Moldrup, Per, Torben Olesen, Seiko Yoshikawa, Toshiko Komatsu, and Dennis E. Rolston. "Three-Porosity Model for Predicting the Gas Diffusion Coefficient in Undisturbed Soil." 2004. *Soil Sci. Soc. Am. J.* 68 (3): 750–759. https://doi.org/10.2136/sssaj2004.7500.

Moradi, Ahmad B., Andrea Carminati, Axel Lamparter, Susanne K. Woche, Jörg Bachmann, Doris Vetterlein, Hans-Jörg Vogel, and Sascha E. Oswald. "Is the Rhizosphere Temporarily Water Repellent?" 2012. *Vadose Zone Journal* 11 (3): vzj2011.0120. https://doi.org/10.2136/vzj2011.0120.

Morel, Jean Louis, Leila Habib, Sylvain Plantureux, and Armand Guckert. "Influence of maize root mucilage on soil aggregate stability." 1991. *Plant Soil* 136 (1): 111–119. https://doi.org/10.1007/BF02465226.

Munjiza, A., D.R.J. Owen, and N. Bicanic. "A combined finite-discrete element method in transient dynamics of fracturing solids." 1995. *Eng. Comput.* 12 (2): 145–174. https://doi.org/10.1108/02644409510799532.

Muñoz, L. A., A. Cobos, O. Diaz, and J. M. Aguilera. "Chia seeds: Microstructure, mucilage extraction and hydration." 2012. *J. Food Eng.* 108 (1): 216–224. https://doi.org/10.1016/j.jfoodeng.2011.06.037.

National Research Council. *Nutrient Requirements of Dairy Cattle: Seventh Revised Edition, 2001.* 2000. https://doi.org/10.17226/9825.

Naveed, M., M. A. Ahmed, P. Benard, L. K. Brown, T. S. George, A. G. Bengough, T. Roose, N. Koebernick, and P. D. Hallett. "Surface tension, rheology and hydrophobicity of rhizodeposits and seed mucilage influence soil water retention and hysteresis." 2019. *Plant Soil* 437 (1-2): 65–81. https://doi.org/10.1007/s11104-019-03939-9.

Naveed, M., L. K. Brown, A. C. Raffan, T. S. George, A. G. Bengough, T. Roose, I. Sinclair, et al. "Plant exudates may stabilize or weaken soil depending on species, origin and time." 2017. *Eur. J. Soil Sci.* 68 (6): 806–816. https://doi.org/10.1111/ejss.12487.

Nazari, Meisam. “Plant mucilage components and their functions in the rhizosphere.” 2021. *Rhizosphere* 18:100344. https://doi.org/10.1016/j.rhisph.2021.100344.

Nazari, Meisam, Samuel Bickel, Pascal Benard, Kyle Mason-Jones, Andrea Carminati, and Michaela A. Dippold. “Biogels in Soils: Plant Mucilage as a Biofilm Matrix That Shapes the Rhizosphere Microbial Habitat.” 2022. *Frontiers in Plant Science* 12.

Ohnesorge, Wolfgang V. “Die Bildung von Tropfen an Düsen und die Auflösung flüssiger Strahlen.” 1936. *ZAMM - Journal of Applied Mathematics and Mechanics / Zeitschrift für Angewandte Mathematik und Mechanik* 16 (6): 355–358. https://doi.org/10.1002/zamm.19360160611.

Oleghe, E., M. Naveed, E. M. Baggs, and P. D. Hallett. “Residues with varying decomposability interact differently with seed or root exudate compounds to affect the biophysical behaviour of soil.” 2019. *Geoderma* 343:50–59. https://doi.org/10.1016/j.geoderma.2019.02.023.

Or, D., B. F. Smets, J. M. Wraith, A. Dechesne, and S. P. Friedman. “Physical constraints affecting bacterial habitats and activity in unsaturated porous media – a review.” 2007. *Advances in Water Resources,* Biological processes in porous media: From the pore scale to the field, 30 (6): 1505–1527. https://doi.org/10.1016/j.advwatres.2006.05.025.

Or, Dani, Sachin Phutane, and Arnaud Dechesne. “Extracellular Polymeric Substances Affecting Pore-Scale Hydrologic Conditions for Bacterial Activity in Unsaturated Soils.” 2007. *Vadose Zone Journal* 6 (2): 298–305. https://doi.org/10.2136/vzj2006.0080.

Patel, Ravi, Janez Perko, and Diederik Jacques. “Yantra: A lattice Boltzmann method based simulation tool modelling physico-chemical processes in concrete at different spatial scales.” 2017.

Penman, H. L. “Gas and vapour movements in the soil: II. The diffusion of carbon dioxide through porous solids.” 1940. *The Journal of Agricultural Science* 30 (4): 570–581. https://doi.org/10.1017/S0021859600048231.

Petrova, Penka, Alexander Arsov, Ivan Ivanov, Lidia Tsigoriyna, and Kaloyan Petrov. "New Exopolysaccharides Produced by Bacillus licheniformis 24 Display Substrate-Dependent Content and Antioxidant Activity." 2021. *Microorganisms* 9 (10): 2127. https://doi.org/10.3390/microorganisms9102127.

Pot, V., S. Peth, O. Monga, L. E. Vogel, A. Genty, P. Garnier, L. Vieublé-Gonod, M. Ogurreck, F. Beckmann, and P. C. Baveye. "Three-dimensional distribution of water and air in soil pores: Comparison of two-phase two-relaxation-times lattice-Boltzmann and morphological model outputs with synchrotron X-ray computed tomography data." 2015. *Adv. Water Resour.* 84:87–102. https://doi.org/10.1016/j.advwatres.2015.08.006.

Raaijmakers, Jos M., Irene De Bruijn, Ole Nybroe, and Marc Ongena. "Natural functions of lipopeptides from Bacillus and Pseudomonas: more than surfactants and antibiotics." 2010. *FEMS Microbiology Reviews* 34, no. 6 (November 1, 2010): 1037–1062. https://doi.org/10.1111/j.1574-6976.2010.00221.x.

Rahim, Riffat, Omid Esmaeelipoor Jahromi, Wulf Amelung, and Eva Kroener. "Rhizosheath formation depends on mucilage concentration and water content." 2024. *Plant and Soil* 495, no. 1 (February 1, 2024): 649–661. https://doi.org/10.1007/s11104-023-06353-4.

Read, D. B., A. G. Bengough, P. J. Gregory, J. W. Crawford, D. Robinson, C. M. Scrimgeour, I. M. Young, K. Zhang, and X. Zhang. "Plant roots release phospholipid surfactants that modify the physical and chemical properties of soil." 2003. *New Phytol.* 157 (2): 315–326. https://doi.org/10.1046/j.1469-8137.2003.00665.x.

Read, D. B., and P. J. Gregory. "Surface Tension and Viscosity of Axenic Maize and Lupin Root Mucilages." 1997. *New Phytol.* 137 (4): 623–628.

Read, D.B., P.J. Gregory, and A.E. Bell. "Physical properties of axenic maize root mucilage." 1999. *Plant and Soil* 211, no. 1 (April 1, 1999): 87–91. https://doi.org/10.1023/A:1004403812307.

Redmile-Gordon, M. A., P. C. Brookes, R. P. Evershed, K. W. T. Goulding, and P. R. Hirsch. "Measuring the soil-microbial interface: Extraction of extracellular polymeric substances (EPS) from soil biofilms." 2014. *Soil Biology and Biochemistry* 72:163–171. https://doi.org/10.1016/j.soilbio.2014.01.025.

Renard, Philippe, and Denis Allard. “Connectivity metrics for subsurface flow and transport.” 2013. *Advances in Water Resources,* 35th Year Anniversary Issue, 51:168–196. https://doi.org/10.1016/j.advwatres.2011.12.001.

Richefeu, Vincent, Farhang Radjai, and Jean-Yves Delenne. “Lattice Boltzmann modelling of liquid distribution in unsaturated granular media.” 2016. *Comput. and Geot.* 80:353–359. https://doi.org/10.1016/j.compgeo.2016.02.017.

Rivoal, J., and A. D. Hanson. “Metabolic Control of Anaerobic Glycolysis (Overexpression of Lactate Dehydrogenase in Transgenic Tomato Roots Supports the Davies-Roberts Hypothesis and Points to a Critical Role for Lactate Secretion.” 1994. *Plant Physiol.* 106 (3): 1179–1185. https://doi.org/10.1104/pp.106.3.1179.

Roberson, Emily B., Claire Chenu, and Mary K. Firestone. “Microstructural changes in bacterial exopolysaccharides during desiccation.” 1993. *Soil Biology and Biochemistry* 25 (9): 1299–1301. https://doi.org/10.1016/0038-0717(93)90230-9.

Roberson, Emily B., and Mary K. Firestone. “Relationship between Desiccation and Exopolysaccharide Production in a Soil Pseudomonas sp.” 1992. *Applied and Environmental Microbiology* 58 (4): 1284–1291. https://doi.org/10.1128/aem.58.4.1284-1291.1992.

Rolston, D. E. “Gas Diffusivity.” 1986. In *Methods of Soil Analysis,* 1089–1102. John Wiley & Sons, Ltd. https://doi.org/10.2136/sssabookser5.1.2ed.c46.

Rolston, Dennis E., and Per Moldrup. “4.3 Gas Diffusivity.” 2018. In *Methods of Soil Analysis,* 1113–1139. John Wiley & Sons, Ltd. https://doi.org/10.2136/sssabookser5.4.c45.

Rosenzweig, Ravid, Uri Shavit, and Alex Furman. “Water Retention Curves of Biofilm-Affected Soils using Xanthan as an Analogue.” 2012. *Soil Science Society of America Journal* 76 (1): 61–69. https://doi.org/10.2136/sssaj2011.0155.

Russell, Edward John, and Alfred Appleyard. “The Atmosphere of the Soil: Its Composition and the Causes of Variation.” 1915. *The Journal of Agricultural Science* 7, no. 1 (March): 1–48. https://doi.org/10.1017/S0021859600002410.

Saha, Abhisekh, Sreedeep Sekharan, and Uttam Manna. “Hysteresis Model for Water Retention Characteristics of Water-Absorbing Polymer-Amended Soils.” 2022. *Journal of Geotechnical and Geoenvironmental Engineering* 148 (4): 04022008. https://doi.org/10.1061/(ASCE)GT.1943-5606.0002764.

Scanlon, Bridget, Jean-Philippe Nicot, and Joel Massmann. “8 Soil Gas Movement in Unsaturated Systems.” 2001. *Soil Physics Companion* (December 28, 2001). https://doi.org/10.1201/9781420041651.ch8.

Scherer, Laura, Jens-Christian Svenning, Jing Huang, Colleen L. Seymour, Brody Sandel, Nathaniel Mueller, Matti Kummu, et al. “Global priorities of environmental issues to combat food insecurity and biodiversity loss.” 2020. *Science of The Total Environment* 730:139096. https://doi.org/10.1016/j.scitotenv.2020.139096.

Schimel, Joshua P. “Life in Dry Soils: Effects of Drought on Soil Microbial Communities and Processes.” 2018. *Annu. Rev. Ecol. Evol. Syst.* 49 (1): 409–432. https://doi.org/10.1146/annurev-ecolsys-110617-062614.

Schmid, Jochen, Volker Sieber, and Bernd Rehm. “Bacterial exopolysaccharides: biosynthesis pathways and engineering strategies.” 2015. *Frontiers in Microbiology* 6. https://doi.org/10.3389/fmicb.2015.00496.

Segura-Campos, Maira Rubi, Norma Ciau-Solís, Gabriel Rosado-Rubio, Luis Chel-Guerrero, and David Betancur-Ancona. “Chemical and Functional Properties of Chia Seed (Salvia hispanica L.) Gum.” 2014. *International Journal of Food Science* 2014 (1): 241053. https://doi.org/10.1155/2014/241053.

Shan, Xiaowen, and Hudong Chen. “Lattice Boltzmann model for simulating flows with multiple phases and components.” 1993. *Phys. Rev. E* 47 (3): 1815–1819. https://doi.org/10.1103/PhysRevE.47.1815.

Shaw, T., M. Winston, C. J. Rupp, I. Klapper, and P. Stoodley. “Commonality of Elastic Relaxation Times in Biofilms.” 2004. *Physical Review Letters* 93, no. 9 (August 24, 2004): 098102. https://doi.org/10.1103/PhysRevLett.93.098102.

Stępniewski, W., Z. Stępniewska, R. P. Bennicelli, and J. Gliński. *Oxygenology in Outline. EU 5th Framework Program QLAM – 2001–00428.* 2005. Lublin: Institute of Agrophysics PAS.

Stoodley, P, R Cargo, C J Rupp, S Wilson, and I Klapper. “Biofilm material properties as related to shear-induced deformation and detachment phenomena.” 2002. *Journal of Industrial Microbiology and Biotechnology* 29, no. 6 (December 1, 2002): 361–367. https://doi.org/10.1038/sj.jim.7000282.

Sukop, Michael C., and Dani Or. “Lattice Boltzmann method for modeling liquid-vapor interface configurations in porous media.” 2004. *Water Resour. Res.* 40 (1). https://doi.org/10.1029/2003WR002333.

Sutherland, Ian W. “Biofilm exopolysaccharides: a strong and sticky framework.” 2001. *Microbiology* 147 (1): 3–9. https://doi.org/10.1099/00221287-147-1-3.

Thorbjørn, Anne, Per Moldrup, Helle Blendstrup, Toshiko Komatsu, and Dennis E. Rolston. “A Gas Diffusivity Model Based on Air-, Solid-, and Water-Phase Resistance in Variably Saturated Soil.” 2008. *Vadose Zone Journal* 7 (4): 1276–1286. https://doi.org/10.2136/vzj2008.0023.

Tolk, Judy A. “Plant available soil water.” 2003. *Encyclopedia of Water Science. Marcel Dekker, Inc., New York, NY,* 669–672.

Troeh, Frederick R., Jalal D. Jabro, and Don Kirkham. “Gaseous diffusion equations for porous materials.” 1982. *Geoderma* 27 (3): 239–253. https://doi.org/10.1016/0016-7061(82)90033-7.

Tsigoriyna, Lidia, Dimitar Ganchev, Penka Petrova, and Kaloyan Petrov. “Highly Efficient 2,3-Butanediol Production by Bacillus licheniformis via Complex Optimization of Nutritional and Technological Parameters.” 2021. *Fermentation* 7 (3): 118. https://doi.org/10.3390/fermentation7030118.

Tuller, Markus, and Dani Or. “Water retention and characteristic curve.” 2004. In *Encyclopedia of Soils in the Environment,* 4:278–289.

Veelen, Arjen van, Monique C. Tourell, Nicolai Koebernick, Giuseppe Pileio, and Tiina Roose. “Correlative Visualization of Root Mucilage Degradation Using X-ray CT and MRI.” 2018. *Front. Environ. Sci.* 6. https://doi.org/10.3389/fenvs.2018.00032.

Vermoesen, A., H. Ramon, and O. Van Cleemput. “Composition of the soil gas phase: Permanent gases and hydrocarbons.” 1991. *Pedologie* 41:119–132.

Vogel, Hans-Jörg. “Morphological determination of pore connectivity as a function of pore size using serial sections.” 1997. *European Journal of Soil Science* 48 (3): 365–377. https://doi.org/10.1111/j.1365-2389.1997.tb00203.x.

Vogel, Hans-Jörg. “Topological Characterization of Porous Media.” 2002. In *Morphology of Condensed Matter,* edited by R. Beig, B. -G. Englert, U. Frisch, P. Hänggi, K. Hepp, W. Hillebrandt, D. Imboden, et al., 600:75–92. Berlin, Heidelberg: Springer Berlin Heidelberg. https://doi.org/10.1007/3-540-45782-8_3.

Volk, Elazar, Sascha C. Iden, Alex Furman, Wolfgang Durner, and Ravid Rosenzweig. “Biofilm effect on soil hydraulic properties: Experimental investigation using soil-grown real biofilm.” 2016. *Water Resources Research* 52 (8): 5813–5828. https://doi.org/10.1002/2016WR018866.

Wen, Tiande, Longtan Shao, and Xiaoxia Guo. “Effect of hysteresis on hydraulic properties of soils under multiple drying and wetting cycles.” 2021. *European Journal of Environmental and Civil Engineering* 25 (10): 1750–1762. https://doi.org/10.1080/19648189.2019.1600037.

Werner, David, Peter Grathwohl, and Patrick Höhener. “Review of Field Methods for the Determination of the Tortuosity and Effective Gas-Phase Diffusivity in the Vadose Zone.” 2004. *Vadose Zone Journal* 3 (4): 1240–1248. https://doi.org/10.2136/vzj2004.1240.

Wesseling, J., W. R. van Wijk, Milton Fireman, Bessel D. van’t Woudt, and Robert M. Hagan. “Land Drainage in Relation to Soils and Crops.” 1957. In *Drainage of Agricultural Lands,* 461–578. John Wiley & Sons, Ltd. https://doi.org/10.2134/agronmonogr7.c5.

Wiant, Harry V. “Has the contribution of litter decay to forest" soil respiration" been overestimated?” 1967. *Journal of Forestry* 65 (6): 408–409.

Wiegleb, Gerhard. “Physikalische Eigenschaften von Gasen.” 2016. In *Gasmesstechnik in Theorie und Praxis: Messgeräte, Sensoren, Anwendungen,* edited by Gerhard Wiegleb, 7–118. Wiesbaden: Springer Fachmedien Wiesbaden. https://doi.org/10.1007/978-3-658-10687-4_2.

Williams, K. A., S. A. Ruiz, C. Petroselli, N. Walker, D. M. McKay Fletcher, G. Pileio, and T. Roose. “Physical characterisation of chia mucilage polymeric gel and its implications on rhizosphere science - Integrating imaging, MRI, and modelling to gain insights into plant and microbial amended soils.” 2021. *Soil Biology and Biochemistry* 162 (November 1, 2021): 108404. https://doi.org/10.1016/j.soilbio.2021.108404.

Wloka, M., H. Rehage, H.-C. Flemming, and J. Wingender. “Rheological properties of viscoelastic biofilm extracellular polymeric substances and comparison to the behavior of calcium alginate gels.” 2004. *Colloid and Polymer Science* 282, no. 10 (August 1, 2004): 1067–1076. https://doi.org/10.1007/s00396-003-1033-8.

Xia, J. H., and Jkm Roberts. “Improved Cytoplasmic pH Regulation, Increased Lactate Efflux, and Reduced Cytoplasmic Lactate Levels Are Biochemical Traits Expressed in Root Tips of Whole Maize Seedlings Acclimated to a Low-Oxygen Environment.” 1994. *Plant Physiol.* 105 (2): 651–657. https://doi.org/10.1104/pp.105.2.651.

Xing, Wei, Min Yin, Qing Lv, Yang Hu, Changpeng Liu, and Jiujun Zhang. “1 - Oxygen Solubility, Diffusion Coefficient, and Solution Viscosity.” 2014. In *Rotating Electrode Methods and Oxygen Reduction Electrocatalysts,* edited by Wei Xing, Geping Yin, and Jiujun Zhang, 1–31. Amsterdam: Elsevier, January 1, 2014. https://doi.org/10.1016/B978-0-444-63278-4.00001-X.

Xu, Xia, J. L. Nieber, and S. C. Gupta. “Compaction Effect on the Gas Diffusion Coefficient in Soils.” 1992. *Soil Sci. Soc. Am. J.* 56 (6): 1743–1750. https://doi.org/10.2136/sssaj1992.03615995005600060014x.

Yang, Runhuai, Tianyun Gao, Didi Li, Haiyi Liang, and Qingqing Xu. “Simulation of fracture behaviour of hydrogel by discrete element method.” 2018. *Micro Nano Lett.* 13 (6): 743–746. https://doi.org/10.1049/mnl.2017.0844.

York, Larry M., Andrea Carminati, Sacha J. Mooney, Karl Ritz, and Malcolm J. Bennett. “The holistic rhizosphere: integrating zones, processes, and semantics in the soil influenced by roots.” 2016. *J Exp Bot* 67 (12): 3629–3643. https://doi.org/10.1093/jxb/erw108.

Young, I. M. “Variation in moisture contents between bulk soil and the rhizosheath of wheat (Triticum aestivum L. cv. Wembley).” 1995. *New Phytol.* 130 (1): 135–139. https://doi.org/10.1111/j.1469-8137.1995.tb01823.x.

Zahra, Noreen, Muhammad Bilal Hafeez, Kanval Shaukat, Abdul Wahid, Sadam Hussain, Rubina Naseer, Ali Raza, Shahid Iqbal, and Muhammad Farooq. “Hypoxia and Anoxia Stress: Plant responses and tolerance mechanisms.” 2021. *Journal of Agronomy and Crop Science* 207 (2): 249–284. https://doi.org/10.1111/jac.12471.

Zarebanadkouki, Mohsen, Mutez A. Ahmed, and Andrea Carminati. "Hydraulic conductivity of the root-soil interface of lupin in sandy soil after drying and rewetting." 2016. *Plant Soil* 398 (1): 267–280. https://doi.org/10.1007/s11104-015-2668-1.

Zarebanadkouki, Mohsen, Theresa Fink, Pascal Benard, and Callum C. Banfield. "Mucilage Facilitates Nutrient Diffusion in the Drying Rhizosphere." 2019. *Vadose Zone Journal* 18 (1): 190021. https://doi.org/https://doi.org/10.2136/vzj2019.02.0021.

Zhang, Ming, Ying Xu, Ke-Qing Xiao, Chun-Hui Gao, Shuang Wang, Di Zhu, Yichao Wu, Qiaoyun Huang, and Peng Cai. "Characterising soil extracellular polymeric substances (EPS) by application of spectral-chemometrics and deconstruction of the extraction process." 2023. *Chemical Geology* 618:121271. https://doi.org/10.1016/j.chemgeo.2022.121271.

Zheng, Wenjuan, Saiqi Zeng, Harsh Bais, Jacob M. LaManna, Daniel S. Hussey, David L. Jacobson, and Yan Jin. "Plant Growth-Promoting Rhizobacteria (PGPR) Reduce Evaporation and Increase Soil Water Retention." 2018. *Water Resources Research* 54 (5): 3673–3687. https://doi.org/10.1029/2018WR022656.

Zickenrott, Ina-Maria, Susanne K. Woche, Jörg Bachmann, Mutez A. Ahmed, and Doris Vetterlein. "An efficient method for the collection of root mucilage from different plant species—A case study on the effect of mucilage on soil water repellency." 2016. *Journal of Plant Nutrition and Soil Science* 179 (2): 294–302. https://doi.org/10.1002/jpln.201500511.

Band / Volume 654
Modellierung der flächendifferenzierten Grundwasserneubildung für Schleswig-Holstein im Beobachtungszeitraum 1961 – 2021 und für Klimaszenarien bis 2100
I. McNamara, B. Tetzlaff, F. Wendland, T. Wolters (2025), 191 pp
ISBN: 978-3-95806-803-2

Band / Volume 655
Entwicklung alternativer Brenngaselektroden für die Hochtemperatur-Elektrolyse
F. E. Winterhalder (2025), vii, 161 pp
ISBN: 978-3-95806-805-6

Band / Volume 656
Oxide-based All-Solid-State Batteries for and from Recycling Processes
V. M. Kiyek (2025), viii, 128 pp, xix
ISBN: 978-3-95806-806-3

Band / Volume 657
Investigation of current and future anthropogenic chemical regimes in simulation chamber experiments
M. Färber (2025), 213 pp
ISBN: 978-3-95806-809-4

Band / Volume 658
Dynamischer Betrieb von Polymer-Elektrolyt-Membran Wasserelektrolyseuren
E. Rauls (2025), XIV, 239 pp
ISBN: 978-3-95806-811-7

Band / Volume 659
Pore-scale reactive transport modeling in cementitious materials: Development and application of a high-performance computing code based on the Lattice-Boltzmann method
S. Rohmen (2025), X, 295 pp
ISBN: 978-3-95806-812-4

Band / Volume 660
Recyclingmöglichkeiten für die Keramikkomponenten einer Festoxidzelle
S. Sarner (2025), VIII, 122 pp
ISBN: 978-3-95806-816-2

Band / Volume 661
Methodological Approach Enabling the Two-phase Flow Investigation in Alkaline Electrolysis under Demanding Conditions
S. Renz (2025), IX, 252 pp
ISBN: 978-3-95806-821-6

Band / Volume 662
Variable renewable energy potential estimates based on high-resolution regional atmospheric modelling over southern Africa
S. Chen (2025), XIII, 141 pp
ISBN: 978-3-95806-822-3

Band / Volume 663
Advances in Understanding Nitrate Aerosol Formation and the Implications for Atmospheric Radiative Balance
A. Milousis (2025), 195 pp
ISBN: 978-3-95806-823-0

Band / Volume 664
Optimization of NaSICON-type lithium-ion conductors for solid-state batteries
A. Loutati (2025), viii, 104 pp
ISBN: 978-3-95806-824-7

Band / Volume 665
Innovative Plasma Sprayed Thermal Barrier Coatings for Enhanced Flexibility in Gas Turbine Operation
J. Igel (2025), V, 153, XXXVI pp
ISBN: 978-3-95806-827-8

Band / Volume 666
Techno-ökonomisches Potenzial dezentraler und autarker Energiesysteme
S. K. A. Risch (2025), xxiii, 210 pp
ISBN: 978-3-95806-829-2

Band / Volume 667
Reactive Field Assisted Sintering of Novel Rare Earth Garnets for Plasma Etching Applications
C. Stern (2025), VII, 101, XXVIII pp
ISBN: 978-3-95806-833-9

Band / Volume 668
Effects of mucilage and extracellular polymeric substances on soil gas diffusion
A. Haupenthal (2025), v, 99 pp
ISBN: 978-3-95806-834-6

Energie & Umwelt / Energy & Environment
Band / Volume 668
ISBN 978-3-95806-834-6

Mitglied der Helmholtz-Gemeinschaft

JÜLICH
Forschungszentrum